



Norwegian University of
Science and Technology

Optimization of NGL Extraction Processes for Floating LNG Processes

Daniel Sætre

Master of Science in Mechanical Engineering

Submission date: February 2016

Supervisor: Truls Gundersen, EPT

Co-supervisor: Donghoi Kim, EPT

Norwegian University of Science and Technology
Department of Energy and Process Engineering

EPT-M-2015-133

MASTER THESIS

for

Student Daniel Sætre

Fall 2015

Optimization of NGL Extraction Processes for Floating LNG Processes*Optimalisering av NGL ekstraksjon i flytende LNG prosesser***Background and objective**

The concept of floating LNG (FLNG) has attracted the attention of the gas industry since natural gas demand is expected to grow in the future. FLNG is a huge and complex facility producing, storing and offloading LNG from an offshore gas field. Processing on an FLNG vessel has, however, required technical developments to be suitable for offshore environment. The removal of heavier hydrocarbons (HHC) in natural gas and the liquefaction of the treated natural gas are the main concerns in this respect. The extraction products are Natural Gas Liquids (NGL) and condensate.

So far, various liquefaction processes have been suggested for FLNG to overcome the drawbacks of the conventional technologies. For large production of LNG, in excess of 2-4 million tons per annum (MTPA), the dual mixed refrigerant (DMR) process has been recommended. This is due to its low specific power, large train capacity and less flammable refrigerant for its pre-cooling cycle compared to the C3MR process, which is the market dominating process. The mixed refrigerant (MR) for the pre-cooling cycle also gives better operational flexibility as it can handle the variation of feed gas composition, pressure and flow rate.

Heavier hydrocarbons like natural gas liquid (NGL) are extracted to prevent freeze-out in the liquefier and to improve project economics as it has a higher value than LNG. Such extraction is performed either upstream or as an integral part of a liquefaction process. The former scheme is achieved by a Joule-Thomson valve, a gas expander or a scrub column. The latter requires an integration of the NGL extraction process with the LNG process, which may increase the complexity of design and operation. Process providers and academic researchers have suggested various HHC extraction systems for each of the two schemes.

The candidate will build further on the specialization project, where 2 upstream and 2 integrated HHC extraction systems were compared in the context of application for FLNG. The AP-DMR process from APCI was used as a representative of the DMR process.

The *main objective* of this Master Thesis is to test the optimization tool in Aspen HYSYS on the different HHC extraction concepts, and to use these results to make a more fair comparison between the 4 alternative extraction processes studied in the specialization project.

The following tasks are to be considered:

1. Brief literature review on relevant publications for numerical optimization, especially non-linear optimization problems and SQP solution algorithms, as well as previous work regarding optimization of NGL and/or LNG processes.
2. Provide a brief presentation of the 4 NGL extraction processes to be optimized with focus on differences, advantages and disadvantages with the different alternatives.
3. Evaluate the robustness of the "Hyprotech SQP" optimizer for the processes with different objective functions and constraints, focusing on computing times and the values of the optima obtained.
4. Analyze the optimization results and compare the performance with those reported in the literature. If possible and as an extra challenge, look for opportunities to improve the existing HHC extraction concepts, while considering the process itself, the heat recovery system, and the drivers (gas turbines).
5. Conclude with a recommendation for the selection of extraction process from criteria such as energy efficiency, process complexity and (if possible) make comments about safety.

-- " --

Within 14 days of receiving the written text on the master thesis, the candidate shall submit a research plan for his project to the department.

When the thesis is evaluated, emphasis is put on processing of the results, and that they are presented in tabular and/or graphic form in a clear manner, and that they are analyzed carefully.

The thesis should be formulated as a research report with summary both in English and Norwegian, conclusion, literature references, table of contents etc. During the preparation of the text, the candidate should make an effort to produce a well-structured and easily readable report. In order to ease the evaluation of the thesis, it is important that the cross-references are correct. In the making of the report, strong emphasis should be placed on both a thorough discussion of the results and an orderly presentation.

The candidate is requested to initiate and keep close contact with his/her academic supervisor(s) throughout the working period. The candidate must follow the rules and regulations of NTNU as well as passive directions given by the Department of Energy and Process Engineering.

Risk assessment of the candidate's work shall be carried out according to the department's procedures. The risk assessment must be documented and included as part of the final report. Events related to the candidate's work adversely affecting the health, safety or security, must be documented and included as part of the final report. If the documentation on risk assessment represents a large number of pages, the full version is to be submitted electronically to the supervisor and an excerpt is included in the report.

Pursuant to “Regulations concerning the supplementary provisions to the technology study program/Master of Science” at NTNU §20, the Department reserves the permission to utilize all the results and data for teaching and research purposes as well as in future publications.

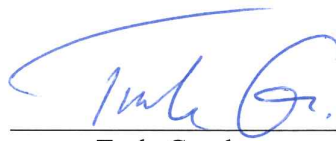
The final report is to be submitted digitally in DAIM. An executive summary of the thesis including title, student’s name, supervisor's name, year, department name, and NTNU's logo and name, shall be submitted to the department as a separate pdf file. Based on an agreement with the supervisor, the final report and other material and documents may be given to the supervisor in digital format.

- Work to be done in lab (Water power lab, Fluids engineering lab, Thermal engineering lab)
 Field work

Department of Energy and Process Engineering, 21 September 2015



Olav Bolland
Department Head



Truls Gundersen
Academic Supervisor

Co-supervisor:

PhD student Donghoi Kim, Department of Energy and Process Engineering, NTNU
E-mail: donghoi.kim@ntnu.no

Preface

This thesis was written during the autumn of 2015 at the Department of Energy and Process Engineering, Norwegian University of Science and Technology (NTNU) in Trondheim. The report is written as a master thesis in the Masters Degree Program of Mechanical Engineering. The thesis is a continuation of my specialization project from the previous semester.

I would like to thank my supervisor at NTNU, Professor Truls Gundersen, for his guidance, his ideas and useful feedback throughout the master thesis. Secondly, I want to express my gratitude to my co-supervisor PhD student Donghoi Kim. He has been available when needed, and help me solve problems I have stumbled upon. I would also like to thank Eirik Rødstøl, who provided valuable insight in the Hyprotech SQP optimizer in HYSYS.

A final thanks goes to my friends and family who have supported me throughout all my years of study.

Trondheim, 24th February, 2016

Daniel Sætre

Abstract

Removal of heavy hydrocarbons from natural gas streams is necessary in all liquefaction processes to prevent freeze-out in the main cryogenic equipment. In addition, more valuable products are obtained giving the process an economical benefit. The process of removing natural gas liquids (NGL) is either done upstream the liquefaction process, or as an integrated part of the pre-cooling of the gas. Both of these possibilities were studied in this master thesis.

The purpose of the thesis is to use the built in Hyprotech SQP optimizer in Aspen HYSYS software program to optimize four different NGL extraction processes. The results have been used to evaluate and compare the different extraction schemes, focusing on performance parameters. Simulation models were used to test the robustness of the optimizer, and to study how it coped with small changes. This is a relevant topic, as the goal for many gas projects is to optimize the process efficiency of the plant.

The results suggest that the Hyprotech SQP optimizer is very sensitive to changes in the setup of the derivative utility. Any changes to input data in the optimizer will affect the results obtained. The optimizer should always be configured after the modeller has made a final decision on the variables start and boundary values. When configured correctly, the optimizer produces good simulation results that satisfy the process constraints.

The optimized processes were improved by 19 - 21 % compared to the initial objective function values. The integrated APCI process proved to be the best performing NGL extraction scheme. It had the best performance for criteria process complexity, process safety, product recovery, and production capacity. The upstream Fluor process had the lowest specific power, and was therefore leading among the schemes in process efficiency.

In conclusion, it is challenging to set up the derivative utility and optimizer parameters properly. On the other hand, if configured correctly, the Hyprotech SQP optimizer has the ability to provide substantial improvements to a process model.



Sammendrag

Fjerning av tyngre hydrokarboner fra en strøm av naturgassføde er nødvendig i alle prosesser for å gjøre en naturgass flytende, for å hindre utfrysning av det kryogene utstyret. I tillegg fremstilles mer verdifulle produkter, noe som gir prosessen en økonomisk fordel. Fjerning av NGL gjøres enten oppstrøms i prosessen eller som en integrert del av forkjølingen av gassen. Begge disse mulighetene er studert i denne masteroppgaven.

Hensikten med denne oppgaven er å bruke den innebygde optimalisatoren Hyprotech SQP i programvaren Aspen HYSYS til å optimalisere fire ulike ekstraksjonsmetoder. Resultatene brukes til å evaluere og sammenligne de ulike ekstraksjonsmetodene, med fokus på ytelsesparametere. Simuleringsmodeller ble brukt til å teste robustheten til optimalisatoren, og undersøke hvordan den håndterte små endringer. Dette temaet er relevant ettersom målet for mange gassprosjekt er å optimalisere prosesseffektiviteten i et NGL-anlegg.

Resultatene tyder på at Hyprotech SQP optimalisatoren er veldig sensitiv for små endringer i oppsettet av derivatverktøyet. Enhver endring i inndata til optimalisatoren vil påvirke de innhentede resultatene. Optimalisatoren bør alltid konfigureres etter at brukeren har gjort en endelig beslutning til variablene sine start- og grenseverdier. Når den er konfigurert riktig, produserer optimalisatoren gode simuleringsresultater som tilfredstiller prosessbegrensningene.

De optimaliserte prosessene ble forbedret med 19 - 21 % i forhold til den opprinnelige verdien av målfunksjonen. Den integrerte APCI prosessen viste seg å være den med best resultat av ekstraksjonsmodellene. Den hadde best ytelse for kriteriene prosesskompleksitet, prosessikkerhet, produktgjenvinning, og produksjonskapasitet. Oppstrømsprosessen Fluor hadde den lavest spesifikke effekten, og var derved best i prosesseffektivitet.

Det konkluderes med at det er vanskelig å sette opp derivatverktøyet og optimalisatorparameterene ordentlig. På den annen side, dersom den er konfigurert riktig, har Hyprotech SQP optimalisatoren mulighet for å gi betydelige forbedringer i en prosessmodell.

Contents

Preface	i
Abstract	iii
Sammendrag	v
List of Figures	xi
List of Tables	xv
Nomenclature	xix
1 Introduction	1
1.1 Background	1
1.2 Objective	3
1.3 Scope of Work	3
1.4 Methodology	4
1.5 Outline of Report	4
2 Optimization	6
2.1 Introduction	6
2.2 Types of Problems	7
2.3 Global and Local Optimization	7
2.4 HYSYS Optimizer	9
2.5 Hyprotech SQP Optimizer	9
2.5.1 Derivative Utility	11
2.5.2 Optimizer Interface	13
2.5.3 Running Results	17
3 NGL Extraction Processes	19
3.1 Upstream NGL Extraction	19
3.1.1 Turbo-expander Process	19
3.1.2 Fluor Process	20
3.2 Integrated NGL Extraction	21
3.2.1 APCI Process	21

3.2.2	Shell Process	23
4	Design Basis	26
4.1	Feed Gas	26
4.2	Product	28
4.3	Liquefaction system	29
4.4	Driver solution	29
4.5	Cooling system	30
4.6	LNG Heat Exchanger	31
4.7	Turbo-machinery	32
4.8	Column	32
4.9	Other Specifications	33
5	Model Development and Optimization Parameters	35
5.1	Liquefaction Unit	35
5.1.1	Warm Mixed Refrigerant Cycle	37
5.1.2	Optimization Parameters WMR	38
5.1.3	Cold Mixed Refrigerant Cycle	41
5.1.4	Optimization Parameters CMR	43
5.2	Turbo-expander NGL Extraction Process	45
5.2.1	Optimization Parameters Turbo-expander Process	47
5.3	APCI NGL Extraction Process	49
5.3.1	Optimization Parameters APCI	50
5.4	Shell NGL Extraction Process	52
5.4.1	Optimization Parameters Shell Process	53
5.5	Fluor NGL Extraction Process	55
5.5.1	Optimization Parameters Fluor Process	57
6	Optimization Setup And Results	60
6.1	Turbo-expander	62
6.1.1	Derivative Utility	62
6.1.2	Optimizer Flags Study	64
6.1.3	Optimizer Setup Study	68
6.2	APCI	79
6.2.1	Derivative Utility	79
6.2.2	Optimizer Setup Study	81

6.3	Shell	90
6.3.1	Derivative Utility	90
6.3.2	Optimizer Setup Study	92
6.4	Fluor	98
6.4.1	Derivative Utility	100
6.4.2	Optimizer Setup Study	101
6.5	Optimizer Setup Trends	103
7	Process Comparison	106
7.1	Process Efficiency	107
7.2	Product Recovery	108
7.3	Production Capacity	111
7.4	Process Complexity	112
7.5	Process Safety	113
7.6	Summary	115
8	Conclusion	116
9	Further Work	119
	References	120
	Appendix A	123
	Appendix B	124
	Appendix C	125
	Appendix D	126
	Appendix E	128
	Appendix F	129
	Appendix G	130
	Appendix H	131
	Appendix I	133

Appendix J	135
Appendix K	138
Appendix L	140
Appendix M	142
Appendix N	144

List of Figures

1.1	Digital impression of Shells Prelude FLNG facility design	2
2.1	Simple illustration of an optimization problem with many local optima and one global optima	8
2.2	Illustration of a merit function	10
2.3	Illustration of the watchdog technique	11
2.4	Default flags configuration for the Hyprotech SQP optimizer	13
2.5	Default setup configuration for the Hyprotech SQP optimizer	14
3.1	Turbo-expander process scheme	19
3.2	Patented Fluor process scheme	21
3.3	APCI process scheme	22
3.4	Shell process scheme	24
4.1	Air Products AP-DMR™ LNG Process	29
4.2	Power output of GE gas turbine LM6000	30
4.3	Direct sea water cooling	31
5.1	Dual mixed refrigerant liquefaction cycle	36
5.2	Warm mixed refrigerant cycle in DMR Process	37
5.3	Cold mixed refrigerant cycle in DMR process	42
5.4	Aspen HYSYS model of Turbo-expander NGL extraction process	46
5.5	Aspen HYSYS model of APCI NGL extraction process	49
5.6	Aspen HYSYS model of Shell NGL extraction process	52
5.7	Fluor model in Aspen HYSYS	56
6.1	Optimizer flags test for perturbation value of 1.00E-5	65
6.2	Optimizer flags test for perturbation value of 1.00E-4	65
6.3	Optimizer flags test for perturbation value of 5.00E-4	66
6.4	Optimizer flags test for perturbation value of 1.00E-3	66
6.5	Optimizer flags test for perturbation value of 3.00E-3	66
6.6	Optimizer setup test for Turbo-expander process with objective scale factor = 0	70

6.7	Optimizer setup test for Turbo-expander process with objective scale factor = 0.001	71
6.8	Optimizer setup test for Turbo-expander process with objective scale factor = 0.01	71
6.9	Optimizer setup test for Turbo-expander process with objective scale factor = 0.1	71
6.10	Optimizer setup test for Turbo-expander process with objective scale factor = 1	72
6.11	Optimizer setup test for Turbo-expander process with objective scale factor = 10	72
6.12	Effect of altering lower boundary value of HP Warm from 35 to 32 bar in Turbo-expander process.	74
6.13	HP Warm value after reducing lower boundary Turbo-expander process . .	76
6.14	Effect of using randomly generated variable values as starting values in Turbo-expander process	77
6.15	Overview of constraint violations in best test result in Turbo-expander process	78
6.16	Average CPU time and gradient evaluations for simulations in Turbo-expander process	79
6.17	Optimizer setup test for APCI process with Objective Scale Factor = 0 . .	82
6.18	Optimizer setup test for APCI process with Objective Scale Factor = 0.001	82
6.19	Optimizer setup test for APCI process with Objective Scale Factor = 0.01	82
6.20	Optimizer setup test for APCI process with Objective Scale Factor = 0.1 .	83
6.21	Optimizer setup test for APCI process with Objective Scale Factor = 1 . .	83
6.22	Optimizer setup test for APCI process with Objective Scale Factor = 10 .	83
6.23	Effect of removing variable N WMR from derivative utility in APCI process	85
6.24	Effect of altering variable boundaries in APCI process	87
6.25	Effect of using randomly generated variable values as starting values in APCI process	88
6.26	Overview of constraint violations in best test result in APCI process	89
6.27	Average CPU time and gradient evaluations for simulations in APCI process	90
6.28	Optimizer setup test for Shell process with Objective Scale Factor = 0 . . .	92
6.29	Optimizer setup test for Shell process with Objective Scale Factor = 0.001	93
6.30	Optimizer setup test for Shell process with Objective Scale Factor = 0.01 .	93
6.31	Optimizer setup test for Shell process with Objective Scale Factor = 0.1 . .	93

6.32	Optimizer setup test for Shell process with Objective Scale Factor = 1 . . .	94
6.33	Optimizer setup test for Shell process with Objective Scale Factor = 10 . . .	94
6.34	Effect of altering variable boundaries in Shell process	96
6.35	Effect of using randomly generated variable values as starting values in Shell process	97
6.36	Overview of constraint violations in best test result in Shell process	98
6.37	Optimizer setup test for Fluor process with Objective Scale Factor = 0 . .	102
6.38	Overview of constraint violations in best test result in Fluor process	103
6.39	Total accepted results for each objective scale factor relative to the number of simulation tests performed	105
6.40	Total accepted results considering perturbation values	105
7.1	Specific power after optimization of NGL extraction processes	107
7.2	Illustration of the degree to which the necessary refrigeration make-up is extracted in each of the NGL extraction schemes	110
7.3	Pressure level of processed gas stream, WMR cycle high pressure and CMR cycle high pressure for best cases of NGL extraction processes	114
A.1	Full HYSYS model of Turbo-expander process	123
B.1	Full HYSYS model of APCI process	124
C.1	Full HYSYS model of Shell process	125
D.1	Full HYSYS model of Fluor process	126
E.1	CPU Time vs Gradient Calculations for Turbo-expander process	128
F.1	CPU Time vs Gradient Calculations for APCI process	129
G.1	CPU Time vs Gradient Calculations for Shell process	130

List of Tables

2.1	Running results in Hyprotech SQP optimizer	18
3.1	Equipment in Figure 3.2	22
3.2	Equipment in Figure 3.3	23
3.3	Equipment in Figure 3.3	24
4.1	Feed gas composition entering NGL extraction processes	27
4.2	Feed gas properties	27
4.3	Product specifications for LNG and NGL	28
4.4	Design specifications in HYSYS LNG heat exchanger	32
4.5	Turbomachinery efficiency parameters in HYSYS models	32
4.6	Design specifications in HYSYS columns	33
4.7	Other specifications	34
5.1	Optimization variables in warm mixed refrigerant cycle in DMR process . .	39
5.2	Optimization constraints in warm mixed refrigerant cycle in DMR process	40
5.3	Optimization variables in cold mixed refrigerant cycle in DMR process . .	43
5.4	Optimization constraints in cold mixed refrigerant cycle in DMR process .	45
5.5	Optimization variables in Turbo-expander process	47
5.6	Optimization constraints in Turbo-expander process	48
5.7	Optimization variables in APCI process	50
5.8	Optimization constraints in APCI process	51
5.9	Optimization variables in Shell process	53
5.10	Optimization constraints in Shell process	55
5.11	Optimization variables in Fluor process	57
5.12	Optimization constraints in Fluor process	59
6.1	Values kept constant for optimizer setup parameters in the derivative utility	60
6.2	Derivative utility values for variables in Turbo-expander process	63
6.3	Derivative utility values for constraints in Turbo-expander process	63
6.4	Flag tests using the Turbo-expander process	64
6.5	Comparison of how the objective value and constraint violations are affected when both "Hyprotech SQP Calc Gradients" and "Include Variable Scales" is checked versus only the latter.	68

6.6	Perturbation values in optimizer setup tests	68
6.7	Constraint violations allowed before test result are rejected in Turbo-expander process.	69
6.8	Termination and failure reasons in Aspen HYSYS which did not provide simulation results in the testing of the optimizer setup.	70
6.9	Top five results from optimizer setup tests in the Turbo-expander process .	73
6.10	Status of variables in derivative utility for test results in Table 6.9 in Turbo-expander process	74
6.11	Status of variables in derivative utility after altering variable bounds in Turbo-expander process	76
6.12	Derivative utility values for variables in APCI process	80
6.13	Derivative utility values for constraints in APCI process	81
6.14	Top five results from optimizer setup tests in the APCI process	84
6.15	Status of variables in derivative utility for test results in Table 6.14 in APCI process	85
6.16	New variable boundaries in optimizer test for APCI process	86
6.17	Status of variables in derivative utility after altering variable bounds in APCI process	87
6.18	Derivative utility values for variables in Shell process	91
6.19	Derivative utility values for constraints in Shell process	92
6.20	Top five results from optimizer setup tests in the Shell process	95
6.21	Stats of variables in derivative utility for test results in Table 6.20 in Shell process	95
6.22	New variable boundaries in optimizer test for Shell process	96
6.23	Derivative utility values for variables in Fluor process	100
6.24	Derivative utility values for constraints in Fluor process	101
6.25	New values for variables and constraints in Fluor process after optimization of the upstream extraction unit.	102
6.26	Accepted results for each process model considering different objective scale factors	104
7.1	Simulation results for the best optimizer results for each NGL extraction process in Chapter 6	106
7.2	Comparison of compressor power in NGL extraction processes	108

7.3	Comparison between the objective value of the extraction models prior to and after optimization using the Hyprotech SQP optimizer.	108
7.4	Scrub column operational parameters in NGL extraction processes	109
7.5	Product recovery of components divided by component molar flow in feed stream in NGL extraction processes	110
7.6	Comparison of production capacity in NGL extraction processes	111
7.7	Major equipment count for NGL extraction processes	112
7.8	Refrigerant circulation for best cases of NGL extraction processes	114
7.9	Comparison summary of NGL extraction schemes	115
H.1	Start values for randomly generated variables in Turbo-expander process for tests done in Section 6.1.3.1	131
H.2	Start values for randomly generated constraints in Turbo-expander process for tests done in Section 6.1.3.1	132
I.1	Start values for randomly generated variables in APCI process for tests done in Section 6.2.2.1	133
I.2	Start values for randomly generated constraints in APCI process for tests done in Section 6.2.2.1	134
J.1	Start values for randomly generated variables in Shell process for tests done in Section 6.3.2.1	136
J.2	Start values for randomly generated constraints in Shell process for tests done in Section 6.3.2.1	137
K.1	Final variable values for the best result in simulation work done by the Hyprotech SQP optimizer for the Turbo-expander process.	138
K.2	Final constraint values for the best result in simulation work done by the Hyprotech SQP optimizer for the Turbo-expander process.	139
L.1	Final variable values for the best result in simulation work done by the Hyprotech SQP optimizer for the APCI process.	140
L.2	Final constraint values for the best result in simulation work done by the Hyprotech SQP optimizer for the APCI process	141
M.1	Final variable values for the best result in simulation work done by the Hyprotech SQP optimizer for the Shell process.	142

M.2	Final constraint values for the best result in simulation work done by the Hyprotech SQP optimizer for the Shell process	143
N.1	Final variable values for the best result in simulation work done by the Hyprotech SQP optimizer for the Fluor process.	144
N.2	Final constraint values for the best result in simulation work done by the Hyprotech SQP optimizer for the Fluor process	145

Nomenclature

Abbreviations

BTX: Aromatic Hydrocarbons (Benzene, Toluene, Xylene)

C1: Methane

C2: Ethane

C3: Propane

C4: Butane

C5+: Condensate containing pentanes and heavier components

CMR: Cold Mixed Refrigerant

CPU: Central Process Unit

CV: Constraint Violation

DMR: Dual Mixed Refrigerant

DPC: Dew Point Controller

FLNG: Floating Liquefied Natural Gas

HHC: Heavy Hydrocarbons

LNG: Liquefied Natural Gas

MR: Mixed Refrigerant

MTPA: Million Tonnes Per Annum

N: Nitrogen

OV: Objective Value

RAM: Random Access Memory

SQP: Sequential Quadratic Programming

WMR: Warm Mixed Refrigerant

Chapter 1 Introduction

1.1 Background

The demand for natural gas is expected to grow in the future, although the value of the gas is currently moving on a downward slope. Due to the increasing demand, an incentive to monetize offshore gas resources exists. Today, offshore gas reserves are typically recovered through pipeline infrastructure to onshore processing plants or liquefied natural gas (LNG) facilities. An attractive alternative to these conventional facilities is the use of floating LNG (FLNG) concepts. Such concepts minimize a projects exposure to security and geopolitical risks, making FLNG a viable option. In addition, the initiation of stricter no-flaring rules that are being applied around the world adds another advantage to FLNG projects. FLNG facilities avoid costly re-injection reservoirs or long distance export pipelines. The construction of offshore FLNG facilities combine existing expertise from onshore facilities with new innovative solutions. The LNG FPSO will produce, process, liquefy, store and transfer LNG to customers worldwide [1].

Currently two FLNG facilities are under construction and will be ready for operations within two years. They are the Petronas Floating LNG Facility (PFLNG 1) located off the coast of Malaysia and Shells Prelude FLNG project located off the coast of Australia. Figure 1.1 displays a digital impression of Shells Prelude FLNG facility design. As illustrated, the size of such facilities is enormous, and especially complicated. Facilities planning on large scale production up towards 5 million tons per anum (MTPA), has a topside weight of as much as 70 000 tonnes. Storage capacities for this sized facility can be 220 000 m^3 for LNG, and 100 000 m^3 for NGL and Condensate storage [1].



Figure 1.1: Digital impression of Shells Prelude FLNG facility design

Prior to liquefaction of the natural gas, Natural Gas Liquids (NGL) need to be extracted. NGL consists of liquid petroleum gases (LPG), which includes ethane (C2), propane (C3), and butane (C4). In addition the more heavier components are categorised as condensate (C5+). The process of removing these components is done for four main reasons [2]:

- Reduce the heating value of the finalized LNG product so that it meets the required specifications.
- Prevent HHC from freezing and plugging the process equipment during the liquefaction stage.
- Use the NGL liquids as refrigerant make-up.
- Give economic benefit in terms of the valuable products obtained. The HHC's can be sold to the petrochemical industry or be used in gasoline blending.

NGL recovery can be accomplished in two ways, either upstream the liquefaction process or as an integrated approach with the liquefaction process. The selection of the best extraction process is dependent on factors such as feed composition, feed condition, sales gas specifications, product recovery, production capacity, process complexity, and process safety. Four extraction systems from Sætre's specialization project [3], two upstream and two integrated, are optimized and compared in this thesis.

1.2 Objective

The main objective of this Master Thesis is to test the optimization tool in Aspen HYSYS on the different HHC extraction concepts. The results are used to make a more fair comparison between the four different extraction processes studied in Sætre's [3] specialization project.

1.3 Scope of Work

The master project work considered, but was not limited to, the following tasks:

1. Review of relevant publications for numerical optimization, especially non-linear optimization problems and SQP solution algorithms, as well as previous work regarding optimization of NGL and/or LNG processes.
2. Provide a brief presentation of the 4 NGL extraction processes to be optimized with focus on differences, advantages and disadvantages with the different alternatives.
3. Evaluate the robustness of the "Hyprotech SQP" optimizer for the processes with different objective functions and constraints, focusing on computing times and the values of the optima obtained.
4. Analyze the optimization results and compare the performance with those reported in the literature. If possible and as an extra challenge, look for opportunities to improve the existing HHC extraction concepts, while considering the process itself, the heat recovery system, and the drivers.
5. Conclude with a recommendation for the selection of extraction process from criteria such as energy efficiency, process complexity and (if possible) make comments about safety.

In agreement with the supervisor of this master thesis, there is a minor change to task 3. The "Hyprotech SQP" optimizer is tested for one objective function and its accompanying constraints, and not for several. In addition, time did not allow looking into improvement opportunities of the existing HHC extraction concept (refer to task 4). The focus was on testing the "Hyprotech SQP" optimizer.

1.4 Methodology

The results of this thesis are based on simulation work done in Aspen Hysys V8.6, as well as a literature study of relevant topics. The literature study was performed to increase the understanding of and insight in NGL extraction, LNG processing, non-linear optimization, and simulation.

1.5 Outline of Report

Chapter 1 Introduction

Contains an explanation of the background, the objective, the scope and the methodology of the thesis work.

Chapter 2 Optimization

Contains information on basic optimization, types of optimization problems, global and local optimization, and the HYSYS Hyprotech SQP optimizer.

Chapter 3 NGL Extraction Processes

Contains descriptions of the upstream and integrated NGL extraction processes, which are in focus in the thesis work.

Chapter 4 Design Basis

Contains the design basis of the process models in which they are modelled in Hysys. Design specifications and assumptions for the four different processes are determined in this chapter.

Chapter 5 Model Development and Optimization Parameters

Contains thorough descriptions of how the models of the four NGL extraction processes were modeled in the process simulation program Aspen HYSYS. The optimization parameters, variables and constraints, are quantified, presented and explained in this chapter.

Chapter 6 Optimization Setup And Results

Contains details on the setup of the Hyprotech SQP optimizer. Studies are performed using different optimizer parameters with the intention of improving the objective value and minimize process constraint violations. Results of the studies are presented and discussed in this chapter.

Chapter 7 Process Comparison

The best optimization results in each process are briefly compared in this chapter. The comparison focuses on process efficiency, production capacity, product recovery, process complexity, and process safety.

Chapter 8 Conclusion

Contains the conclusion of results from studies performed in Chapters 6 & 7.

Chapter 9 Further Work

A recommendation for further work within this master thesis's discipline is presented in this chapter.

Chapter 2 Optimization

2.1 Introduction

The concept of optimization is used to solve complex problems. Multiple methods exist within the field of optimization that focus on solving various types of problems. Using optimization philosophy, complex decision problems that include variables and constraints can be solved focusing on a single objective function. The objective function is designed to measure the quality of the decisions made during optimization runs, resulting in an improved objective value. The objective value is a quantitative measure of the performance of the system under study [4]. The goal of the optimization is to find values for the variables that yield the best objective value, while upholding the process constraints. The objective value is either minimized or maximized depending on the formulation of the problem [5].

When dealing with complex problems it is hard to represent the complexities of variable interactions, and constraint restrictions. Constraints in a problem will often limit the optimizer in picking certain values for particular variables. It is therefore necessary that the modeller has good understanding of relevant theory and of the modelled process. Skillful modelling will support in capturing the most important variables in a process, and defining their boundaries appropriately [5].

An optimization algorithm can be used to find a solution once a model has been formulated. Depending on the model, a suitable optimization algorithm is picked to solve the particular type of optimization problem. The choice of algorithm is important, and can make the difference of whether the problem is solved or not. In addition, certain algorithms may solve certain problems quicker than others, saving time. After an algorithm has been applied to a problem, the modeller must be able to recognize whether or not it has succeeded in its task of finding a solution. In cases where the solution is not acceptable, the solution may be improved by changing specifications set either in the process model or as optimization parameters [4].

2.2 Types of Problems

Solving equations can be separated mathematically into three diverse types of problems. The first, also the simplest, is where the the number of equations, $N_{equations}$, equals the number of variables, $N_{variables}$. This case can be referred to as the completely specified case, and is therefore not an optimization problem. In this case the problem can both be linear or nonlinear, and the challenge is to find a method of solving it. A unique solution exists for the linear problem, while multiple or no solutions exist in the case of a nonlinear problem.

The second type of problem is where the number of equations exceed number of variables, $N_{variables} < N_{equations}$. This case is referred to as the overspecified case. Consequently, the set of equations are unsolvable unless some of the equations are linear combinations of the others.

The third type of problem is where the number of variables exceed the number of equations $N_{variables} > N_{equations}$. In this case the problem is underspecified, and the way of solving is done through iteration. This is the type of problem that arises when dealing with optimization work. The way of solving such a problem is by selecting a portion of the variables and use them as decision variables, N_D . The decision variables are iteratively adjusted to achieve an optimal solution to the function one wants to optimize.

$$N_D = N_{variables} - N_{equations} \quad (2.1)$$

[6]

2.3 Global and Local Optimization

Both global and local optima exist in non-linear optimization problems. Many local optima can exist in a single optimization problem, but only one global optima can exist. Figure 2.1 illustrates a function where multiple local optima exist. The red dots highlight locations of local optima, while the single green dot represents the global optimized solution.

In non-linear optimization problems it is difficult to find the global optima, because the problem may contain several feasible regions. In such optimization problems the algorithm

tends to trap itself in the search region of a local optima. A local solution will find a point at which the objective function is smaller than at all other feasible points in its proximity. For this reason, it is important to set up the optimizer in such a way that both the initial search conditions and search range cover an area where the expected global optima exists.

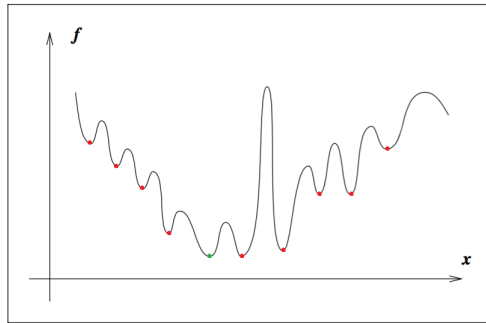


Figure 2.1: Simple illustration of an optimization problem with many local optima and one global optima [4]

Optimization algorithms search for the solution through the use of iteration. An initial guess of the the model's variables generates a starting point. The optimizer uses this starting point to generate a sequence of improved estimates until it reaches a solution. The method in which the algorithm iterates varies depending on the type of optimization algorithm. Despite the solving method, all algorithms should possess the following properties:

- Efficiency: should solve the problem without the use of excessive computing time and storage.
- Accuracy: should find precise solution without being overly sensitive to data and arithmetic rounding errors that occur during solving.
- Robustness: should perform well in a range of problems within its class, for all reasonable choices of initial variables.

The general formulation of a non-linear constrained mathematical programming problem can be stated as:

$$\begin{aligned}
& \underset{\mathbf{x}}{\text{minimize}} && f(\mathbf{x}) \\
& \text{subject to} && h_i(\mathbf{x}) = 0, \quad i = 1, 2, \dots, m. \\
& && g_j(\mathbf{x}) \leq 0, \quad j = 1, 2, \dots, r \\
& && \mathbf{x} \in S.
\end{aligned} \tag{2.2}$$

In this formulation, \mathbf{x} is an n -dimensional vector of unknowns, $\mathbf{x} = (x_1, x_2, \dots, x_n)$. The parameters h_i and g_j are real-valued functions of the variables (x_1, x_2, \dots, x_n) . S is a subset of n -dimensional space, and f is the objective function of the problem. The equations equality constraints and inequality constraints are represented by m and r , respectively [5].

2.4 HYSYS Optimizer

Aspen HYSYS uses a multi-variable steady state optimizer. A built and already converged process flowsheet can be optimized (maximized or minimized) in relation to an objective function [7]. The objective function can be anything from minimizing energy use, minimizing equipment size, or maximizing profits, depending on the purpose of the optimization. The optimizer can control a range of variables which influence the operating conditions of the specific process, making it a powerful tool. There are three different optimizer configurations available in Aspen HYSYS V8.6; Original, Hyprotech SQP and MDC Optim. Based on earlier work, the optimizer most appropriate when dealing with advanced liquefaction processes is the Hyprotech SQP optimizer [8]. The other two will be disregarded and not examined. The Hyprotech SQP optimizer is the newest addition to the optimizers available in HYSYS.

2.5 Hyprotech SQP Optimizer

The Hyprotech SQP optimizer is a sequential quadratic programming (SQP) algorithm, which handles both equality and inequality constraints. SQP is considered to be one of the most efficient optimization algorithms when solving minimization problems with general linear and non-linear constraints. This is true considering reasonable starting values are

used, and the number of primary variables is small [7]. In this thesis the number of optimization variables will vary from 25-30 in each process.

The optimizer features step size restriction, decision variable scaling, objective function scaling, and a problem-independent and scale independent relative convergence test. The algorithm also ensures that the model is evaluated only at points feasible with respect to the variable bounds. The solver utilizes a line search procedure referred to as the "watchdog" technique and a merit function in solving the optimization problem [7].

A merit function ϕ is a scalar-valued function of x . The function points out whether or not a new iteration value is better or worse than the previous one. Algorithms focusing on minimizing the objective function will require a decrease for each new iteration. Figure 2.2 shows an illustration of a merit function [8].

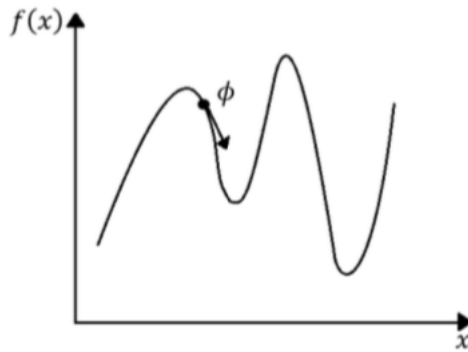


Figure 2.2: Illustration of a merit function [8]

The watchdog technique allows a certain number of iterations in the merit function to be accepted. These iterations steps are referred to as "relaxed steps", and aim towards finding a better objective value when stuck in a local optima pit. The strategy is illustrated in Figure 2.3. If a better objective function is not found within a certain number of iterations, another technique is performed [8].

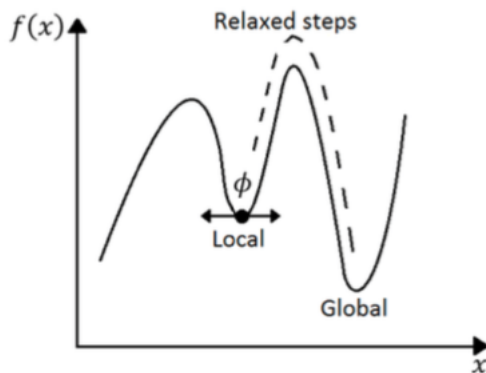


Figure 2.3: Illustration of the watchdog technique [8]

To get started with the optimizer, it needs to be configured with the necessary input data. This is done through the addition of a derivative utility and optimizer interface. The derivative utility defines how the optimizer is set up, while the interface determines how the optimizer reaches a solution.

2.5.1 Derivative Utility

The first step in creating a functioning optimizer is to initiate the setup of the derivative utility. The derivative utility has three main components; variables, constraints, and an objective function. The variables in the derivative utility are independent properties that are changed to satisfy the dependent variables, which are the constraints. This is done simultaneously to achieve an optimized objective function within the feasible boundaries of the problem [9].

Objective Function:

The objective function is the function which is to be maximized or minimized. This function can either be one specific variable from the process flowsheet, or a number of objective function variables which are combined into a single variable. The latter is the most probable type of objective function, and gives the user a huge amount of flexibility. A spreadsheet can be used to import multiple process variables, which are used to create an objective function. Typical objective functions can be total power consumption or an economical analysis of a process. The function for minimizing the objective function is shown in Equation 2.2.

Variables:

Variables are decision variables for the optimization problem. Variables are imported from the flowsheet, and are the parameters that are altered to minimize/maximize the objective function. Any process parameter that is user-specified can be used as a variable in the derivative utility. Upper and lower bounds are set for each independent variable. The range between the upper and lower bound is used to set the search range for the optimizer. In the case of a search range not being user-specified, the optimizer calculates it as:

$$\text{Range} = \text{Upper bound} - \text{Lower bound}$$

Since the search range is user-specified for each variable, the range might not be wide enough to find the optimal objective value. On the other hand, if the variable range is set too big, a feasible solution to the problem might be hard to find due to the search region being too broad. Therefore, the upper and lower boundaries should be set accordingly based on knowledge of the process.

After the optimizer has run, each variable will present a status in the derivative utility. The status of the variable can show three different messages. If the optimizer has succeeded in finding a variable value in between the upper and lower bound, the status will present "Inactive". This means that the variable does not prevent the optimizer in its search for the best value. In the case of the value equaling the lower bound, it will present "Active Low". The search region in this case is limited by the lower boundary. Lowering the value could in this case be advantageous. In the case of the value equaling the upper bound, it will present "Active high". In this case, increasing the value could improve the objective value.

Constraints:

Constraints are bounded variables for the optimization problem. The Hyprotech SQP can handle both inequality and equality constraints. The constraints set for an optimization problem are process parameters that have been constrained to a certain value or a range of numbers. Constraints can be one-sided unlike for variables, meaning they have the option of defining either a maximum or minimum limit. An example can be upholding a minimum approach temperature of 3°C in a heat exchanger, while having no upper limit.

The constraint also has a scale parameter that can be specified. The scale parameter can

be viewed upon as the constraint's tolerance, and is feasible if:

$$(Minimum - Scale) \leq Current Value \leq (Maximum + Scale)$$

A large scale value will ease the optimizer in solving complicated non-linear problems. The feasible region of the constraint parameter will increase proportionally with the the scale value.

2.5.2 Optimizer Interface

The method the optimizer uses to search for a feasible solution is determined in the optimizer interface. It also gathers the data provided in the derivative utility and supplies it to the optimizer. Two configuration sections exist in the optimizer interface; Setup and Flags.

Optimizer Flags

A total of nine options exist in the flags section. The default option in Aspen HYSYS is shown in Figure 2.4. An explanation of the options follows [10].

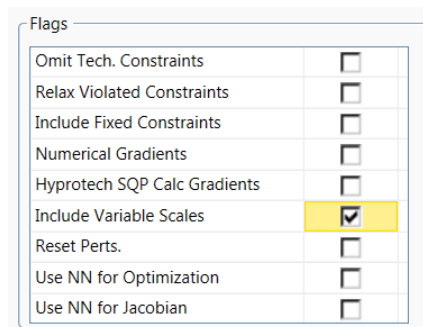


Figure 2.4: Default flags configuration for the Hyprotech SQP optimizer

Omit. Tech Constraints: Not used.

Relax Violated Constraints: Not used.

Include Fixed constraints: If this checkbox is selected, variables from the derivative utility that have equal lower and upper boundaries will be included in the optimization.

Numerical Gradients: Not used.

Hyprotech SQP Calc Gradients: If this checkbox is selected, the Hyprotech SQP algorithm itself carries out numerical calculations of any gradient elements needed.

Include Variable Scales: This checkbox is selected by default when using the Hyprotech SQP optimizer. The variable ranges for each variable, which is set in the derivative utility, is used as scaling factors within the algorithm.

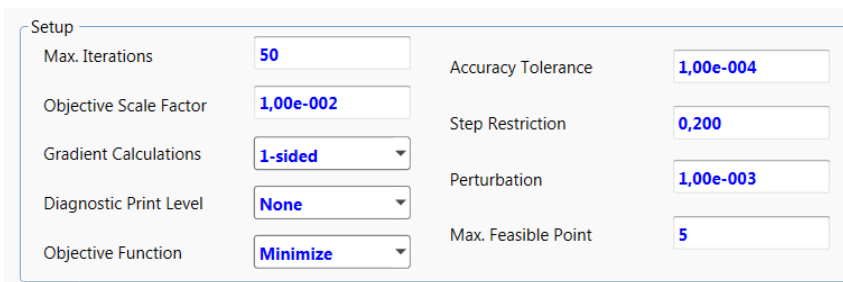
Reset Perts.: If this checkbox is selected, the gradient calculations will remove noise elements in the process flowsheet when the optimization starts.

Use NN for Optimization: Allows you to use any trained Neural Network in the flowsheet to replace the traditional HYSYS solver for optimization. This improves the robustness and reduced CPU time. However, the accuracy in the solution depends upon how the NN is trained and upon the data available. Neural networks are found the parametric utility in Hysys, which is outside the scope of this thesis. This flag option will therefore not be tested.

Use NN for Jacobian: Allows you to use any trained Neural Network to calculate the Jacobian. This is used to determine the next step in the Optimization process. This increases the CPU time as well as the accuracy. As mentioned above, this is option is outside the scope of this thesis.

Optimizer Setup

The second part to the optimizer configuration is the setup. In this section, the user has the option to change values of certain parameters to support the process flowsheet in converging while upholding the specified constraints. Figure 2.5 illustrates the default options for the setup of the Hyprotech SQP optimizer. Explanation of the parameters are described below.



Parameter	Value
Max. Iterations	50
Objective Scale Factor	1,00e-002
Gradient Calculations	1-sided
Diagnostic Print Level	None
Objective Function	Minimize
Accuracy Tolerance	1,00e-004
Step Restriction	0,200
Perturbation	1,00e-003
Max. Feasible Point	5

Figure 2.5: Default setup configuration for the Hyprotech SQP optimizer

Maximum Iterations

Maximum iterations indicates the maximum number of major iterations possible in the optimization process. One major iteration consists of a chain of minor iterations that focus on minimizing a linearly constrained sub-problem. Choosing an appropriate value for this feature depends on the size, complexity, noise, number of variables, and number of constraints in the flowsheet.

Objective Scale Factor

The objective scale factor is used to specify the factor for scaling the objective function. The specified factor is multiplied by the objective function, giving the optimizer a relative weight between the objective function and feasible search region. Low values can help in solving non-linear optimization problems.

Positive values are used as-is, and negative values use the absolute value of the scale factor. When the objective scale factor is set to 0, the optimizer itself picks a suitable value for the objective scale [7].

Accuracy Tolerance

The accuracy tolerance parameter specifies the relative accuracy tolerance used in the convergence test. The convergence test used is:

$$Convergence\ Sum \leq Accuracy\ Tolerance \times \max(|F(x)|, 1.0) \quad (2.3)$$

The convergence sum is a weighted sum of the possible improvement to the objective function considering the constraint violations. It has the same units as the objective function. This value, and therefore also the convergence test, is independent of the objective scale factor. The lower the accuracy tolerance value, the more accurate the objective function will be [7].

Step Restriction

The step restriction specifies the line search step-size restriction factor used during the first three iterations. Values higher than 1.0 indicate that no step restriction is set. For other values, lower step restriction results in larger restrictions.

Perturbation

The perturbation is the step size of the scaled variable used for gradient and Jacobian calculations. The size of the perturbation applied to each variable is determined by its

individual Range x perturbation [7]. Smaller values give faster gradient calculations, but may be inaccurate if the simulation contains a significant amount of noise [10].

Gradient Calculations

The two available options for gradient calculations are 1-sided or 2-sided.

- 1-sided: This option utilizes forward differences when constructing gradient approximations.

$$\frac{dc}{dv} = \frac{c(v + \Delta v) - c(v)}{\Delta v} \quad (2.4)$$

where:

v : optimizer variable

c : objective function or constraint

- 2-sided: This option utilizes central differences when constructing gradient approximations. Twice the number of calculations for a given solution is needed compared to the 1-sided option. The advantage of this is more accurate estimates of both the constraints and objective gradients. A disadvantage is an increase in CPU calculation time. This option is preferred for problems where the function is highly non-linear or has a lot of noise.

$$\frac{dc}{dv} = \frac{c(v + 0.5\Delta v) - c(v - 0.5\Delta v)}{\Delta v} \quad (2.5)$$

[7][10]

Max Feasible Point

The maximum number of iterations allowed in the line search procedure is specified in this parameter. When the Hysys optimizer has reached this point, it terminates the search and displays an error message of Step Convergence. When this occurs, it means that the required optimization accuracy is not achievable. If this parameter is set high enough, the Step Convergence error message is not due to the number of iterations. On the other hand, if the error message occurs early in the optimization, the initial values of the optimization variables might be set inappropriately [7].

Diagnostic Print Level

The diagnostic print level specifies the amount of information included in the optimizers diagnostic file. Six options exist; None, Partial_1, Partial_2, Partial_3, Full, and Excessive.

The diagnostic print level has nothing to do with how the optimizer solves the optimization problem.

Objective Function

In this parameter, the modeller chooses whether the objective function is to be maximized or minimized.

2.5.3 Running Results

After each optimization problem, the optimizer presents a set of results. The "Termination Reason Field" of the optimizer also presents the reason for termination. Five types of terminations are possible:

- **OK** If the problem has converged finding a feasible solution within the given constraints, variable boundaries, and optimizer configuration, the termination reason is presented as a green OK.
- **Step Convergence** If the stepping back procedure results in a step collapse to below the step restriction tolerance, step convergence is presented in the yellow banner. This is the solution type in most simulation cases. Step convergence is also displayed in cases when the optimizer is not able to provide results due to unsolved scrub columns in the process flowsheet.
- **Unbounded** If the defined variables and/or constraints are set or scaled badly, an unbounded error message is presented. In this case the optimizer terminates before it has begun.
- **Stopped** If two object's in the simulation are calculating different values for the same variable or an objects calculations are conflicting with existing specifications. A inconsistency error occurs and the simulation stops.

In addition, a fifth termination reason exists. In cases where the optimizer uses an excessive amount of time to solve the problem, HYSYS will shut down. This seems to occur due to a maximum amount of random access memory (RAM) available in the program. If the RAM cap, which was experienced to be 3.2 gigabytes, is reached prior to the termination reasons above, an error message declaring "Low Memory" will present itself in the program. This type of termination has nothing to do with the configuration of the optimizer, unlike the others. Simulation results in optimizer tests due to program failure are unobtainable. This

is unfortunate since the simulations that seem to provide the best results use a prolonged amount of time.

When the optimizer has reached one of the above termination reasons, a set of results are presented in the Running Results window of the Hyprotech SQP optimizer. The ones of interest are listed Table 2.1 along with a description.

Running Result	Description
Objective Value	This is the optimized objective value. This value can be compared to the starting objective value to determine the improvement of the process.
CPU Time	The total time the optimizer uses to solve the problem. This value depends on the processing power of the computer.
Gradient Evaluations	The number of gradient evaluations performed during the course of the optimization. This number is equal to the number of major iterations performed.
Model Evaluations	The number of model evaluations performed during the course of the optimization.
Feasible Point Iterations	The number of minor iterations since the last major iteration. If the optimizer terminates due to step convergence, this value will always equal the predetermined Max. Feasible Point.

Table 2.1: Running results in Hyprotech SQP optimizer

In addition to the running results, final variable and constraint values are presented in the optimizers derivative utility. Whether or not the optimizer has upheld the constraints is the most important factor along with the resulting objective function value. If constraints have been badly violated, the objective value should be discarded.

Chapter 3 NGL Extraction Processes

3.1 Upstream NGL Extraction

3.1.1 Turbo-expander Process

The Turbo-expander process is an upstream NGL extraction unit. There are a number of process configurations based on utilizing expansion to refrigerate the gas stream. The one used in this study is based on the first turbo-expander process patent which was issued to Bucklin in 1966 [11]. Instead of utilizing this exact patented version of the turbo-expander process, a similar process model from previous work has been used [12]. An illustration of the process is shown in Figure 3.1.

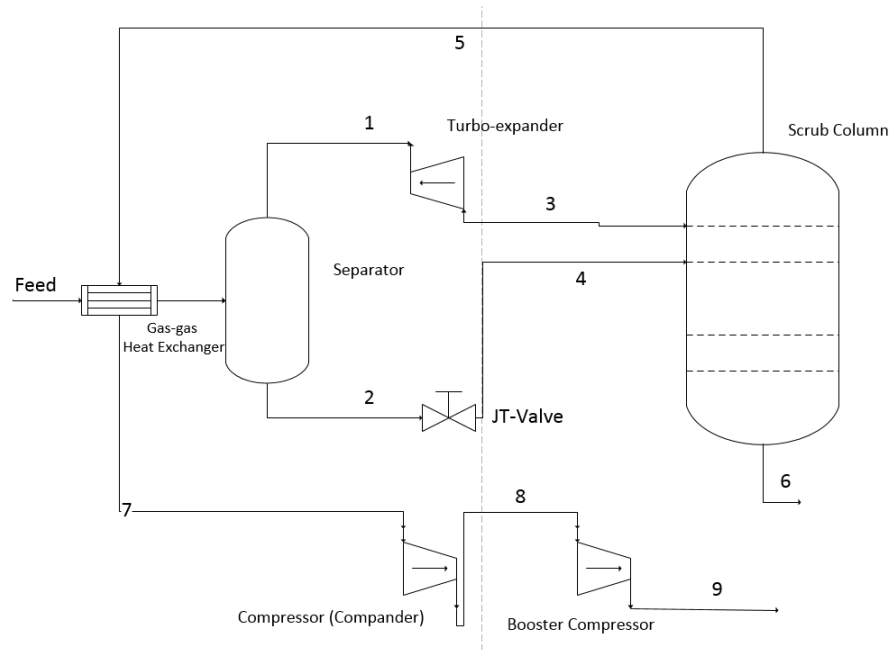


Figure 3.1: Turbo-expander process scheme

Feed gas enters the gas-gas heat exchanger, and is cooled down to a temperature limited by the minimum approach in the exchanger. From here it enters a separation column, which separates the stream into two phases; a vapour and liquid phase. The vapour phase (1) is isentropically expanded through a turbo-expander, reducing its temperature

and pressure. The pressure level after expansion is decided depending on the operational pressure of the scrub column. The pressure of the stream has to be low enough to result in a sufficiently low temperature for the wanted NGL extraction to take place. The liquid phase (2) is isenthalpically expanded through a JT-valve with the same expansion ratio as the vapour stream. The temperature reduction over the JT-valve is slightly lower than over the turbo-expander. A lower temperature is achieved in isentropic expansion due to work being taken out of the system from the turbo-expander.

The vapour and liquid streams enter the scrub column at the top stage. The bottom product (6), NGL, can either be further fractionated into separate products or can be sold as is. The top product (5) is a leaner gas stream, no longer containing heavy components. This stream's cold duty is used to chill the feed gas stream. The turbo-expander is linked to a compressor, known as a compander. The expansion power from the turbo-expander can therefore be used to re-compress the lean gas stream. This helps increase the plants overall efficiency. It is normal to add an additional compressor to boost the pressure of the stream, as a higher pressure could reduce the compression power needed in the liquefaction process. The stream is cooled and enters the liquefaction process.

3.1.2 Fluor Process

A process configuration for upstream NGL removal was introduced by Mak on behalf of Fluor Technologies Corporation in US Patent No. 20140060114. This patented scheme removes the need for additional external refrigeration in the scrub column, as well as utilizing its own residue gas stream for re-boiling in the fractionation column. Figure 3.2 is taken from the above mentioned patent and will, in this paper, be referred to as the Fluor process. Other figures in the patent are illustrations of previously known configurations, and are used as a basis for this configuration. Table 3.1 informs about the main equipment shown in Figure 3.2.

The feed gas is cooled at high pressure resulting in partial condensation. Vapour and liquid phases are then separated in separator 53, with the liquid phase (5) being expanded to a lower pressure to provide cooling for the feed gas. The liquid stream is further fed to the lower part of the scrub column (59).

The vapour phase from the separator is expanded through a turbo-expander (55). From here, stream 8 enters another separator, which is not illustrated in Figure 3.2, but described

Number	Equipment
52	Coil-wound Heat Exchanger
53	Separator
54	JT-valve
55	Expander in Compander
56	Compressor in Compander
57	Booster Compressor
58	Cooler
59	Scrub Column
62	Reboiler
63	Compressor
70	Absorber

Table 3.1: Equipment in Figure 3.2

on ships, barges, or on an offshore platform where space is at a premium. It is mentioned that both equipment size and number is reduced to a minimum [14]. The configuration is shown in the mentioned patent and as Figure 3.3, along with major equipment in Table 3.2.

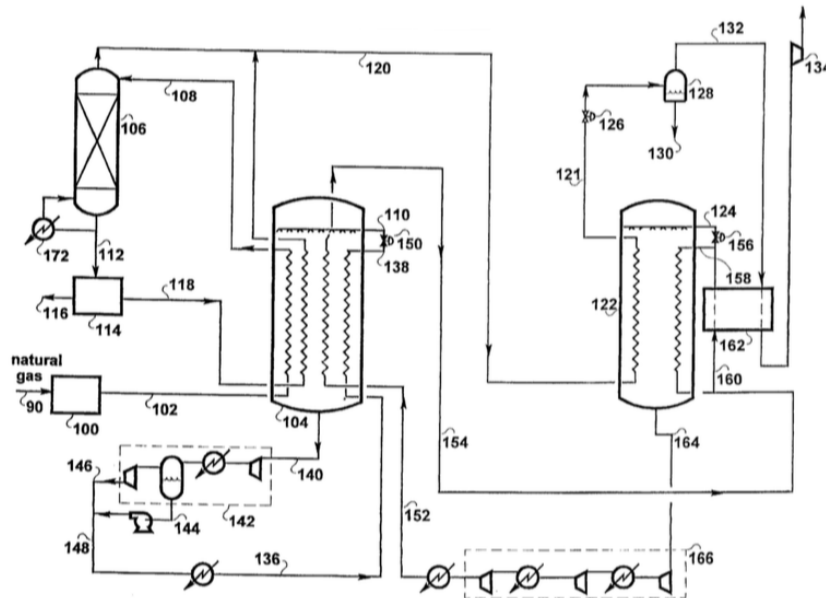


Figure 3.3: APCI process scheme [14]

Number	Equipment
100	Cooler
104	Coil-wound Heat Exchanger
106	Scrub Column
114	NGL fractionation unit
122	Coil-wound Heat Exchanger
128	Storage Tank
142	WMR compression train
162	Heat Exchanger
166	CMR compression train
172	Reboiler

Table 3.2: Equipment in Figure 3.3

Natural gas is dried and cleaned in the pre-treatment section (100) before entering the coil-wound heat exchanger 104. The feed gas, still containing HHC, is cooled to an intermediate temperature depending on feed composition and desired LNG product specifications. The cooled feed stream is directed to the scrub column (106) for removal of hydrocarbons heavier than methane. The bottom product from this column is sent to the fractionation unit (114), where pentane and heavier components (C5+) are recovered (116). Butane and lighter components (118) are cooled in the warm mixed refrigerant (WMR) coil-wound heat exchanger (104), and added to the overhead product (120) from the scrub column (106). The mixed stream is further cooled and liquefied in cold mixed refrigerant (CMR) coil-wound heat exchanger (122) to form the end product of LNG.

3.2.2 Shell Process

A process configuration for integrated NGL removal was introduced by Grootjans, Nagelvoort and Vink on behalf of Shell Oil Company. The configuration is shown and described in US Patent No. 6370910B1. The scheme aims towards lowering the temperature at the cold end of the auxiliary heat exchanger (97), so that the amount of cooling duty needed to liquefy the stream enriched in methane is reduced [15]. Figure 3.4 shows an illustration of the patented scheme, and Table 3.3 refers to the major equipment.

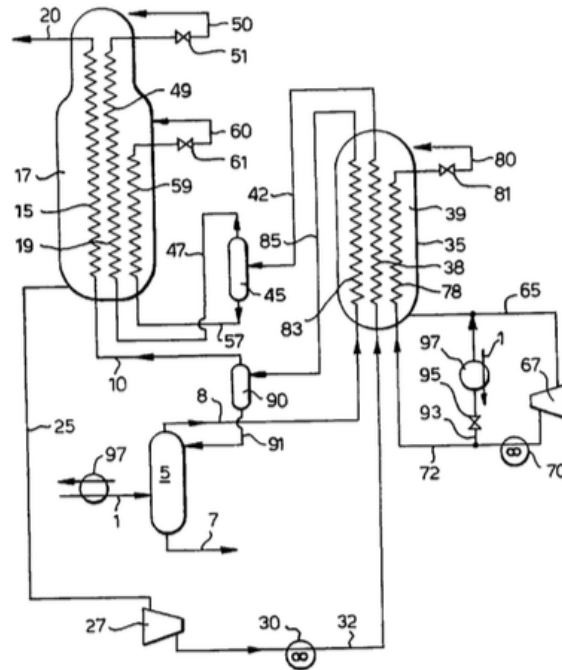


Figure 3.4: Shell process scheme [15]

Number	Equipment
5	Scrub Column
17	Coil-wound Heat Exchanger
27	CMR compression train
30	Cooler
39	Coil-wound Heat Exchanger
45	Separator
67	WMR compression train
70	Cooler
90	Condensor
97	Auxiliary Heat exchanger

Table 3.3: Equipment in Figure 3.3

Feed gas is pre-cooled by the auxiliary heat exchanger (97) and supplied at an elevated pressure to the scrub column (5), where hydrocarbons heavier than methane are removed. The method of pre-cooling comes from a bleed stream from the WMR stream 72. As seen in Figure 3.4, the WMR stream is split before entering the WMR CWHE (39). The

pressure of the bleed stream is reduced through a JT-valve, reducing its temperature so that it can cool the natural gas feed. The pressure is set equivalent to the pressure of the WMR prior to the first compression stage.

In the scrub column (5), the HHC's are withdrawn from the bottom and sent to the NGL fractionation unit. The gaseous stream (8), which now has a higher methane concentration than the feed stream, is withdrawn from the top of the column. This stream is partly condensed through the WMR CWHE (39), and separated (90) to form a vapour and condensate stream. The vapour stream (57), now containing an even higher methane concentration is sent to the liquefaction and sub-cooling unit (17). The cooled condensate stream (91) is returned to the scrub column (5) as reflux.

Chapter 4 Design Basis

A good design basis is essential when comparing and evaluating different process schemes. The main step towards achieving this is to assess the details of the simulation for each process scheme. Since each NGL extraction scheme introduced in Chapter 3 utilizes different equipment, both in number, size and price, it may prove hard to have an equal comparison [16].

Optimization of certain variables in each NGL extraction process improve the possibilities to having an equal comparison. The objective function of each model can be improved by altering the variables that impact it. On the other hand, one wants to keep specifications that do not affect the objective function fixed. This way the advantages of one model as compared to another can be identified, and a more authentic comparison made.

This chapter will present the process specifications that are kept fixed for all the NGL extraction process schemes. Only the most necessary parameters are included. Some of the fixed parameters presented in this chapter may be advantageous in certain processes. The benefits in form of an improved objective function because of them are assumed to be low compared to the optimization variables presented in Chapter 5.

4.1 Feed Gas

The feed stream is a dry and sour free gas, which has been pre-treated in acid gas removal and dehydration units. Its composition and properties, which are used in the HYSYS simulator, are shown in Tables 4.1 and 4.2. The feed stream can be characterized as a medium lean stream. The feed temperature, pressure, composition and molar flow rate are set, and will be equal in all models.

Component	Mole Fraction [%]
Nitrogen	0.01
Methane	0.91
Ethane	0.049
Propane	0.017
i-Butane	0.0035
n-Butane	0.004
i-Pentane	0.0015
n-Pentane	0.0015
n-Hexane	0.0013
n-Heptane	0.001
n-Octane	0.0004
n-Nonane	0.0001
n-Decane	0.0001
Benzene	0.0003
Toluene	0.0002
m-xylene	0.0001
Total	1.0000

Table 4.1: Feed gas composition entering NGL extraction processes

Property	Value	Unit
Temperature	22	°C
Pressure	60	bar
Flow rate	35000	kgmole/hr
Vapour phase	0.9986	-
Liquid phase	0.0014	-

Table 4.2: Feed gas properties

4.2 Product

NGL extraction processes result primarily in two end products, the first being the produced LNG, and the second the extracted NGL. If desired, the extracted NGL can be further fractionated into pure components. Components such as ethane (C2), propane (C3), butane (C4), and condensate (C5+) can be separated from each other. Ethane, propane, and butane are often extracted to be used as refrigerant makeup in the refrigeration cycles, especially for FLNG operations. C5+ condensate is sold as a more valuable product than LNG to the market.

The extraction processes in this thesis will not fractionate the extracted NGL. The reason for this is that for each pure component separated, an extra fractionation column is required. The number of iterations to solve the optimization problem increases drastically for each additional column. The CPU time spent solving each optimizer evaluation will also escalate due to the increased number of iterations. Additionally, when columns are arranged in a series as they are in a fractionation train, convergence can prove to be difficult or impossible when the optimization variables are constantly changing.

The molar flow and composition of the produced NGL and LNG will vary depending on which extraction method is used. The produced LNG has a few restrictions as presented in Table 4.3. BTX represents the hydrocarbon components Benzene, Toluene, and Xylene. Due to the restrictions of the LNG product, the extracted NGL is in reality only a byproduct. A restriction has been set anyhow, allowing only a certain amount of methane in the NGL stream. This restriction operates as a column specification for column convergence.

Component	LNG	NGL	Unit
C1	-	<6	mol-%
N	<1	-	mol-%
C5+	<0.1	-	mol-%
BTX	<10	-	ppm

Table 4.3: Product specifications for LNG and NGL

4.3 Liquefaction system

The liquefaction process used in the simulations is a dual mixed refrigerant process (DMR). The model used is referred to as the AP-DMR liquefaction process. A simplified illustration of the process can be seen in Figure 4.1. Utilizing a second mixed refrigerant (MR) instead of a pure refrigerant such as propane has many advantages. The MR enables the process to deal with changes in the feed composition, seasonal ambient temperatures, and variable flow rates during the projects lifetime. The DMR has also been proven a good choice for plants operating at high capacity (above 4 MTPA), as in this project. In the case of offshore applications, flexibility of the operation is of high importance [17].

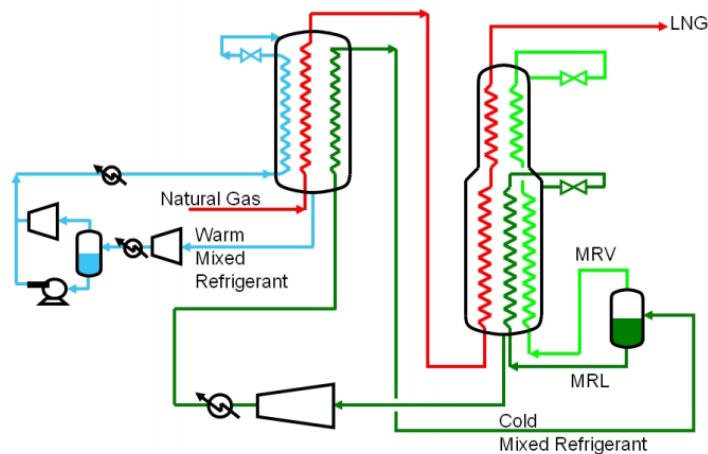


Figure 4.1: Air Products AP-DMRTM LNG process [18]

4.4 Driver solution

The driving solution of an FLNG project brings forward many restrictions, such as train capacity and compressor size. Other criteria include space and weight limitations, safety considerations, and maintenance. The trend for midsized FLNG plants is aeroderivative gas turbines. Fuel efficiency in such turbines is improved by 15-25 % compared to traditional gas turbines or steam turbines. Other reasons the aeroderivative gas turbine is preferred is smaller package and lighter weight. Parts can also easily be removed and replaced with spare parts. A disadvantage is the maximum power this type of turbine can deliver compared to industrial gas turbines [19]. The aeroderivative gas turbine GE LM

6000 is chosen as the driving solution. As shown in Figure 4.2, this turbine has a power output varying from 28-50 MW depending on the ambient air temperature.

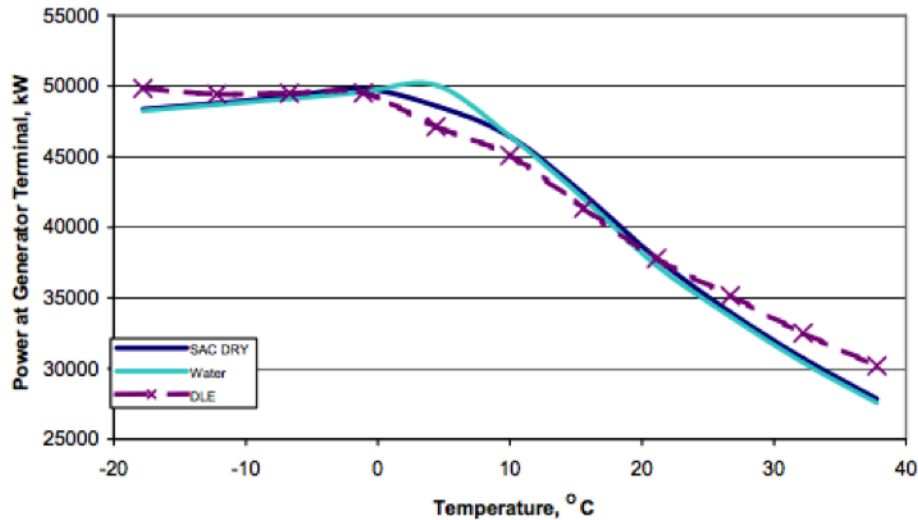


Figure 4.2: Power output of GE gas turbine LM6000

The focus is on optimizing NGL extraction schemes, and therefore no upper limit is set for the available compressor power in each process. This means that the number of gas turbines can vary from one process to another. Compression power in each MR cycle will also vary depending on the outlet temperature of the pre-cooling LNG heat exchanger. The fuel used to run the gas turbines can be assumed to come from flash gas produced at the end of the LNG liquefaction process.

4.5 Cooling system

The cooling system used is a closed loop cooling system chilled by seawater. When operating with large heat duties the most common and efficient approach is direct seawater cooling. [20] A possible cooling system is presented in Figure 4.3.

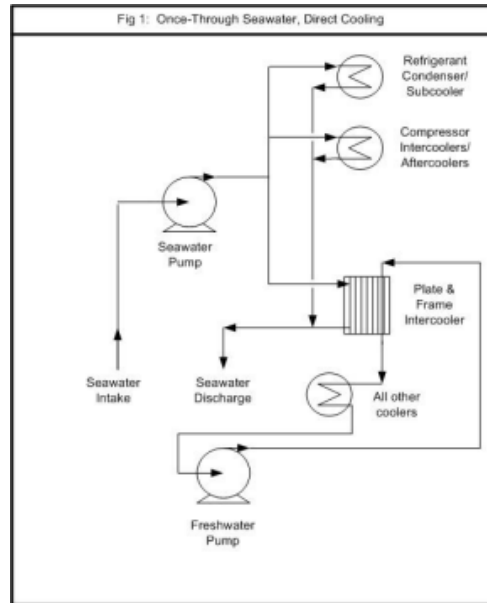


Figure 4.3: Direct sea water cooling [20]

The reason water-cooling is preferred to air-cooling is the smaller footprint required. The location of the FLNG facility is unknown, and therefore the ambient seawater temperature is also unknown. For this study it is assumed that the cooling system has a seawater temperature of 19 °C. Adding a minimum temperature approach of 3K, the cooling system can supply cooling down to 22 °C through heat exchangers. This is used as the process temperature in the models.

4.6 LNG Heat Exchanger

Coil wound heat exchangers (CWHE), are used as the equipment for pre-cooling and liquefaction of the gas. This type of exchanger is known to withstand high LNG capacity, and has great turndown capability. They are robust and can handle high thermal stresses created by high heat transfer rates. The shell enclosing the heat exchanger prevents leakage of natural gas or refrigerants to the environment [21]. The minimum temperature approach in all CWHE have been set to 3K. There is assumed no pressure drop through the heat exchangers.

Two adjustable design specifications exist for the LNG heat exchanger in HYSYS; Error Tolerance and Maximum Iterations. Regulating these can enhance the performance of

the heat exchanger in optimization work. Tightening the error tolerance of the exchanger results in significantly less derivative calculation errors in the optimizer [10]. Table 4.4 shows the default settings and the new values set for the optimization work.

Design Specifications	Default Value	New Value
Error Tolerance	0.0001	0.000001
Maximum Iterations	25	25

Table 4.4: Design specifications in HYSYS LNG heat exchanger

4.7 Turbo-machinery

The conditions used for turbines, compressors, and companders are based on previous work [22]. The values are presented in Table 4.5.

Equipment	Efficiency	
Compressor	Polytropic	78%
Expander	Polytropic	85%
Compressor in Compander	Polytropic	73%
Expander in Compander	Polytropic	83%
Pump	Adiabatic	75%
Hydraulic Turbine	Adiabatic	75%

Table 4.5: Turbomachinery efficiency parameters in HYSYS models

4.8 Column

A column is the most important equipment when dealing with NGL extraction. Two types of columns are used in the process models in Chapter 5. These are reboiled absorber columns, referred to as scrub columns, and absorber columns. The difference between the two is that bottom product in the reboiled absorber columns enter a reboiler. In the reboiler heat is added to vaporize the lighter components from the condensed natural gas and reinsert it in to the bottom of the column as boilup. This increases the separation efficiency in the column.

Adjustable solving options exist for all columns in HYSYS. The default HYSYS values and the values used are listed in Table 4.6. A decrease in the maximum number of iterations by a factor of 10 is necessary to keep the solving time of an optimization problem low. The column will more than likely find a solution, if possible, within this limit. The Error Tolerances have been tightened for the same reasons as mentioned in Section 4.6.

Design Specification	Default Value	New Value
Maximum Number of Iterations	10000	1000
Equilibrium Error Tolerance	1×10^5	1×10^6
Heat / Spec Error Tolerance	5×10^4	1×10^6

Table 4.6: Design specifications in HYSYS columns

The convergence of a column in HYSYS depends solely on the specifications of the column. It is therefore important, when setting up the derivative utility of the optimizer, that the columns variables are within values that provide column convergence. If either the upper or lower boundary are set to a value which cannot provide convergence, the optimizer will not be able to provide a result. The reason for this is that once the column has tried to solve for values which are unsolvable, the solving algorithm in the column will not be able to solve for values that can provide convergence.

4.9 Other Specifications

The plant availability is set to 330 days per year. This is a typical value for an LNG process. Adding NGL extraction to the process will reduce the number of operational days per year depending on the equipment utilized. This is due to the reliability of the equipment, with especially rotating equipment in mind. In reality, the various schemes will therefore have different plant availability, but that is not taken into account.

Parameter	Value	Unit
Plant availability	330	days per year
LNG product temperature	-157.7	°C
LNG temperature at CMR CWHE upper bundle outlet	-148	°C

Table 4.7: Other specifications

Most of stream properties considering pressure, temperature and composition are optimization variables in all processes. Only a few unavoidable specifications remain and are listed in Table 4.7. The outlet temperature of the CMR CWHE upper bundle is set to -148 °C. This value is set to achieve sufficient temperature drop through the end flash to achieve the specified LNG product temperature.

Chapter 5 Model Development and Optimization Parameters

The processes introduced in Chapter 3 have been modeled in the process simulation program Aspen HYSYS V8.6. All models are built upon the DMR liquifaction system briefly described in Section 4.3.

5.1 Liquefaction Unit

The liquefaction unit is a system consisting of two mixed refrigerant cooling cycles. The warm mixed refrigerant operates as a pre-cooling mixed refrigerant, which chills the gas to an intermediate temperature. The cold mixed refrigerant is used to liquefy and sub-cool the gas to produce the end product of LNG. A full scaled model of the process is illustrated in Figure 5.1. Subchapters 5.1.1 and 5.1.3 will explain in detail the cycle of each mixed refrigerant, its possible optimization variables and its constraints. It should be noted that the components tag names may vary for the different NGL extraction processes. The following descriptions and explanations should therefore be compared to Figure 5.1, and not to figure models in the following sections.

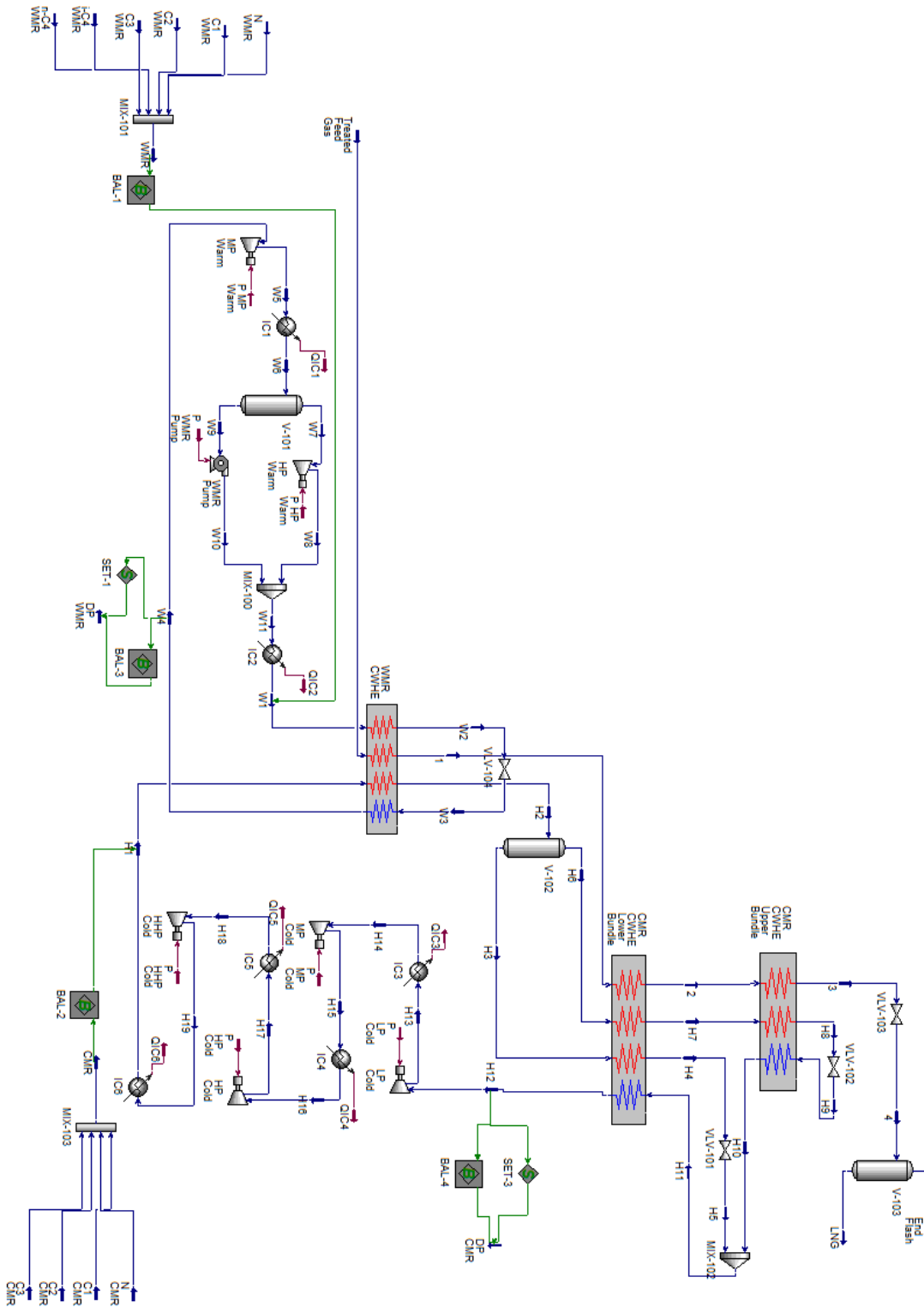


Figure 5.1: Dual mixed refrigerant liquefaction cycle

intermediate temperature (W2) by the colder counter-flowing mixed refrigerant stream W3. The temperature reduction in stream W3 comes from expansion through VLV-104. The vapour and liquid phase fraction of stream W3 will vary depending on the temperature prior to expansion, as well as the pressure decrease across the valve. W3 is evaporated through WMR CWHE supplying cooling duty to the Treated Feed Gas, the upward flowing WMR, and the CMR from the second refrigeration cycle (H1).

Stream W3 exits WMR CHWE as W4 and is controlled by a Dew Point Controller (DPC). The purpose of the DPC is to ensure that no two-phase flow exists. This is to protect compressor MP Warm from possible damage done by liquid droplets. A temperature above the dew point is therefore necessary [23]. The controller works by transferring the molar composition and pressure from W4 using a balance function (BAL-3) and a set function (SET-1). The data is imported to stream DP WMR, where a liquid fraction of 1.0 is stated. The corresponding temperature is sent to a worksheet where a temperature difference between W4 and DP WMR is set as a constraint.

Stream W4 continues through compressor MP Warm increasing its pressure to an intermediate level (W5), is cooled by cooler IC1 (W6), and enters separator V-101. The separator ensures no liquid flow enters the HP Warm compressor. Vapour exits the top of the separator (W7), and is compressed through compressor HP Warm (W8) increasing its pressure to the cycle high pressure. Liquid exits the bottom (W9) and is compressed through pump WMR Pump (W10) to the same pressure as W8. Stream W9 and W10 are mixed in MIX-100 (W11), and cooled by IC2 to a chosen process temperature. From here the cycle repeats itself.

5.1.2 Optimization Parameters WMR

The DMR liquefaction system has many changeable variables that help decrease the cycle power and increase the process efficiency. In the WMR cycle only one parameter is set constant. The process temperature of the inter-stage coolers are set to 22 °C. In other words, the temperature in streams W6 and W11 after coolers IC1 and IC2 are 22 °C. The remaining optimization variables for pressure, temperature, and molar flow are displayed in Table 5.1.

Component	Variable	Unit	Connections	Derivative Utility Tag
N WMR				N WMR
C1 WMR				C1 WMR
C2 WMR	Molar Flow	kgmole/h	Outlet: x Inlet: MIX-101	C2 WMR
C3 WMR				C3 WMR
i-C4 WMR				i-C4 WMR
n-C4 WMR				n-C4 WMR
W3	Pressure	bar	Outlet: LP Valve Inlet: WMR CWHE	LP Warm
W5	Pressure	bar	Outlet: MP Warm Inlet: IC1	MP Warm
W8/W10	Pressure	bar	Outlet: HP Warm / WMR Pump Inlet: MIX-100	HP Warm
W2/1/H2	Temperature	°C	Outlet: WMR CWHE Inlet: LP Valve / Lower Bundle CMR CWHE / V-102	Temp WMR CWHE

Table 5.1: Optimization variables in warm mixed refrigerant cycle in DMR process

The column header marked "Derivative Utility Tag" informs about the variables tag name in the derivative utility in Chapter 6. This applies to all column headers in the coming sections marked with "Derivative Utility Tag". A description of each component in Tabel 5.1 and how they influence the process follows:

N WMR, C1 WMR, C2 WMR, C3 WMR, i-C4 WMR, n-C4 WMR

These components make up the WMR stream. Varying the molar flow of each component will change the evaporation temperature of the mixed refrigerant, focusing on optimized cooling in the WMR CWHE. The components are mixed in MIX-101, resulting in a combined MR displayed as WMR in Figure 5.2.

W3:

The W3 stream defines the low pressure in the WMR refrigeration cycle. Varying the low pressure will work towards increasing the process efficiency. The pressure ratio and compressor power in MP Warm is affected by this pressure.

W5:

Outlet pressure of MP Warm compressor. The W5 stream defines the medium pressure in the WMR refrigeration cycle. Varying the medium pressure will work towards increasing the process efficiency. This pressure affects the pressure ration and compressor power in both MP Warm as well as HP Warm.

W8/W10:

Outlet pressure of HP Warm compressor and WMR Pump. The W8 and W10 streams define the high pressure in the WMR refrigeration cycle. Varying the high pressure will work towards increasing the process efficiency. The pressure ratio and compressor power in HP Warm is affected. The high pressure regulates the evaporation temperature of the components in the mixed refrigerant in the WMR CWHE.

W2/1/H2:

Outlet temperature of LNG heat exchanger WMR CWHE. In upstream NGL extraction processes stream 1 is set as the optimization variable focusing on an improved intermediate temperature before entering the second LNG heat exchanger. In integrated NGL extraction processes the temperature of stream 1 is decided considering the HHC separation in the scrub column. Streams W2 and H2 are set to have an identical temperature to the optimized stream 1.

As well as optimization variables, optimization constraints are set to constrict the process in certain ways. The constraints in the WMR cycle are few, but are necessary to uphold. Table 5.2 lists the constraints.

Component	Constraint	Unit	Value	Connections	Derivative Utility Tag
WMR CWHE	Minimum Temperature Approach	°C	3	Inlets: Treated Feed Gas, W1, H1, W3 Outlets: 1, W2, H2, W14	MinApp Upstream
W4	Temperature Approach Dew Point Controller	°C	5	Inlet: MP Warm Outlet: WMR CWHE	Dew Point WMR
W1	Liquid Fraction	%	100	Inlet: WMR CWHE Outlet: IC2	Liquid input WMR

Table 5.2: Optimization constraints in warm mixed refrigerant cycle in DMR process

The importance of upholding the constraints are explained.

WMR CWHE:

The minimum temperature approach of the coil wound heat exchanger in the warm mixed refrigerant cycle is restricted. The main factor that comes into play when selecting the minimum approach is to avoid temperature cross in the exchanger.

W4:

A constraint is required for the inlet stream of the MP Warm compressor. This is to prevent damage to the compressor from liquid droplets. Setting a temperature constraint above the dew point temperature of stream W4 prevents liquid from entering the compressor. Adding this constraint gives the WMR CWHE less working room, as it restricts the outlet temperature of the exchanger.

W1:

To avoid two phase flow of the WMR refrigerant in the WMR CWHE, a liquid fraction is set. This ensures that no vapour remains in stream W1 after intercooler IC2. This constraint results in single-phase flow in the CWHE.

5.1.3 Cold Mixed Refrigerant Cycle

The Cold Mixed Refrigerant Cycle is illustrated in Figure 5.3. The composition of the CMR stream is made up of components nitrogen (N CMR), methane (C1 CMR), ethane (C2 CMR), and propane (C3 CMR). Adding components such as i-butane and n-butane would increase the phase envelope of the mixture, meaning a higher range of temperatures containing two phase flow. The composition of the Cold Mixed Refrigerant varies based on the stream/streams that are to be cooled.

The composition of the CMR stream is connected to the Cold Mixed Refrigerant cycle stream H1 through a balance function (BAL-2). The temperature of stream H1 comes from IC6, which cools the stream to the selected process temperature. The pressure is the outlet pressure of compressor HHP Cold, which is the highest pressure of the CMR cycle. Stream H1 is cooled through LNG heat exchanger WMR CWHE, exiting as stream H2. Stream H2 is divided in separator V-102 into a vapour and liquid part. The separation of stream H2 is to separate the components which have lower boiling points and therefore the ability to be cooled extensively.

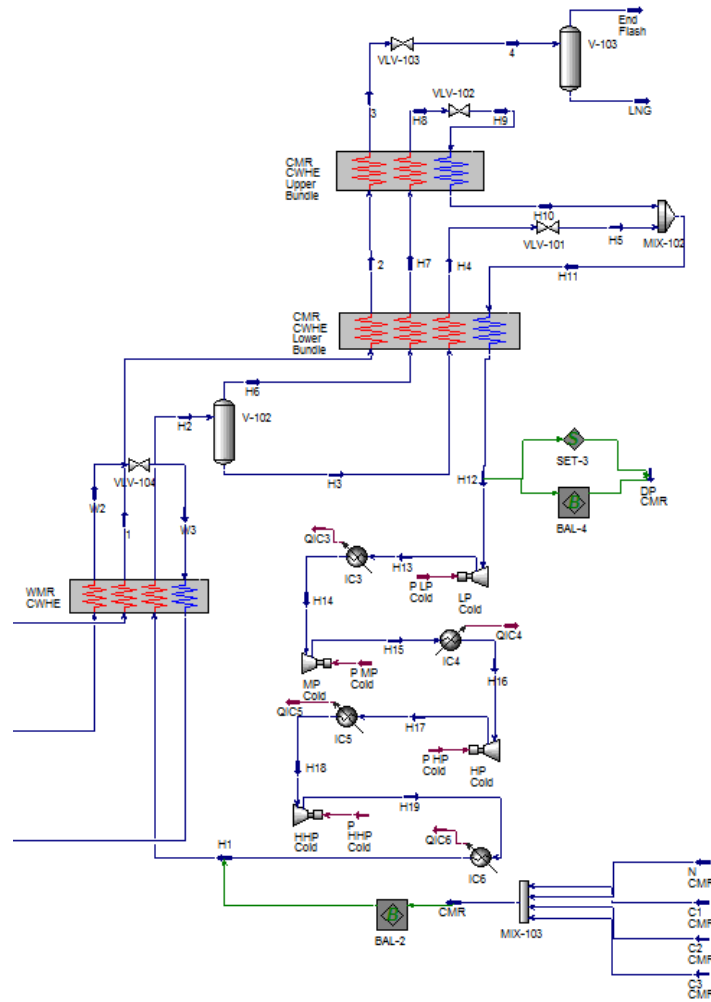


Figure 5.3: Cold mixed refrigerant cycle in DMR process

The heavier components of the CMR exit the bottom of the separator as stream H3, and are further sub-cooled through LNG heat exchanger CMR CWHE Lower Bundle. The cooling stream of the heat exchanger is explained hereafter. Stream H4 exits the heat exchanger and is expanded through valve VLV-101 to the cycle's lowest pressure. In addition to pressure reduction, stream H5 achieves a lower temperature due to isenthalpic expansion. The top products, stream H6, of separator V-102 are light components still in vapour phase. This stream is cooled through CMR CWHE and sub-cooled through LNG heat exchanger CMR CWHE Upper Bundle. Stream H8 exits the heat exchanger at a defined temperature of $-148\text{ }^{\circ}\text{C}$, is throttled in JT-valve VLV-102 to the equivalent pressure of H5, and exits as stream H9 with a lower temperature. Stream H9 enters CMR CWHE Upper Bundle and is the cooling medium of the exchanger. Stream H9 evaporates

through the exchanger, exits as stream H10, and is mixed together with stream H5. The two-phase mixed stream (H11) operates as the cooling medium for LNG heat exchanger CMR CWHE Lower Bundle. The stream evaporates and exits solely as vapour phase.

A series of four compression stages with inter-stage cooling to the process temperature follows. The pressure levels between compressors vary depending on the mixed refrigerant composition and the Feed Gas entering the DMR process. After reaching the cycle's highest pressure, the cycle repeats itself.

5.1.4 Optimization Parameters CMR

The optimization variables and constraints in the CMR cycle are very similar to the WMR cycle. In addition to the process temperature of the interstage coolers, a predefined outlet temperature of CMR CWHE Upper Bundle is set. With these two exceptions, multiple optimization variables exist in the cycle. Table 5.3 lists all the variables, followed by how they affect the cycles performance. The optimization constraints are listed in Table 5.4.

Component	Variable	Unit	Connections	Derivative Utility Tag
N CMR				N CMR
C1 CMR	Molar Flow	kgmole/h	Outlet: - Inlet: MIX-103	C1 CMR
C2 CMR				C2 CMR
C3 CMR				C3 CMR
H11	Pressure	bar	Outlet: MIX-102 Inlet: CMR CWHE Lower Bundle	LLP Cold
H13	Pressure	bar	Outlet: LP Cold Inlet: IC3	LP Cold
H15	Pressure	bar	Outlet: MP Cold Inlet: IC4	MP Cold
H17	Pressure	bar	Outlet: HP Cold Inlet: IC5	HP Cold
H19	Pressure	bar	Outlet: HHP Cold Inlet: IC6	HHP Cold

Table 5.3: Optimization variables in cold mixed refrigerant cycle in DMR process

N CMR, C1 CMR, C2 CMR, C3 CMR:

These components make up the CMR stream. Varying the molar flow of each component will change the evaporation temperature of the mixed refrigerant, focusing on optimized cooling in the CMR CWHE Lower and Upper Bundle. The components are mixed in MIX-103, resulting a a combined MR displayed as CMR in Figure 5.3.

H11:

Outlet pressure of VLV-101 and VLV-102. The outlet streams of these valves are H5 and H9. Stream H9 is evaporated through CMR CWHE Upper Bundle, exiting as H10. Streams H5 and H10 are mixed with each other to produce H11. The H11 stream defines the low pressure in the CMR refrigeration cycle. The streams pressure affects the pressure ratio and compressor power in LP Cold.

H13:

Outlet pressure of LP Cold compressor. The H13 stream defines the low-medium pressure in the CMR refrigeration cycle. The streams pressure affects the pressure ratio and compressor power in LP Cold and MP Cold.

H15:

Outlet pressure of MP Cold compressor. The H15 stream defines the medium pressure in the CMR refrigeration cycle. The streams pressure affects the pressure ratio and compressor power in MP Cold and HP Cold.

H17:

Outlet pressure of HP Cold compressor. The H17 stream defines the medium-high pressure in the CMR refrigeration cycle. The streams pressure affects the pressure ratio and compressor power in HP Cold and HHP Cold.

H19:

Outlet pressure of HHP Cold compressor. The H19 stream defines the high pressure in the CMR refrigeration cycle. The streams pressure affects the pressure ratio and compressor power in HP Cold. The high pressure also regulates the evaporation temperature of the components in the mixed refrigerant in all of the CWHE.

Component	Constraint	Unit	Value	Connections	Derivative Utility Tag
CMR CWHE Lower Bundle	Minimum Temperature Approach	°C	3	Inlet: 1, H3, H6, H11 Outlet: 2, H4, H7, H12	MinApp LB CMR CWHE
CMR CWHE Upper Bundle	Minimum Temperature Approach	°C	3	Inlet: 2, H7, H10 Outlet: 3, H8, H9	MinAPP UP CMR CWHE
H12	Temperature Approach Dew Point Controller	°C	5	Inlet: LP Cold Outlet: CMR CWHE Lower Bundle	Dew Point CMR

Table 5.4: Optimization constraints in cold mixed refrigerant cycle in DMR process

CMR CWHE Lower Bundle:

The minimum temperature approach of the CWHE Lower Bundle in the cold mixed refrigerant cycle is restricted. The same reason as for WMR CWHE applies.

CMR CWHE Upper Bundle:

The minimum temperature approach of the CWHE Upper Bundle in the cold mixed refrigerant cycle is restricted. The same reason as for WMR CWHE applies.

H12:

A constraint is required for the inlet stream of the LP Cold compressor. This is to prevent damage to the compressor from liquid droplets. Setting a temperature constraint above the dew point temperature of stream W4 prevents liquid from entering the compressor.

5.2 Turbo-expander NGL Extraction Process

The HYSYS model of upstream NGL extraction in the Turbo-expander process is illustrated in Figure 5.4. A full process model is displayed in Appendix A. Pre-treated natural gas (Feed) enters the gas-gas heat exchanger (LNG-100), is cooled and partly condensed by counter flowing stream 4. Stream 4 is the top product from the Scrub Column. The

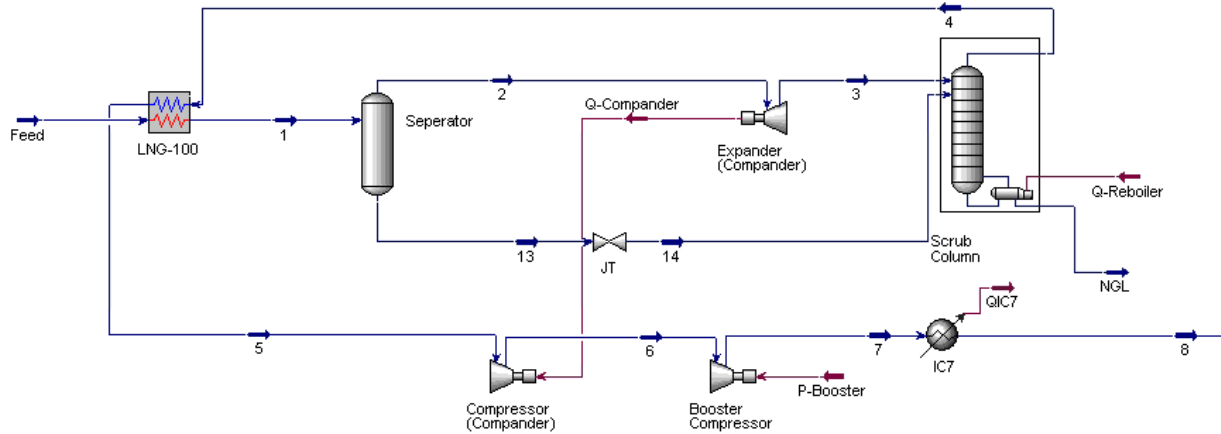


Figure 5.4: Aspen HYSYS model of Turbo-expander NGL extraction process

amount of cooling achieved in the heat exchanger is limited by the minimum approach temperature of 3K and inlet temperature of stream 4. Stream 1 exits the heat exchanger and enters the Separator. Vapour and liquid are separated into streams 2 and 13, respectively. Stream 2 is expanded through an expander to stream 3, reducing its pressure to an optimized value as well as decreasing its temperature. Alongside stream 13 is expanded through JT-Valve, decreasing its pressure equal to stream 3, and exits as stream 14. The temperature of stream 14 will be lower than that of stream 3 due to isenthalpic expansion versus an expander's isentropic expansion. The pressure is kept as high as possible, while still achieving the necessary NGL separation in the scrub column. The lower the operational pressure of the scrub column, the easier it is to achieve the wanted separation. Keeping this pressure as high as possible reduces the needed re-compression work prior to entering the liquefaction process.

Both streams (3 & 14) enter the top of the Scrub Column. The column is modelled as a reboiled absorber column, meaning no external refrigeration is supplied. Heat duty is supplied to the reboiler to achieve the wanted C1 fraction in the bottom stream. Cold lean gas leaves the top of the scrub column as stream 4, and cools the inlet feed stream as mentioned. Stream 4 exits the gas-gas heat exchanger as stream 5. It is further compressed by a compressor linked to the expander increasing its pressure and temperature. Further, the pressure is increased through a booster compressor. Increasing the pressure of the stream prior to entering the liquefaction process will reduce the cooling duty needed. The pressure of stream 7 is an optimization variable. Therefore the stream has the possibility of being reduced in pressure as well. In this case, the booster compressor will function as an expander. An inter-cooler (IC7) cools stream 7, and exits as stream 8, which is the

inlet feed stream to the DMR liquefaction process.

The bottom product of the Scrub Column exits as stream NGL. The solely liquid stream contains mostly ethane and heavier components. From here it has the option of being further fractionated into ethane, propane, butane and condensate. These components are either used as refrigerant makeup in the refrigeration cycles or sold on the market. The optimization work in Chapter 6 will not include fractionation of the NGL liquid, as this will introduce an additional 3-4 distillation columns. With each distillation column comes several thousand iterations, and excessive CPU Time.

5.2.1 Optimization Parameters Turbo-expander Process

In the Turbo-expander process an additional four variables and one constraint are added to the derivative utility. The constraint is a minimum temperature approach due to an added heat exchanger. The variables include two pressure, one temperature, and one molar fraction variable. Tables 5.5 and 5.6 have information regarding the added parameters. All possible optimizable variables and constraints from the Turbo-expander process are included in the derivative utility. In other words, no additional components have fixed values, except for components that fall under specifications explained in Chapter 4.

Component	Variable	Unit	Connections	Derivative Utility Tag
1	Temperature	°C	Outlet: LNG-100 Inlet: Separator	Temp Upstream
3 / 14	Pressure	bar	Outlet: Comander Expander / JT-Valve Inlet: Scrub Column	ScrubCol Pressure
7	Pressure	bar	Outlet: Booster Compressor Inlet: IC7	Booster Pressure
NGL	C1 Molar Fraction	%	Outlet: Scrub Column Inlet: -	C1 to NGL

Table 5.5: Optimization variables in Turbo-expander process

Description of variable components:

1:

The outlet temperature of the gas-gas heat exchanger is desired as low as possible. This is to ensure increased separation in the separator, allowing the scrub column operational pressure to be as high as possible.

3 / 14:

The scrub column inlet pressure (operational pressure) is decided by these components. The higher the pressure is kept in the scrub column, the less power is needed in the booster compressor for re-compression of the gas before entering the liquefaction process. The pressure has to be low enough to ensure upheld constraints put on the NGL stream. This pressure affects the expander duty (Q-Compander).

7:

The booster compressor can increase the pressure of the treated feed gas prior to entering the liquefaction process. The optimal pressure varies depending on the gas's composition, which affects its phase envelope, and the WMR composition. Increasing the pressure can reduce the overall compression power needed in the refrigeration cycles.

NGL:

The methane molar fraction in stream NGL gives a good indication of the separation efficiency in the scrub column. The higher the molar fraction, the lower the separation efficiency has been between methane and the heavier components. However, to obtain a low molar fraction, high reboiler duty is necessary to boil off higher quantities of methane. The methane molar fraction in the NGL stream is set as a an optimization variable to give the scrub column room to converge. A fixed variable here could hinder the column in converging.

Component	Constraint	Unit	Value	Connections	Derivative Utility Tag
LNG-100	Minimum Temperature Approach	°C	3K	Outlet: 1 / 5 Inlet: Feed / 4	MinApp Upstream
4	C5+ Molar Fraction	%	0.1	Outlet: Scrub Column	C5+ to LNG
	BTX Molar Fraction	ppm	10	Inlet: LNG-100	BTX to LNG

Table 5.6: Optimization constraints in Turbo-expander process

Description of constraint components:

LNG-100:

The LNG-100 heat exchanger cools the feed gas prior to separation. As in the other heat exchangers, it is important to uphold the minimum temperature approach to avoid temperature cross in the exchanger. This ensures sufficient heat transfer as well as a reasonable size of the exchanger.

4:

Removing components C5+ and BTX prevents freeze-out in the piping, as well as providing an economic gain.

5.3 APCI NGL Extraction Process

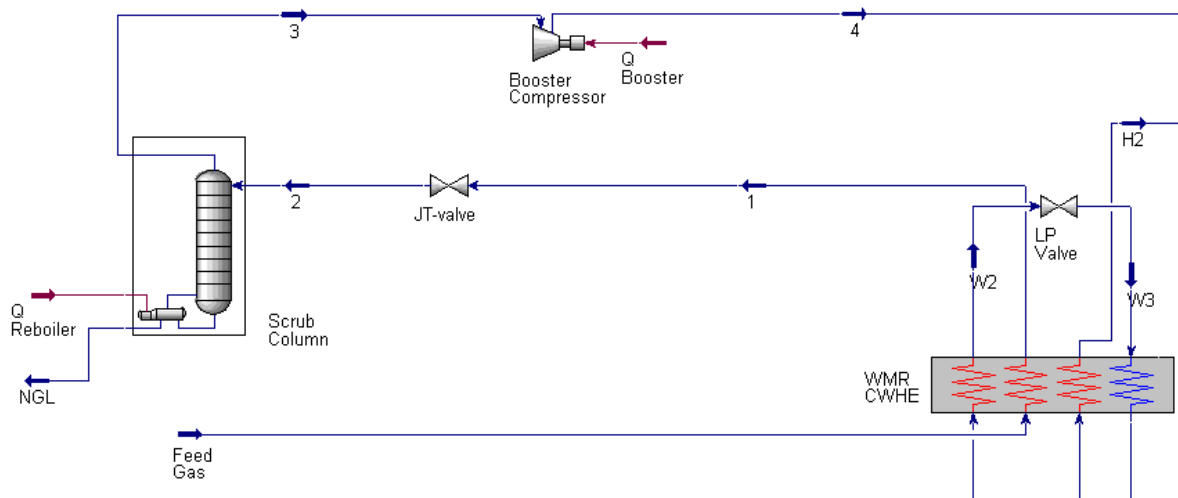


Figure 5.5: Aspen HYSYS model of APCI NGL extraction process

The HYSYS model of the integrated NGL extraction in the APCI process is illustrated in Figure 5.5. A full model process model is displayed in Appendix B. Pretreated natural gas (Feed Gas), still containing HHC, enters the WMR CWHE at a predefined temperature and pressure. The stream is partially condensed to an optimized temperature and is expanded through a JT-valve to an optimized pressure. The outlet pressure of the JT-valve has to be low enough to remove the desired amount of C5+ and BTX in the scrub column, as specified in Table 4.3. The pressure decrease will reduce the gas's temperature, supporting in the separation. Depending on the temperature decrease over the WMR

CWHE, a pressure decrease may not be necessary to achieve the requested separation. On the other hand, a pressure decrease might still be required for the column to operate properly and succeed in converging.

Stream 2 enters the scrub column at the top stage. The top product (3) of the scrub column exits as a cold lean gas, only containing a small fraction of HHC. The pressure and temperature of this stream is equal to the scrub column feed stream. Stream 3 has the option of being boosted in pressure in cases where this will decrease the objective value of the optimization. In some cases, depending on multiple other optimization variables, a reduction in pressure might be more favorable. In this case the booster compressor actually works as a turbine to decrease the pressure. The gas stream exits the compressor as stream 4 and enters the liquefaction unit.

A liquid stream (NGL) leaves the bottom of the scrub column. This stream is mostly stripped of methane, leaving its composition of ethane, propane, butane, and heavier components. The specification providing convergence in the scrub column depends solely on the molar fraction of methane. This value is set as an optimization variable. The reboiler duty in the column depends on the value of the specification. For low molar fractions of methane, higher reboiler duty is needed. For high molar fractions, lower reboiler duty is needed.

5.3.1 Optimization Parameters APCI

Component	Variable	Unit	Connections	Derivative Utility Tag
2	Pressure	bar	Outlet: JT-valve Inlet: Scrub Column	ScrubCol Pressure
4	Pressure	bar	Outlet: Booster Compressor Inlet: Lower Bundle CMR CWHE	Booster Pressure

Table 5.7: Optimization variables in APCI process

Description of variable components:

2:

The outlet pressure of the JT-valve affects separation in the scrub column. The separation

increases for decreasing pressure. The energy efficiency in the process takes advantage of high pressure in the column. This way the compressor duty in the booster compressor is reduced.

4:

The outlet pressure of the booster compressor affects the compressor power. In addition, the evaporating temperature of the components will vary depending on the pressure of the stream. This is applicable as the stream enters the liquefaction process.

Component	Constraint	Unit	Value	Connections	Derivative Utility Tag
3	C5+ Molar Fraction	%	0.1	Outlet: Scrub Column	C5+ to LNG
	BTX Molar Fraction	ppm	10	Inlet: Booster Compressor	BTX to LNG

Table 5.8: Optimization constraints in APCI process

Description of constraint components:

3:

Removing components C5+ and BTX prevents freeze-out in the piping, as well as an economical gain.

5.4 Shell NGL Extraction Process

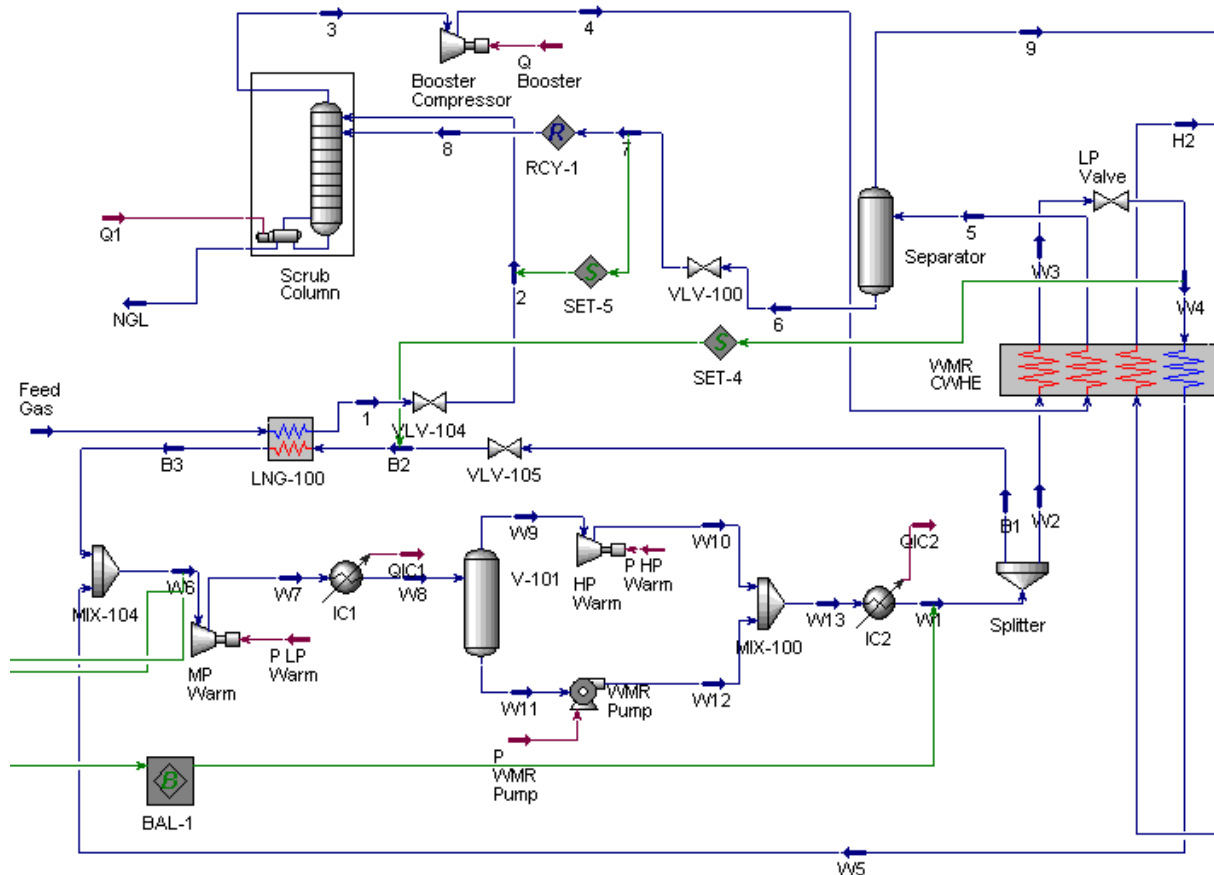


Figure 5.6: Aspen HYSYS model of Shell NGL extraction process

The HYSYS model of the integrated NGL extraction in the Shell process is illustrated in Figure 5.6. A full process model is displayed in Appendix C. In this process, the WMR refrigeration cycle is split, establishing a bleed stream (B1). The bleed stream creates a second circuit, where its task is to cool the pre-treated feed gas. Stream B1 is reduced in pressure from the WMR cycles optimized high pressure, to the optimized low pressure. The temperature of stream B2 is reduced from the process temperature of 22 °C. The feed gas is pre-cooled to an optimized temperature in an upstream heat exchanger (LNG-100), while upholding the heat exchanger’s constraint. Stream B2 exits the heat exchanger and is mixed back together with the original warm mixed refrigerant.

The pre-cooled feed gas (1) exits LNG-100, is optimized in pressure over a JT-valve (VLV-104), before it enters the top stage of the scrub column. A lean vapour stream (3) leaves the top of the column. Stream 3 is compressed to an optimized pressure level in the booster

compressor (Booster) prior to entering the WMR CWHE. It is cooled to an optimized intermediate temperature, exiting as a two-phase flow stream 5. Stream 5 enters the separator where the liquid part and vapour part are separated. The vapour part (9), now an even leaner gas than when exiting the scrub column, is further cooled and liquefied in the CMR cycle.

The liquid stream (6) exits the bottom of the separator. It is reduced in pressure to the same optimized pressure as stream 2. This is accomplished by the use of the set function SET-5, which transfers the pressure of stream 2 to stream 7. Stream 7 enters a recycle icon (RCY-1). The reason a recycle icon is needed is because the scrub column has problems converging without it during optimizer iterations. More information on the recycle icon is found in Appendix D. The stream that exits the recycle icon (8) enters the top stage of the Scrub Column.

5.4.1 Optimization Parameters Shell Process

Component	Variable	Unit	Connections	Derivative Utility Tag
1	Temperature	°C	Outlet: LNG-100 Inlet: VLV-104	LNG-100 Temp
Splitter	Flow Ratio	%	Outlet: B1 / W2 Inlet: W1	Split Ratio
2 / 7	Pressure	bar	Outlet: VLV-104 / VLV-100 Inlet: Scrub Column	ScrubCol Pressure
4	Pressure	bar	Outlet: Booster Compressor Inlet: WMR CWHE	Booster Pressure
NGL	C1 Molar Fraction	%	Outlet: Scrub Column Inlet: -	C1 to NGL

Table 5.9: Optimization variables in Shell process

Description of variable components:

1:

The outlet temperature of upstream heat exchanger, LNG-100, affects the phase of the stream. A higher amount of the stream is in liquid phase for colder temperatures. This is beneficial when entering the scrub column since part of the separation has already

been achieved. The scrub column can operate at an elevated pressure when the streams temperature is low.

Splitter:

The splitter determines how big a part of the inlet stream W1 will continue the WMR cycle through WMR CWHE. When increasing the split ratio, the molar flow of the bleed stream will lessen. To counteract the decrease in molar flow, the UA value of the upstream heat exchanger, LNG-100, needs to increase to achieve an equal amount of cooling duty.

2 / 7:

The inlet pressure of the scrub column affects the separation of HHC. Lower pressure means lower temperature, and therefore also higher separation efficiency in the column. The pressure has to be low enough to achieve the required stream specifications in Section 4.2.

4:

The booster compressor can increase the pressure of the gas prior to entering the liquefaction process. The optimal pressure varies depending on the gas's composition which affects its phase envelope. Increasing the pressure can reduce the overall compression needed in the refrigeration cycles.

NGL:

The methane molar fraction in stream NGL gives a good indication of the separation efficiency in the scrub column. The higher the molar fraction, the lower the separation efficiency has been between methane and the heavier components. However, to obtain a low molar fraction, high reboiler duty is necessary to boil off higher quantities of methane. The methane molar fraction in the NGL stream is set as a an optimization variable to give the scrub column room to converge. A fixed variable here could hinder the column in converging.

Component	Constraint	Unit	Value	Connections	Derivative Utility Tag
LNG-100	Minimum Temperature Approach	°C	3K	Outlet: 1 / 5 Inlet: Feed / 4	MinApp Upstream
3	C5+ Molar Fraction	%	0.1	Outlet: Scrub Column	C5+ to LNG
	BTX Molar Fraction	ppm	10	Inlet: Booster Compressor	BTX to LNG

Table 5.10: Optimization constraints in Shell process

Description of constraint components:

LNG-100:

The constraint in LNG-100 is set to avoid temperature cross in the upstream heat exchanger.

3:

The composition constraints in stream 3 are set to achieve the required separation in the scrub column.

5.5 Fluor NGL Extraction Process

The HYSYS model of upstream NGL extraction in the Fluor process is illustrated in Figure 5.7. A full process model is displayed in Appendix D. Pretreated natural gas (Feed) enters the upstream CWHE at 22 °C and 60 bar. The stream is cooled by multiple counter flowing streams. Stream 1 exits the heat exchanger as a two-phase flow at an optimized temperature, which satisfies the minimum temperature approach in the heat exchanger. The gas stream enters separator 1, where it is separated into a vapour stream and a liquid stream. A leaner vapour stream leaves the top of the separator as stream 5. The vapour stream is relieved in pressure over an expander to an optimized value. As well as pressure reduction, the temperature drops, making stream 6 a two-phase flow once again. From here it enters a second separator. An even leaner stream leaves the top, free of the majority of C5+ molecules. The liquid phase exits the bottom of separator 2 and enters the top of the absorber, acting as reflux. The operating pressure of the absorber

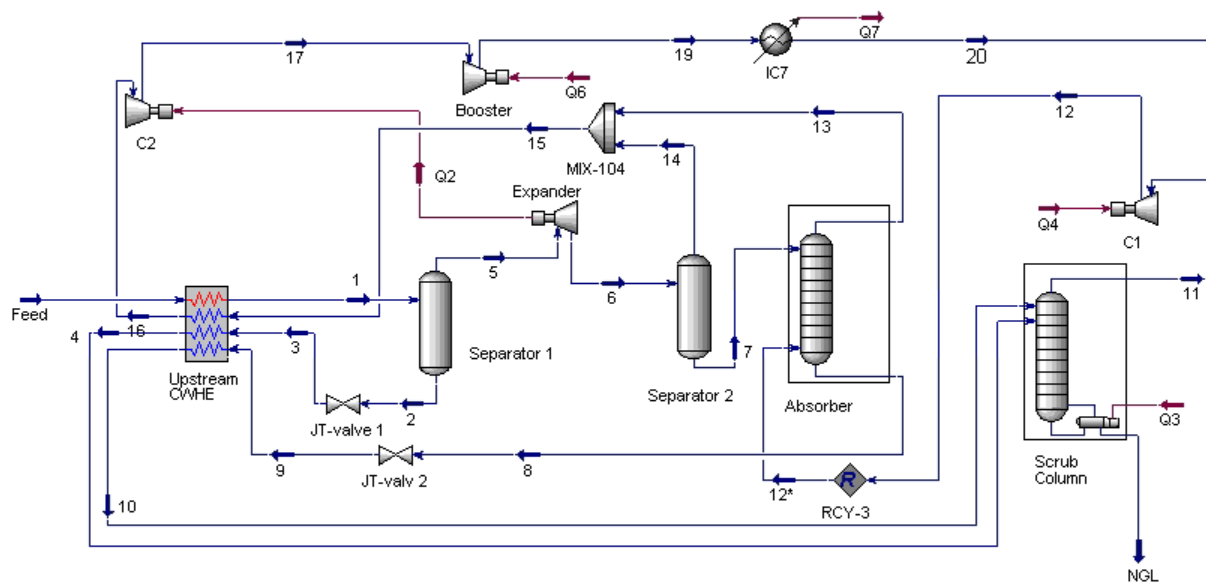


Figure 5.7: Fluor model in Aspen HYSYS

is equal to the expanded pressure of stream 6. The lean top product of the absorber and separator 2 (13 & 14) are mixed with each other, creating stream 15. Stream 15 is one of three streams that act as a cooling medium for the feed in the upstream CWHE.

A liquid stream (2) leaves the bottom of separator 1, containing both light and heavy components. The stream is expanded through JT-valve 1 to an optimized pressure. This pressure is also the operational pressure of the scrub column. Stream 3, primarily liquid, enters the upstream CWHE, also working as a cooling medium for the feed stream. Stream 3 exits the heat exchanger as stream 4, now primarily made up of vapour. From here it is directed towards the top stage of the scrub column. The third stream acting as a cooling medium for the feed gas, is the bottom product of the absorber. Stream 8 contains most of the heavy components which were not separated in separator 2. It is expanded through JT-valve 2, to the same optimized pressure as stream 3. The cooling duty provided by this stream compared to streams 3 & 15 is minimal, as the molar flow is less and the temperature is higher. Stream 10 exits the heat exchanger and is directed towards the top stage of the scrub column.

The scrub column has no need for external refrigeration due to the fact that most of the light components have already been removed in separator 1, separator 2, and the absorber. The operating pressure of the column is equal to both inlet streams (4 & 10). Only one specification value exists in the column to provide convergence. This is the molar

fraction of methane in the NGL stream. The value is set as an optimization variable in the derivative utility. NGL exits the bottom of the scrub column as a liquid stream containing mainly HHC and aromatic compounds. From here, NGL can be further fractionated in a fractionation train into pure components. The lighter components, consisting mainly of methane, exits the top of the column as a vapour stream (11). The gas is compressed in compressor C1 to the operational pressure of the absorber. Stream 12 is recycled to the bottom of the absorber to operate as a stripping gas. A recycle icon is needed to support the scrub column and absorber in convergence (explained in Appendix D).

Stream 16 exits the upstream CWHE as a warm, lean gas stream free of pentane and heavier components. First, the stream is compressed through compressor C2, provided power by the expander used to expand stream 5. The available compression power depends on the optimized pressure of stream 6. The lower the pressure of stream 6, the more power is available to re-compress stream 16. Stream 17 exits the compressor and is additionally compressed over the booster compressor to an optimized pressure level. The lean gas stream is further cooled to the system cooling temperature prior to entering the liquefaction process as stream 20.

5.5.1 Optimization Parameters Fluor Process

Component	Variable	Unit	Connections	Derivative Utility Tag
1	Temperature	°C	Outlet: Upstream CWHE Inlet: Separator 1	Temp Upstream
6 / 12 / 12*	Pressure	bar	Outlet: Expander / C1 / RCY-3 Inlet: Separator 2 / RCY-3 / Absorber	Absorber Pressure
4 / 10	Pressure	bar	Outlet: Upstream CWHE Inlet: Scrub Column	ScrubCol Pressure
NGL	Methane Molar Fraction	%	Outlet: Scrub Column Inlet: -	C1 in NGL
19	Pressure	bar	Outlet: Booster Inlet: IC7	Booster Pressure

Table 5.11: Optimization variables in Fluor process

Description of variable components:

1:

The outlet temperature of the feed gas from the coil wound heat exchanger is preferred as low as possible. This is to ensure increased separation in separators 1 & 2. Separating as much of the heavy components as early as possible will give the system the opportunity of operating the absorber and scrub column at elevated pressures, while still achieving the necessary separation of HHC. This will save power when recompressing the gas before entering the liquefaction process.

6 / 12 / 12*:

The absorber's operational pressure is decided by the pressure of the inlet streams. The separation between components in the gas stream is easier for low pressures. The pressure needs to be low enough for the necessary constraints set on stream 20, but are desired as high as possible to save process power.

4 / 10:

The scrub column's operational pressure is decided by the pressure of the inlet streams. The scrub column has two inlet streams (4 & 10). The pressure in the column should be as high as possible for the same reasons stated for the absorber.

NGL:

The methane molar fraction in stream NGL gives a good indication of the separation efficiency in the scrub column. A large portion of methane is already separated from the inlet streams (4 & 10) to the scrub column. Both inlet streams are therefore already rich in components heavier than methane, making the separation in the scrub column easier. An operational pressure as high as possible in the scrub column is desirable while still achieving a rich enough bottom product.

19:

The booster compressor can increase the pressure of the treated feed gas prior to entering the liquefaction process. The optimal pressure varies depending on the gases composition which affects its phase envelope. Increasing the pressure can reduce the overall compression needed in the refrigeration cycles.

Component	Constraint	Unit	Value	Connections	Derivative Utility Tag
Upstream CWHE	Minimum Temperature Approach	°C	3K	Outlet: 1 / 4 / 10 / 16 Inlet: Feed / 3 / 9 / 15	MinApp Upstream
20	C5+ Molar Fraction	%	0.1	Outlet: IC7 Inlet: Liquefaction	C5+ to LNG
	BTX Molar Fraction	ppm	10	Process	BTX to LNG

Table 5.12: Optimization constraints in Fluor process

Description of constraint components

Upstream CWHE:

The heat exchanger helps with cooling the feed gas prior to separation in separator 1 & 2, absorber, and scrub column. The minimum temperature approach is important to uphold to avoid temperature cross in the exchanger. This ensures sufficient heat transfer as well as a reasonable size of the exchanger.

20:

Removing components C5+ and BTX prevents freeze-out in the piping, as well as providing an economical gain.

Chapter 6 Optimization Setup And Results

The optimization interface for the four extraction processes have been configured. The interface needs to be configured prior to running the optimizer simulation. Multiple options exist in determining how the Hyprotech SQP optimizer will solve a problem. In Chapter 2 under Section 2.5.2 the optimizer flags and optimizer setup were introduced. Additionally, upper and lower bounds need to be determined for all variables and constraints in the derivative utility.

Thorough optimization work regarding the optimizer setup, explained in Chapter 2, was performed by Rødstøl in 2015 [8]. The work focused on optimization of two different liquefaction schemes, whereof one was the DMR liquefaction process. In his studies, many of the optimization setup parameters proved to obtain their best performance results with certain values. Since each extraction process studied in this thesis utilizes the DMR liquefaction process, it has been assumed that equivalent conclusions would be made. Therefore the values which were concluded in Rødstøls thesis have been included in the optimization work in this thesis.

Setup Parameter	Value
Maximum Iterations	2000
Gradient Calculations	2-sided
Accuracy Tolerance	1.00E-8
Step Restriction	1.00
Maximum Feasible Points	400

Table 6.1: Values kept constant for optimizer setup parameters in the derivative utility

The parameters were Maximum Iterations, Gradient Calculations, Accuracy Tolerance, Step Restriction, and Maximum Feasible Points. Table 6.1 shows values of the parameters which will stay constant throughout all optimizer simulation problems. Maximum Iterations and Maximum Feasible Points are set high to avoid search limitations in the optimization problem. A Step Restriction value of 1 tells the optimizer that there should not be any step restriction. Gradient Calculations are set to be 2-sided to avoid limiting the optimizer in searching for optimized values. Lastly, a low Accuracy Tolerance value

allows the optimizer to provide an as accurate as possible objective value considering the values of the other setup parameters and derivative utility values.

This leaves only two adjustable optimizer setup parameters in the Hyprotech SQP optimizer; Objective Scale Factor and Perturbation. These two parameters are altered against each other with the task of finding the best possible combination to improve the objective value, while upholding the given constraints.

The optimizer flags have to be determined as well. A total of eight flags could either be checked or unchecked. The importance of each flag and its necessity was investigated using the Turbo-expander process. It was assumed that whether or not a flag was checked or not would affect each process model in a similar way as they were all built in HYSYS under the same circumstances. The upstream Turbo-expander process is therefore explored first, to determine the flag setup for all simulations. The processes are thereafter studied by increasing complexity. Firstly the APCI process was studied, followed by the Shell process, and lastly the Fluor process.

A common objective function is used for all simulations of the process models. The objective was to minimize the total amount of compressor power needed to process the feed gas stream relative to the amount of produced LNG and NGL. Total compressor power is distributed between compressors in the WMR cycle, CMR cycle, and NGL extraction scheme. All extraction processes have the same number of compressors in the WMR and CMR cycles. Compressors in the specific extraction process may vary. The objective function can be seen in Equation 6.1.

$$\min f(x) = \frac{W_{Compressors}}{\dot{m}_{LNG} + \dot{m}_{NGL}} \quad (6.1)$$

where:

f = objective function [kWh/ton]

W = compressor power [kW]

\dot{m} = mass flow [ton/h]

6.1 Turbo-expander

6.1.1 Derivative Utility

The derivative utility is the first part of the optimizer that needs to be configured. The upper and lower bounds for variables are chosen. Additionally, the minimum and maximum values for constraints are determined. The boundaries in the process are set based on the assumed range needed to allow the optimizer a big enough area to search for a solution. Using knowledge obtained by multiple simulations, the variable boundaries presented in Table 6.2 were decided. During testing, it was found that when the search range for multiple variables was set too high, the optimizer was not able to run. In these cases the optimizer presented a termination reason displaying "Unbounded". If this occurred, upper and lower bounds for variables with big ranges had to be tightened. Still, the optimizer needs variable boundary ranges to be broad enough to allow an effective search for a good objective function value.

The start value of each variable in the process is based on values achieved in earlier work [3]. It is advantageous for the optimizer to have start values that uphold the given constraints in the process. Table 6.3 show the resulting start values of the process constraints. All constraints are upheld except for "Liquid input WMR". The violation of this constraint allows the WMR to enter the WMR CWHE with a small fraction of vapour.

The starting objective value with the start values from Tables 6.2 and 6.3 is 264.3 kWh/ton.

Tag Name	Variable	Unit	Lower Bound	Start Value	Upper Bound
N WMR	Molar Flow	kgmole/h	0	0	2000
C1 WMR	Molar Flow	kgmole/h	1000	9300	13000
C2 WMR	Molar Flow	kgmole/h	20000	29345	38000
C3 WMR	Molar Flow	kgmole/h	2000	6956	14000
i-C4 WMR	Molar Flow	kgmole/h	100	4139	9000
n-C4 WMR	Molar Flow	kgmole/h	100	2610	9000
N CMR	Molar Flow	kgmole/h	2000	6200	10000
C1 CMR	Molar Flow	kgmole/h	10000	16900	25000
C2 CMR	Molar Flow	kgmole/h	10000	18766	25000
C3 CMR	Molar Flow	kgmole/h	500	1722	12000
LP Warm	Pressure	bar	5	10	13
MP Warm	Pressure	bar	15	22	29
HP Warm	Pressure	bar	35	51	55
LLP Cold	Pressure	bar	2	5	8
LP Cold	Pressure	bar	8	15.5	23
MP Cold	Pressure	bar	22	38	46
HP Cold	Pressure	bar	30	45.5	52
HHP Cold	Pressure	bar	40	55.5	62
Temp WMR CWHE	Temperature	°C	-53	-48.3	-30
Temp LB CMR CWHE	Temperature	°C	-135	-125.7	-110
Temp Upstream	Temperature	°C	-40	-33	-20
ScrubCol Pressure	Pressure	bar	30	40	50
Booster Pressure	Pressure	bar	50	65	70
C1 to NGL	Molar Fraction	-	0.01	0.02	0.06

Table 6.2: Derivative utility values for variables in Turbo-expander process

Tag Name	Constraint	Unit	Minimum	Start Value	Maximum
MinApp WMR CWHE	Minimum Approach	°C	3	5.1002	-
MinApp LB CMR CWHE	Minimum Approach	°C	3	3.3946	-
MinApp UP CMR CWHE	Minimum Approach	°C	3	4.002	-
Dew Point WMR	Minimum Approach	°C	5	7.0334	-
Dew Point CMR	Minimum Approach	°C	5	6.3207	-
MinApp Upstream	Minimum Approach	°C	3	3.4191	-
C5+ to LNG	Molar Fraction	-	-	0.0002	0.0010
Liquid input WMR	Fraction	-	1	0.9967	-
BTX to LNG	Molar Fraction	ppm	-	4.4490	10

Table 6.3: Derivative utility values for constraints in Turbo-expander process

6.1.2 Optimizer Flags Study

Determining which flags to check or uncheck in the Hyprotech SQP optimizer was tested using the Turbo-expander process. The results of this test were utilized in all other processes. The flag test was performed prior to testing of the optimizer setup parameters. The purpose of the test was to find out whether or not the default flags configuration presented in Figure 2.4 is the best choice. To run a flag test, optimizer setup parameters also needed to be defined. The values in Table 6.1 were used as well as an Objective Scale Factor of 0. 0 is used because for this value the optimizer picks its own suitable objective scale factor. Only the Perturbation remained to be varied in comparison to the optimizer flags. Five perturbation values and nine flag arrangements were compared, resulting in a total of 45 tests. Table 6.4 shows the arrangement of which flags are checked and unchecked for each test. An x indicates that the flag was checked.

Flags	Test 1	Test 2	Test 3	Test 4	Test 5	Test 6	Test 7	Test 8	Test 9
Omit Tech Constraints	x								
Relax Violated Constraints	x	x							
Include Fixed Constraints	x	x	x						
Numerical Gradients	x	x	x	x					
Hyprotech SQP Calc Gradients	x	x	x	x	x	x		x	
Include Variable Scales	x	x	x	x	x	x	x		
Reset Perts	x	x	x	x	x				
Use NN for Optimization									
Use NN for Jacobian									

Table 6.4: Flag tests using the Turbo-expander process

It was mentioned in Section 2.5.2 that the flags "Use NN for Optimization" and "Use NN for Jacobian" would not be used in this optimization work. They are therefore unchecked for all tests. Otherwise the tests were done systematically with all flags checked in Test 1 and reduced gradually until no flag was checked in Test 9. The results are shown graphically in Figures 6.1 - 6.5. The orange colored line represents total constraint violations for the four heat exchangers in the process. The grey colored line represents total constraint violations for the two dew point controllers in the process. The lower the values in each category, the better the result.

Constraint violations for molar fractions and liquid fraction are not displayed for two

reasons. The first is that violations of these constraints will only affect the objective value minimally. The second is that for all tests, the violations were a maximum of one thousandth of the value of the defined constraint.

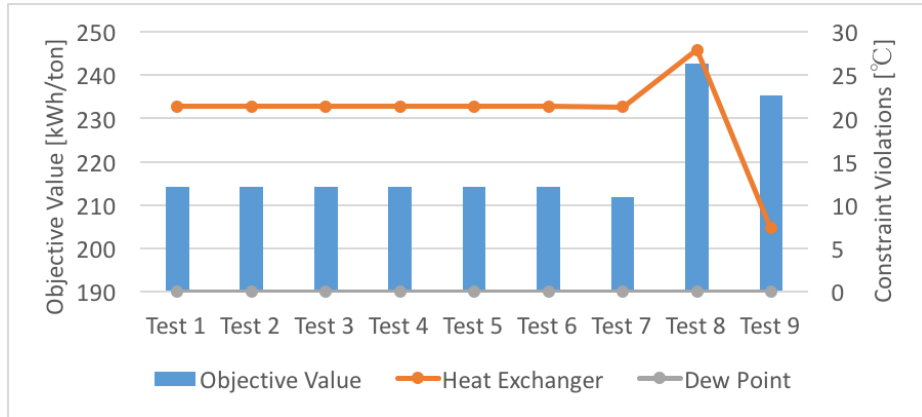


Figure 6.1: Optimizer flags test for perturbation value of 1.00E-5

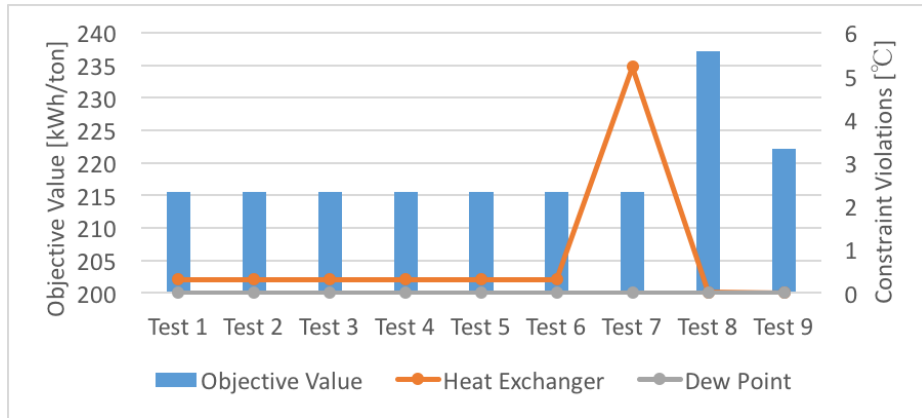


Figure 6.2: Optimizer flags test for perturbation value of 1.00E-4

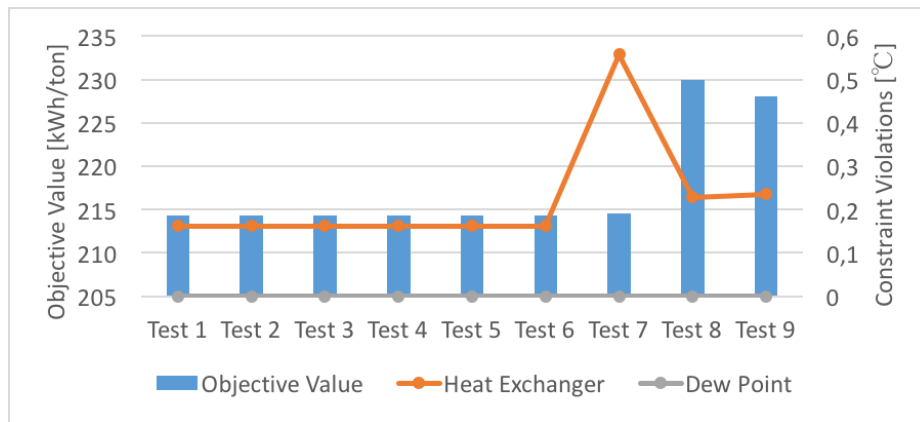


Figure 6.3: Optimizer flags test for perturbation value of 5.00E-4

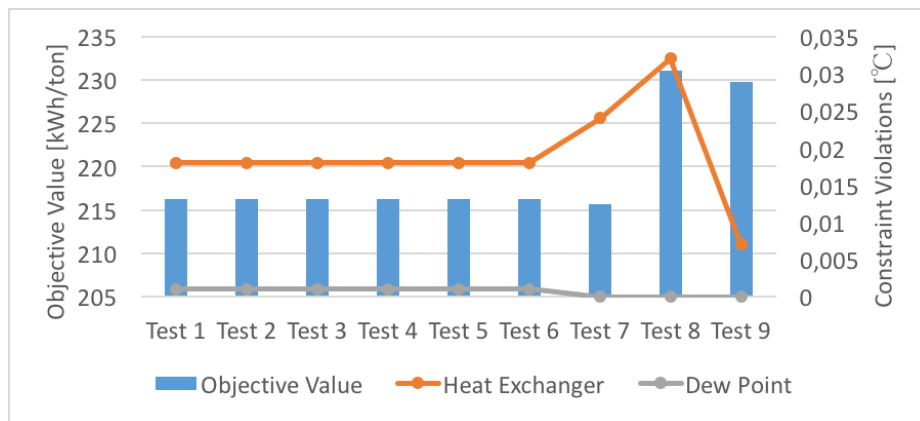


Figure 6.4: Optimizer flags test for perturbation value of 1.00E-3

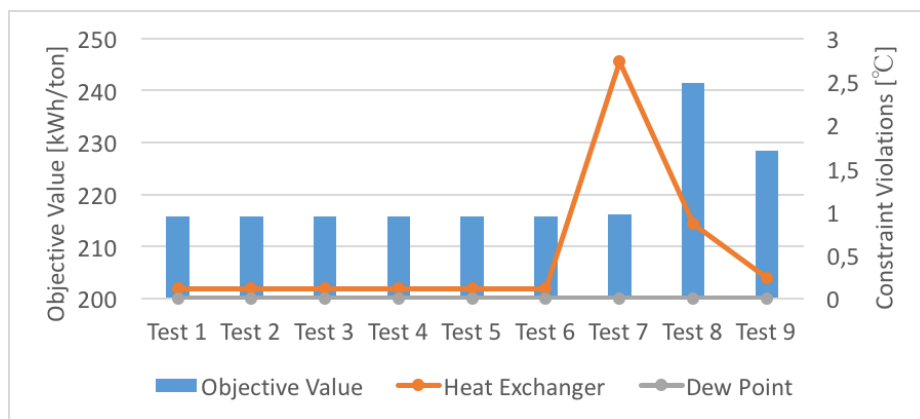


Figure 6.5: Optimizer flags test for perturbation value of 3.00E-3

Before analyzing the results, notice that the primary and secondary y-axes have different

bounds for different perturbation values. The clearest result from the graphs is that tests 1 through 6 for each perturbation value show equal outcomes. Hence, the following flags from Table 6.4 do not affect the outcome: Omit Tech Constraints, Relax Violated Constraints, Include Fixed Constraints, Numerical Gradients, and Reset Perts.

It was somewhat expected that flags Omit Tech Constraints, Relax Violated Constraints and Numerical Gradients would have no affect. The reason for this is that the information presented in Section 2.5.2 had no description of the purpose of these flags. The flag "Include Fixed Constraints" proves to have no use as none of the variables in the derivative utility have equal lower and upper bounds. None of the NGL extraction processes studied in this thesis will have equal lower upper bounds. It should be noted that if there were such variables, then this flag should be checked. The flag "Reset Perts" was supposed to remove noise elements in the process flowsheet when the optimization starts. Either the flowsheet has no noise or noise elements do not affect how the optimizer solves its problem. There could be a possibility that more noise exists in the other processes, which could affect the optimizer, but this is not expected as all processes have their bases in the DMR liquefaction process.

The two remaining flags that have an impact on the objective value and constraint violations are "Hyprotech SQP Calc Gradients" and "Include Variable Scales". In test 7 & 8 one of them is checked in each, while in test 9 none are checked. Tests 8 & 9 show a big increase in objective value compared to tests 1 - 7. No trend is evident on how tests 8 & 9 affect the heat exchanger and dew point constraint violations. Some perturbation values upheld the constraints better, while others were worse. Considering the big increase in objective value and no visible advantages for constraint violations, keeping only flag "Hyprotech SQP Calc Gradients" is not an option. On the other hand, checking only flag "Include Variable Scales" provides low objective values, but violates constraints heavily. This flag will stay checked as it was in the default flag settings.

The question comes down to whether or not flag "Hyprotech SQP Calc Gradients" should be ticked along with "Include Variable Scales". For perturbation values of $1E-5$ (Figure 6.5), constraint violations are over $5\text{ }^{\circ}\text{C}$ in all tests. Violations of this magnitude is way too high, so these values will not be evaluated further. Tests 6 & 7 for the remaining perturbation values were compared. Table 6.5 shows how keeping both remaining flags checked versus only "Include Variable Scales" affects the objective value, heat exchanger and dew point constraint violations.

Perturbation	Objective Value	Heat Exchanger	Dew Point
1.00E-04	Equal	Improved	Equal
5.00E-04	Improved	Improved	Equal
1.00E-03	Worsened	Improved	Equal
3.00E-03	Improved	Improved	Equal

Table 6.5: Comparison of how the objective value and constraint violations are affected when both "Hyprotech SQP Calc Gradients" and "Include Variable Scales" is checked versus only the latter.

The heat exchanger constraint violations were improved for all perturbation values. Improving this value means that the cooling curves in the heat exchangers are closer together, which results in reduced compressor power in the mixed refrigerant cycles. No benefits for dew point constraint violations are visible. The objective value has been improved in two out of the four cases, as well as being equal in a third. Due to the overall positive outcome, it was decided to keep both of the remaining flags, "Hyprotech SQP Calc Gradients" and "Include Variable Scales", ticked.

6.1.3 Optimizer Setup Study

In the optimizer setup study hundreds of optimization tests were executed. Perturbation and objective scale factors were tested to find out how the optimizer used these parameters in solving a simulation problem. The objective scale factor was tested for six values, starting at 0, and increasing logarithmically from 1E-3 to 10. For each objective scale factor, a number of perturbation values were tested. During the early stages of testing it was found that small changes in perturbation values often resulted in major changes to the objective value as well as constraint violations. Therefore it was decided to test a broad range of perturbation values. A total of 23 perturbation values were tested, and are displayed in Table 6.6. The perturbation values were increased with equal steps within each test section.

Test #	1 - 9	10 - 19	20 - 23
Perturbation Value	1E-5 to 9E-5	1E-4 to 9E-4	1E-3 to 5E-3

Table 6.6: Perturbation values in optimizer setup tests

During testing only a fraction of all the tests were accepted as solutions. The reason for this being that for some combinations of perturbation values and objective scale factors, the constraint violations were very high. It was decided that tests with constraint violations of more than a certain amount would be rejected. The allowable constraint violation was set to 1 % of the constraint value. The constraint rejection amounts are presented in Table 6.7.

Constraint	Value	Unit
Total Heat Exchanger Violations	0.12	°C
Dew Point CMR	0.05	°C
Dew Point WMR	0.05	°C
C5+ to LNG	0.001	mol-%
BTX to LNG	0.1	ppm
Liquid input WMR	0.99	%

Table 6.7: Constraint violations allowed before test result are rejected in Turbo-expander process.

The compositional constraints listed in Table 6.7 are constraints linked directly to the NGL extraction process. The magnitude in which they affect the objective value is small. Small variations in the compositional values will represent basically no change to the objective value. As long as these constraints are upheld, in respect to the allowed amounts, they will be accepted without the need of further analyzing in the coming sections.

The constraints that are related to temperature are all linked to a heat exchanger. The minimum temperature approach in the heat exchangers have a big impact on the objective value. Therefore, violation of these constraints can hugely improve the objective value. Closer cooling curves in the heat exchangers will lead to lower compressor power needed in the refrigeration cycles. The total violations of these constraints will therefore be analyzed against the objective value. Figures 6.6 - 6.11 show all accepted test results for the Turbo-expander process.

Termination Reason	Failure Reason
HYSYS Error	The maximum amount of RAM is reached. Aspen HYSYS is forced to quit due to low memory available.
Step Convergence	The scrub column in the process is unsolvable at provided specifications, variable boundaries, constraint boundaries, and starting values.
Stopped	A consistency error occurs in the flowsheet.

Table 6.8: Termination and failure reasons in Aspen HYSYS which did not provide simulation results in the testing of the optimizer setup.

In addition to test results being rejected due to high constraint violations, multiple tests were not able to provide results. Section 2.5.3 provided information on the termination reasons of the optimizer. Test results were not provided in cases where any of the outcomes in Table 6.8 occurred. The unsolved optimizer tests were unavoidable for the tests declaring a termination reason of "Step Convergence" or "Stopped". Otherwise, it was a shame that the test results due to a HYSYS error were not obtainable. Very often these tests seemed to develop positive results, which were forfeited due to error occurrence.

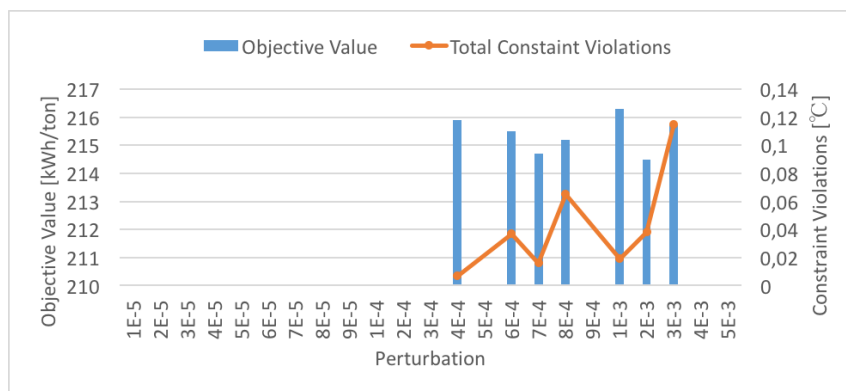


Figure 6.6: Optimizer setup test for Turbo-expander process with objective scale factor = 0

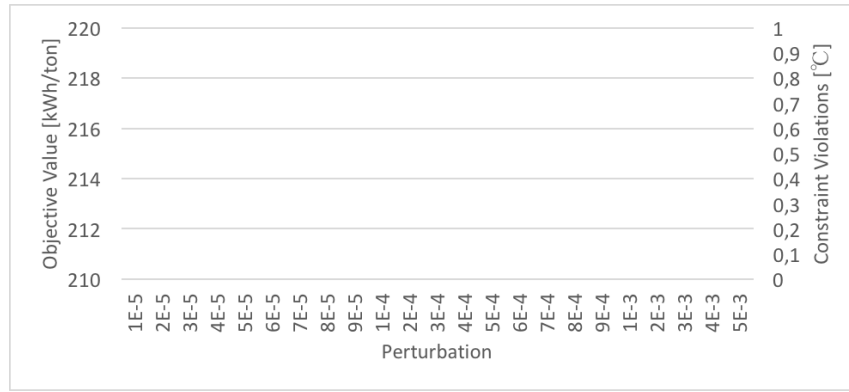


Figure 6.7: Optimizer setup test for Turbo-expander process with objective scale factor = 0.001

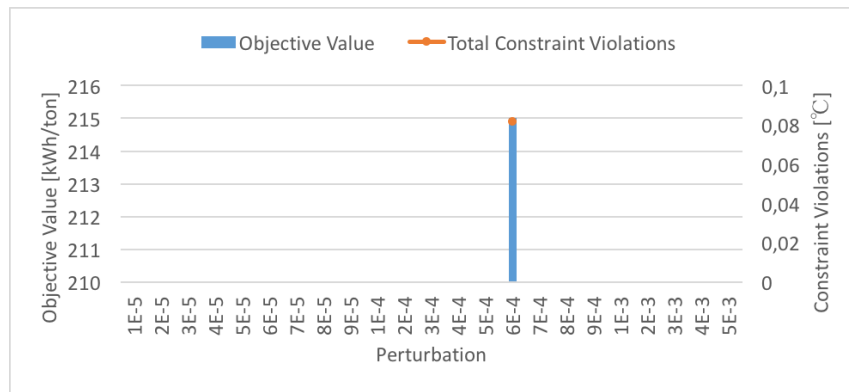


Figure 6.8: Optimizer setup test for Turbo-expander process with objective scale factor = 0.01

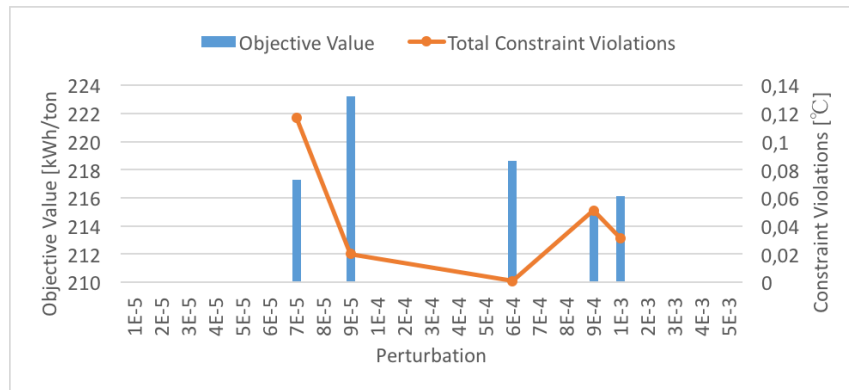


Figure 6.9: Optimizer setup test for Turbo-expander process with objective scale factor = 0.1

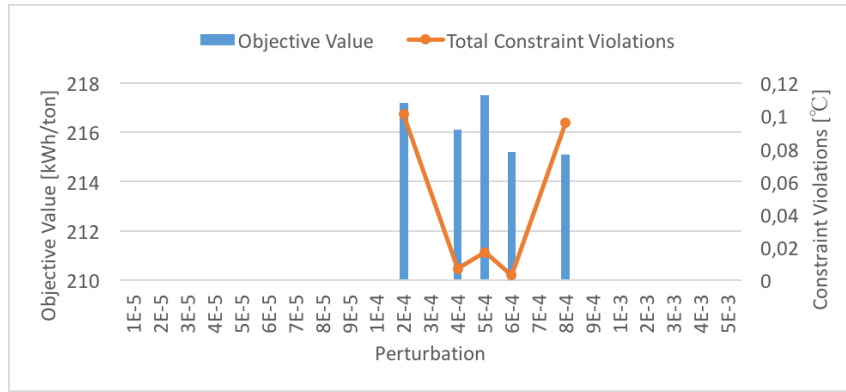


Figure 6.10: Optimizer setup test for Turbo-expander process with objective scale factor = 1

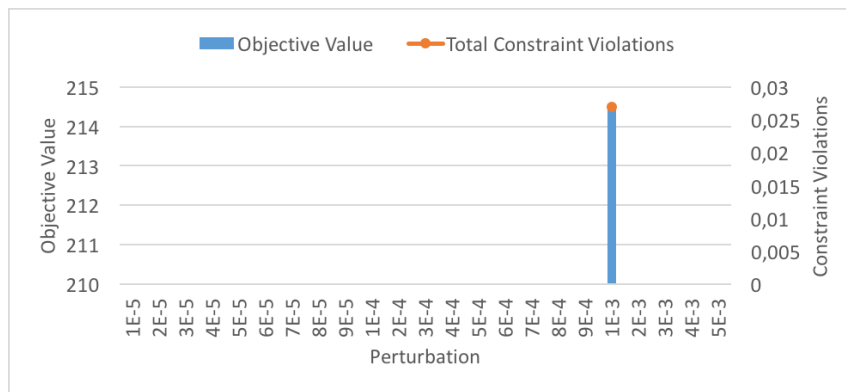


Figure 6.11: Optimizer setup test for Turbo-expander process with objective scale factor = 10

Acceptable test results were achieved for all objective scale factors except for 0.001. An objective scale factor of 0 had the most with seven acceptable results. When the optimizer has this value, it chooses its own suitable scale factor to solve the problem. However, Figure 6.6 shows that no acceptable results were found for perturbation values below 4E-4. Nonetheless, results were found for perturbation values below this when the objective scale factor was manually chosen to be 0.1 and 1. This means that although the optimizer picks a suitable value, it is not always able to find the value that gives the best possible solution.

Only one result was obtained from the two lowest objective scale factors. The result was obtained using a perturbation value of 6E-4. This perturbation value in particular proved to provide solutions in four of six scale factors tested. This is possibly the best

perturbation value to use when testing the Turbo-expander process.

The objective values obtained varied from 214.5 - 223.5 kWh/ton. Constraint violations varied from 0 - 0.12 °C (within the allowable amounts from Table 6.7).

6.1.3.1 Robustness

The optimizer was tested in different ways to see how it coped with changes to variable start values and variable boundaries. The best test results from Section 6.1.3 were included in the study. Picking the best results was done by looking at the constraint violations compared to the optima obtained. As mentioned earlier, high constraint violations in the process will support in lowering the objective value. Having this factor in mind, the focus was on obtaining a low objective value with low constraint violations. The top five out of the 19 results obtained are collected in Table 6.9. Three of the top five results had an objective scale factor of 0.

Name Tag	Objective Scale Factor	Perturbation	Objective Value	Total Constraint Violations
Test 1	0	4E-04	215.9	0.007
Test 2	0	7E-04	214.7	0.016
Test 3	0	2E-03	214.5	0.029
Test 4	1	6E-04	215.2	0.0003
Test 5	10	1E-03	214.5	0.027

Table 6.9: Top five results from optimizer setup tests in the Turbo-expander process

Altering Variable Boundaries

The derivative utility results were looked at for each of the optimizer tests in Table 6.9 to see if any variables were preventing the optimizer from searching for a better solution. Table 6.10 shows the variables that were affecting the search range and in which way they were obstructing the optimizer. Variables that were "Inactive" for all tests are not presented. The variable N WMR is listed as "Active Low" for tests 3 & 4. Since the lower boundary for this variable is 0, it can not be reduced further. Tests 2 & 3 are therefore both within the set boundaries of all the variables.

Name Tag	HP Warm	MP Cold	HHP Cold	N WMR
Test 1	Active Low	Active Low	Active Low	Inactive
Test 2	Inactive	Inactive	Inactive	Inactive
Test 3	Inactive	Inactive	Inactive	Active Low
Test 4	Active Low	Inactive	Inactive	Active Low
Test 5	Active Low	Inactive	Inactive	Inactive

Table 6.10: Status of variables in derivative utility for test results in Table 6.9 in Turbo-expander process

Otherwise, it is variable HP Warm that prevents the search region of the optimizer in the remaining tests 1, 4 & 5. The optimizer was tested once again after reducing the lower boundary value of HP Warm from 35 to 32 bar. This was the only change to the process.

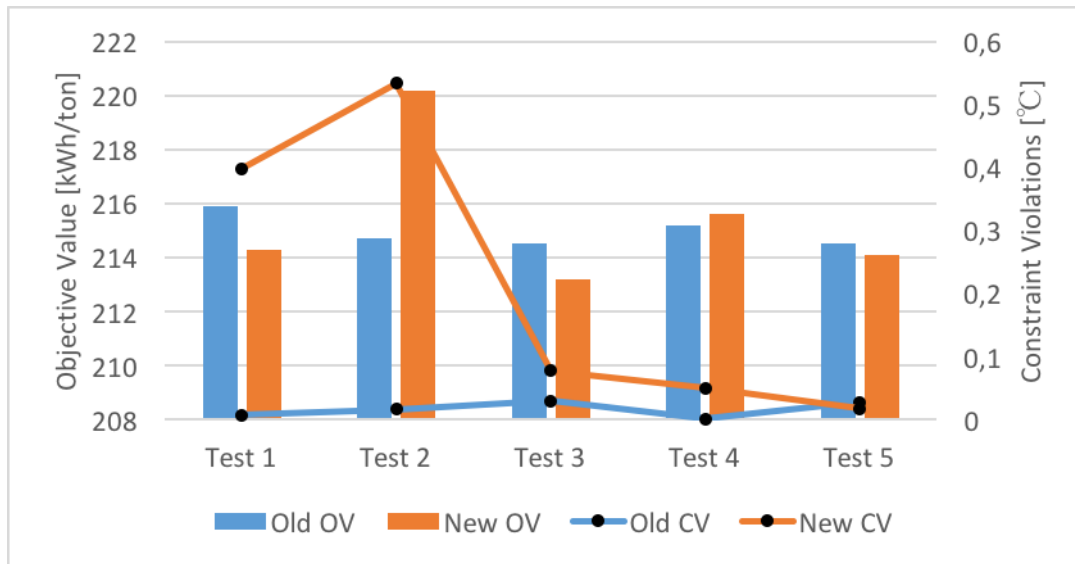


Figure 6.12: Effect of altering lower boundary value of HP Warm from 35 to 32 bar in Turbo-expander process.

Displayed in Figure 6.12 are the unexpected results of the test. OV in the figures legend stands for objective value. CV in the figures legend stands for constraint violations. By lowering the boundary, it was expected that the new objective value would result in one of two scenarios. Either the objective value would not change in the case where 35 bar was the optimal solution, or it would decrease while finding an improved high pressure value in the warm refrigeration cycle. The reason it would decrease is because a lower outlet pressure in the HP Warm compressor would reduce the compressor power in the

WMR cycle. The necessary compressor power depends on the molar flow of the warm mixed refrigerant. If the molar flow stays unchanged, a lower outlet pressure would result in lower overall compressor power and an improved objective value.

Despite expectations, the optimizer only did this in two out of the five tests. Test 5 proved to lower the objective value as well as marginally lowering the constraint violations. HP Warm's status changed from "Active Low" to "Inactive". The best objective value resulted from test 3, lowering the optima value to 213.2 kWh/ton. The constraint violations for this test increased from 0.029 to 0.077, but this still a number well within the rejection amounts stated in Table 6.7. The status of HP Warm in test 3 was still "Active Low" after decreasing the pressure to 32 bar. A further decrease could therefore result in an even better result.

The reduction of the objective value in test 1 can be looked at as a chain reaction due to an increase of constraint violations. The increase in constraint violations could be affected by the fact that variables MP Cold and HHP Cold are unchanged when having the status "Active Low". These variables were not reduced, as "Inactive" as the status in the other four tests. In a second attempt, all three variables in test 1 were reduced by three bar. The result was even bigger constraint violations as well as a higher objective value than the initial one in Table 6.9.

The fact that there are smaller changes to the optimizer result in tests 4 & 5 can have to do with the objective scale factor value. Since the optimizer picks a suitable value if the factor is set to 0, the objective scale factor will most likely change in tests 1,2, and & 4. On the other hand the fixed values in tests 4 & 5 stay the same when altering the variable boundaries. Looking closer into this, Figure 6.13 presents the new values for HP Warm in each test.



Figure 6.13: HP Warm value after reducing lower boundary Turbo-expander process

Four of the five tests found a solution using a lower HP Warm value than the original. Looking especially at tests 4 & 5 it is shown that they both found a value within the old and new lower boundary value (The value for test 5 is 32.02 bar). The new lower boundary in this variable also affected the values achieved in multiple of the other optimization variables in the process. Another look at the status of variables in the derivative utility is presented in Table 6.11.

Name Tag	HP Warm	MP Cold	HHP Cold	N WMR	N CMR
Test 1	Inactive	Inactive	Inactive	Inactive	Inactive
Test 2	Inactive	Inactive	Inactive	Active Low	Inactive
Test 3	Active Low	Inactive	Inactive	Active Low	Inactive
Test 4	Inactive	Inactive	Inactive	Inactive	Inactive
Test 5	Inactive	Inactive	Inactive	Inactive	Active Low

Table 6.11: Status of variables in derivative utility after altering variable bounds in Turbo-expander process

Test 4 has achieved a solution where all specifications in the derivative utility are "Inactive". This was expected to show that the optimizer used some type of logical solving method to find a better solution. Instead, looking back at Figure 6.12, it shows that the objective value as well as the constraint violations were worsened.

Test 5 now has an "Active Low" status for a new variable N CMR. The optimizer seemingly got an advantage in test 5 as both the constraint violation and objective value were

improved. A further decrease of variable N CMR proved to not achieve an improvement of the result in the process.

Randomly Generated Start Variables

A second experiment was done by randomly generating starting variables for the process. This was done in order to check if the starting point of the variables affected the optimizer's result. The generated variables were in between the lower and upper bounds. Accordingly, the constraints were also subjected to new start values. The randomly generated variables and constraints can be seen in Appendix H. Results of this study are presented in Figure 6.14.

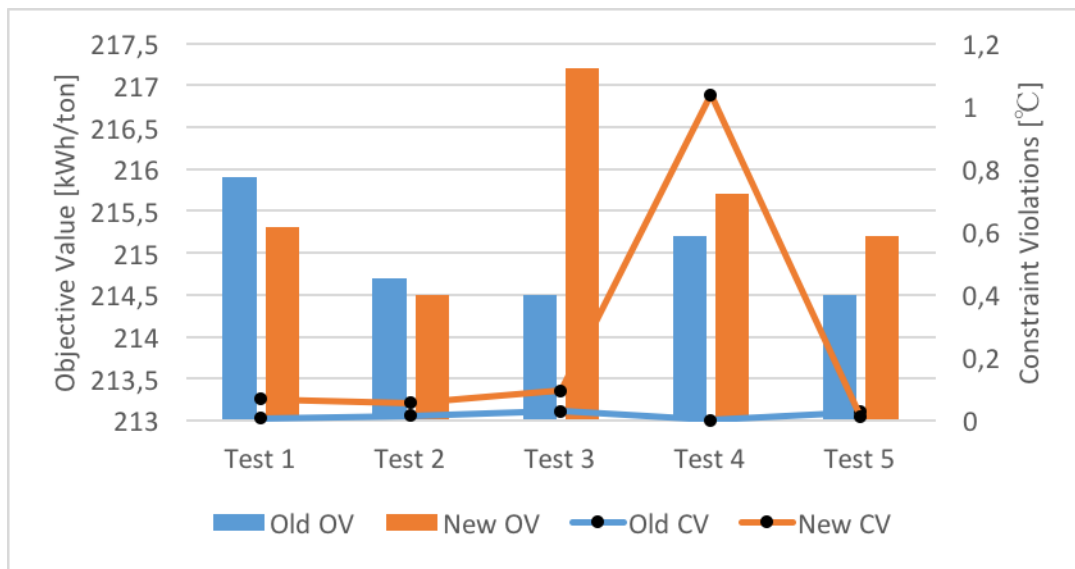


Figure 6.14: Effect of using randomly generated variable values as starting values in Turbo-expander process

The search range of the optimizer remained unchanged, making it possible for this study to result in identical values as in Table 6.9. Clearly this was not the case. In all five tests, both the objective value and the constraint violations changed. This evidently means that the start values influence the optimizer solving algorithm.

The objective value of tests 1 & 2 are reduced, with a minor increase in constraint violations. Whether or not these tests have improved or not, depends on how much the constraint violation affects the objective value. This relationship is unknown. What can be understood is that the value of the start variables barely affected the result in any way. Looking at the start variables and constraints in Appendix H it can be seen how

badly the starting point of the process flowsheet is. For example, the minimum approach temperature in CMR CWHE Upper Bundle is -174.2 °C.

Tests 3,4 & 5 result in increased objective values. The constraint violations increase slightly in test 3, severely in test 4, and improve negligibly in test 5. In this test case, the objective scale factor value of 0 seems to have played a role in the simulation result. Two of the tests with this value had minor changes in the simulation results. This could mean that it is the perturbation value in the optimizer that is a more important parameter when the flowsheet has bad initial conditions.

A downside to this study is that it is unknown how simulation tests resulting in bad results would react to initial variable changes. It is possible that some of the tests which resulted in horrendous constraint violations would perform better when drastically changing the start condition.

Best Overall Test Result

The best result in the Turbo-expander process was obtained from test 5 after altering variable bounds. This test result will be used in the process comparison in Chapter 7. The final values of variables and constraints in the test can be seen in Appendix K. Figure 6.15 shows an overview of the degree of constraint violations in this result.

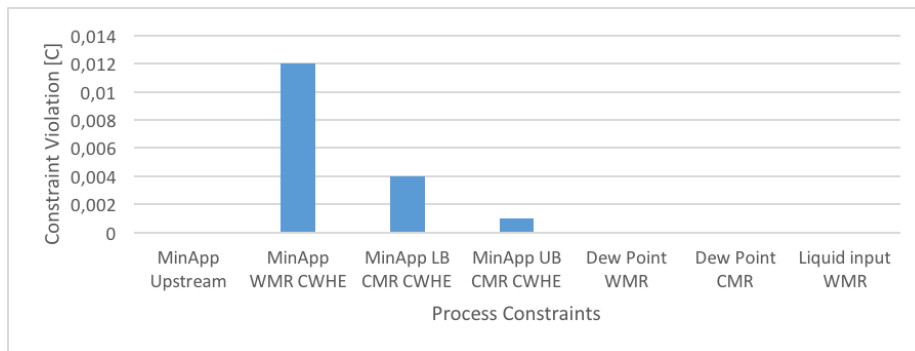


Figure 6.15: Overview of constraint violations in best test result in Turbo-expander process

6.1.3.2 CPU TIME

The time it took the optimizer to solve simulation problems varied from one test to another. It was discovered that the time the optimizer used to solve a simulation problem was comparable to the number of gradient evaluations. Results of this for all of the tests done with

the Turbo-expander process is shown in Appendix E. The graphs clearly show that the line representing gradient evaluations follow almost precisely to the columns representing CPU time. An important note to mention is that if results for certain perturbation values in graphs in Appendix E are not shown, then the result was unobtainable in accordance to reasons in Table 6.8.

The CPU time was checked for test results that were within the allowable constraint violations in Table 6.7. The average CPU time in the 19 test results was 16.1 minutes. On the other hand, the average CPU time for all tests done in the Turbo-expander process was 13.3 minutes. In this process, simulations that lasted longer produced results with less constraint violations.

Whether or not the objective value had an effect on CPU time and gradient evaluations was also investigated. The average CPU time and average gradient evaluations for each objective value was calculated. The results of the calculations are presented in Figure 6.16. Nothing stands out specifically. The value of the objective scale factor does not seem to affect the calculation time or the amount of evaluations in the simulation.

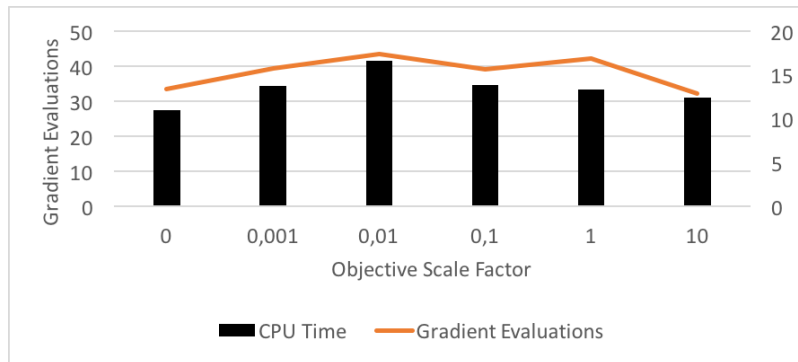


Figure 6.16: Average CPU time and gradient evaluations for simulations in Turbo-expander process

6.2 APCI

6.2.1 Derivative Utility

The starting values that have been selected for the APCI process can be seen in Table 6.12. Once again the focus has been on using starting values which uphold the constraints

to a certain degree. The starting values in the compression stages in both the warm and cold mixed refrigerant cycles are the same as in the Turbo-expander process. The exit temperature of the WMR CWHE and the CMR CWHE Lower Bundle are also matched.

The constraints obtained using the starting variables are presented in Table 6.13. The only constraint not upheld is the "Liquid input WMR", where the constraint violation is minimal.

The starting objective value with start values from Tables 6.12 and 6.13 is 267.7 kWh/ton.

Tag Name	Variable	Unit	Lower Bound	Start Value	Upper Bound
N WMR	Molar Flow	kgmole/h	0	0	2000
C1 WMR	Molar Flow	kgmole/h	1000	9747	13000
C2 WMR	Molar Flow	kgmole/h	20000	30752	38000
C3 WMR	Molar Flow	kgmole/h	2000	7290	14000
i-C4 WMR	Molar Flow	kgmole/h	100	4338	9000
n-C4 WMR	Molar Flow	kgmole/h	100	2737	9000
N CMR	Molar Flow	kgmole/h	2000	6400	10000
C1 CMR	Molar Flow	kgmole/h	10000	17456	25000
C2 CMR	Molar Flow	kgmole/h	10000	19369	25000
C3 CMR	Molar Flow	kgmole/h	500	1777	12000
LP Warm	Pressure	bar	5	10	13
MP Warm	Pressure	bar	15	22	29
HP Warm	Pressure	bar	35	51	55
LLP Cold	Pressure	bar	2	5	8
LP Cold	Pressure	bar	8	15.5	23
MP Cold	Pressure	bar	22	38	46
HP Cold	Pressure	bar	30	45.5	52
HHP Cold	Pressure	bar	40	55.5	62
Temp WMR	Temperature	°C	-53	-48.3	-30
Temp LB CMR	Temperature	°C	-135	-125.7	-110
ScrubCol Pressure	Pressure	bar	40	45	55
Booster Pressure	Pressure	bar	50	65	70
C1 to NGL	Molar Fraction	-	0.01	0.02	0.06

Table 6.12: Derivative utility values for variables in APCI process

Tag Name	Constraint	Unit	Minimum	Start Value	Maximum
MinApp WMR CWHE	Minimum Approach	°C	3	4.5212	-
MinApp LB CMR CWHE	Minimum Approach	°C	3	3.1486	-
MinApp UP CMR CWHE	Minimum Approach	°C	3	5.4329	-
Dew Point WMR	Minimum Approach	°C	5	8.5336	-
Dew Point CMR	Minimum Approach	°C	5	16.6951	-
C5+ to LNG	Molar Fraction	-	-	0.0001	0.0010
Liquid input WMR	Fraction	-	1	0.9967	-
BTX to LNG	Molar Fraction	ppm	-	3.7020	10

Table 6.13: Derivative utility values for constraints in APCI process

6.2.2 Optimizer Setup Study

The optimizer setup study for the APCI process was constructed in the same way as for the Turbo-expander process. The tests were done for perturbation values as stated in Table 6.6. Each perturbation value was simulated with six different objective scale factors. The objective scale factors were the same as in the Turbo-expander process. Once again, simulation results with high constraint violations were rejected. In this process, the allowable constraint violations for "Total Heat Exchanger Violations" is reduced. The APCI process has no upstream heat exchanger, since it uses the WMR CWHE as pre-cooling of the gas prior to separation. Because of this, one less heat exchanger exists in the process, and the allowable violation is reduced from 0.12 °C to 0.09 °C. Otherwise, the constraint violation rejection values are as stated in Table 6.7.

The simulation results for the APCI process are displayed in Figures 6.17 - 6.22. A total of 21 results were accepted.

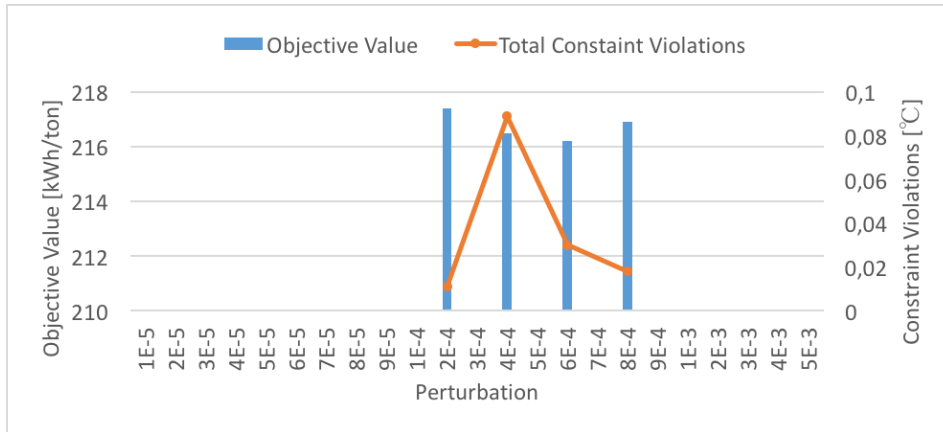


Figure 6.17: Optimizer setup test for APCI process with Objective Scale Factor = 0

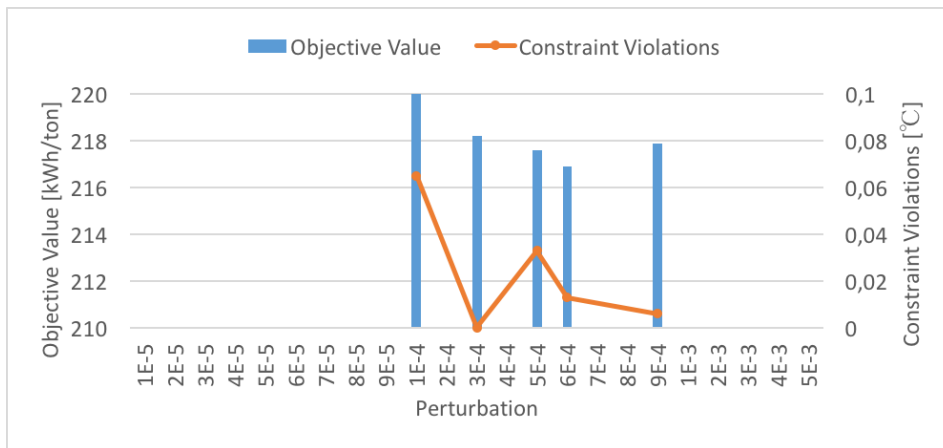


Figure 6.18: Optimizer setup test for APCI process with Objective Scale Factor = 0.001

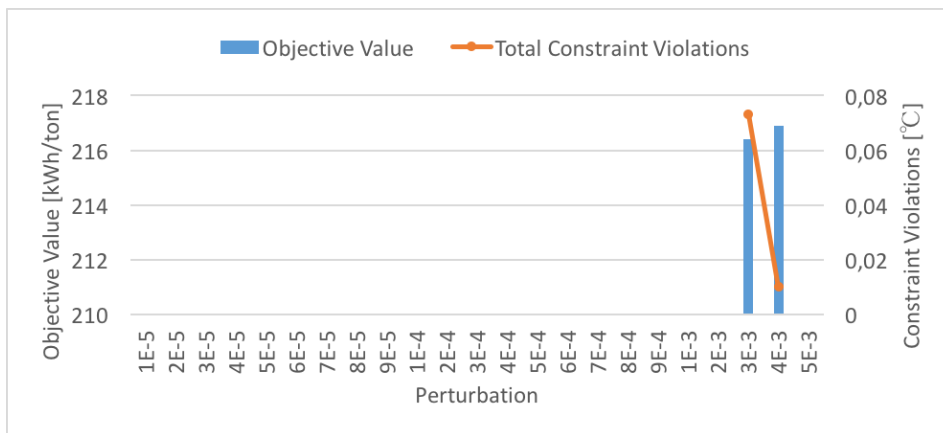


Figure 6.19: Optimizer setup test for APCI process with Objective Scale Factor = 0.01

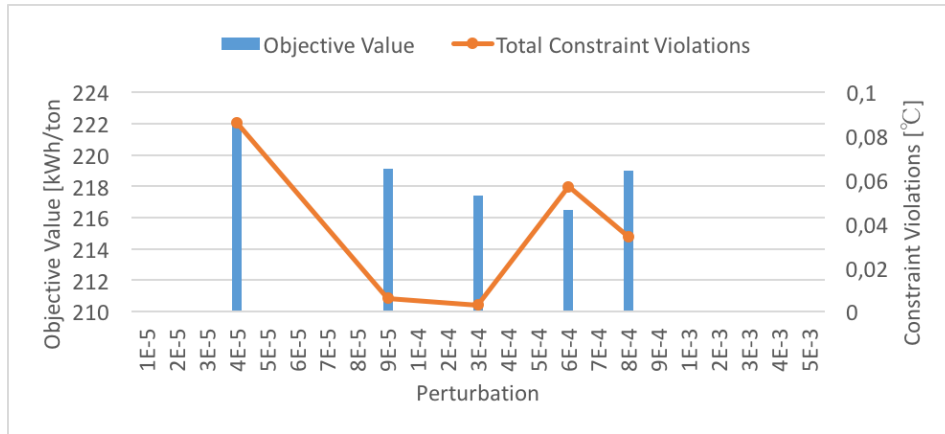


Figure 6.20: Optimizer setup test for APCI process with Objective Scale Factor = 0.1

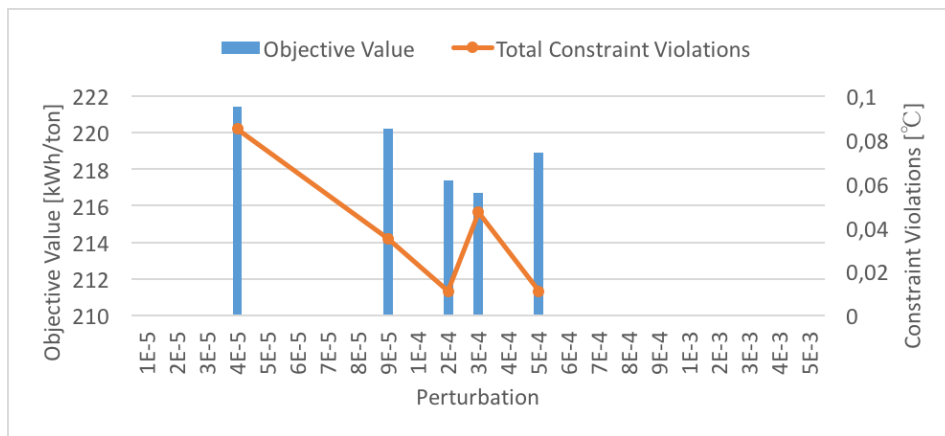


Figure 6.21: Optimizer setup test for APCI process with Objective Scale Factor = 1

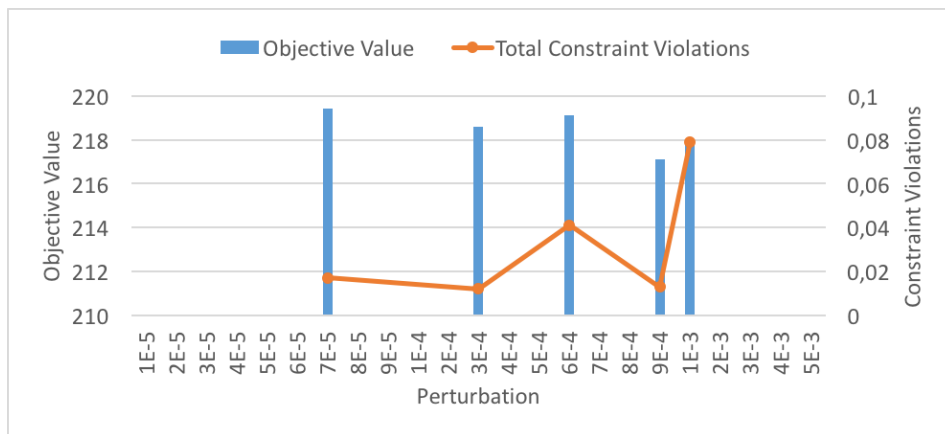


Figure 6.22: Optimizer setup test for APCI process with Objective Scale Factor = 10

In the APCI process, the value of the objective scale factor did not seem to hinder the optimizer in achieving good results. A minimum of two test results are accepted for the various objective scale factors. Perturbation values in the E-4 range produced most of the results. Once again values in the E-5 range only produced a handful of results. As mentioned in Section 2.5.2, smaller perturbation values give faster gradient calculations but with a decreased accuracy. The inaccuracy seems to be too big for good simulation results in the APCI process. All in all, the optimizer provided solutions in many simulations, meaning that it is of value in this process.

The objective values obtained varied from 216 - 222 kWh/ton. Constraint violations varied from 0 - 0.09 °C.

6.2.2.1 Robustness

The optimizer was tested in different ways to see how it coped with changes in the derivative utility. The top five results from Section 6.2.2 were used to test the robustness of the optimizer. The tests are shown in Table 6.14. Between the top five results, there were small differences in objective values and total constraint violations.

Name Tag	Objective Scale Factor	Perturbation	Objective Value	Total Constraint Violations
Test 6	0	6E-04	216.2	0.030
Test 7	0.001	6E-04	216.9	0.013
Test 8	0.01	4E-03	216.9	0.010
Test 9	0.1	3E-04	217.4	0.003
Test 10	10	9E-04	217.1	0.013

Table 6.14: Top five results from optimizer setup tests in the APCI process

Altering Variable Boundaries

The APCI process was tested with altered variable boundaries to examine changes in the results. To find which variables were hindering the optimizers search range, the derivative utility status for each variable was checked. The status of variables from test results presented in Table 6.14 are shown in Table 6.15.

Name Tag	N WMR	HP Warm	C1 to NGL	HHP Cold	N CMR	MP Cold	HP Cold
Test 6	Active Low	Active Low	Inactive	Inactive	Inactive	Inactive	Inactive
Test 7	Active Low	Inactive	Active High	Inactive	Inactive	Inactive	Inactive
Test 8	Active Low	Inactive	Active High	Inactive	Inactive	Inactive	Inactive
Test 9	Inactive	Inactive	Inactive	Active Low	Inactive	Inactive	Inactive
Test 10	Active Low	Inactive	Active Low	Inactive	Active Low	Active Low	Active Low

Table 6.15: Status of variables in derivative utility for test results in Table 6.14 in APCI process

The status of variable N WMR is "Active Low" in four out of the five tests. The lower boundary of this variable is 0, and can therefore not be reduced further. Instead, the optimizer has been tested by removing this variable from the derivative utility. The starting value of molar flow of nitrogen in the WMR cycle is kept at 0, without the possibility of increasing. By testing this, it is expected that the optimizer will find identical solutions as in Table 6.14, with the possibility of reduced CPU time. Figure 6.23 shows the result of this test compared to the original values.

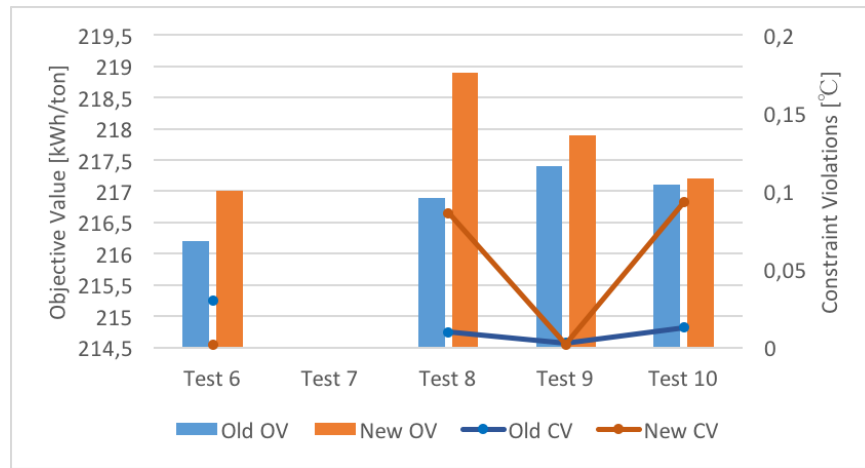


Figure 6.23: Effect of removing variable N WMR from derivative utility in APCI process

In contrast to the expectations, the objective values increased. Test 7 resulted in "Low Memory" in HYSYS, and therefore did not provide a new result. It is illogical that the optimizer was not able to provide the same results as the old ones. The optimal value for N WMR was pre-defined, relieving the optimizer in searching for other values for this component. Still, it provided increased objective values, as well as increased constraint violations in three of the four tests. The only result that has a reasonable solution is Test

6, where the objective scale factor is 0. This test presented an increased objective value, along with a decrease in constraint violations. Since these adversely affect each other, it is hard to know if the old or the new result is the better one. It is clear that removing searchable variables from the optimizers derivative utility does not help in solving the problem. This is especially true in searches where the objective scale factor is not 0.

No significant changes were noticed in the CPU Time used to solve the optimization problem. This was expected since only one variable was removed from the derivative utility. The N WMR variable was also of no importance in most of the previous test cases.

Another variable boundary test was performed. Variable boundaries for certain variables in Table 6.15 were altered. In addition to N WMR, variable C1 to NGL is not adjustable. The lower and upper boundary for C1 to NGL is 0.01 and 0.06. The product specification in Table 4.3 restricts a fraction of methane in the NGL stream of more than 0.06. The lower boundary is set to 0.01 to support the scrub column in converging. If the lower boundary value of this variable was set to 0, the column would start searching for an unfeasible solution (explained in Section 4.8). The remaining variables were altered as displayed in Table 6.16, for tests 6-10. The result of the test is shown in Figure 6.24. Note the high constraint violation values on the y-axis.

Variable	Altered Boundary	Old Value	New Value	Unit
HP Warm	Lower	35	32	bar
HHP Cold	Lower	40	37	bar
N CMR	Lower	2000	1500	Molar flow
MP Cold	Lower	22	19	bar
HP Cold	Lower	30	27	bar

Table 6.16: New variable boundaries in optimizer test for APCI process

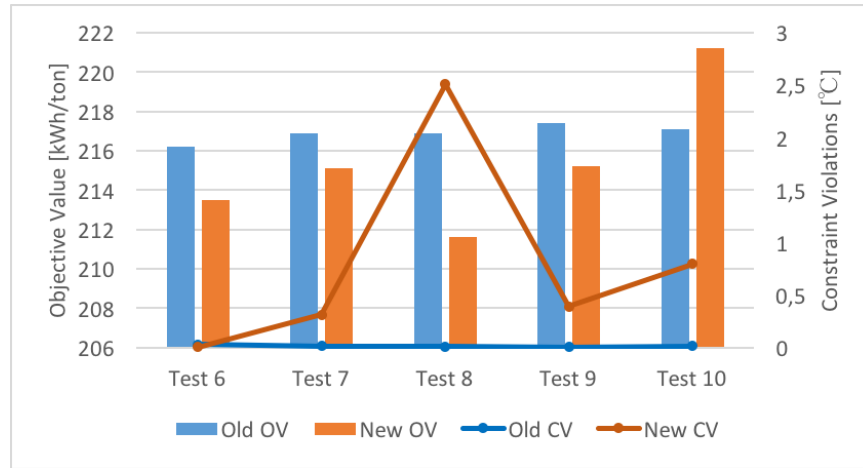


Figure 6.24: Effect of altering variable boundaries in APCI process

All boundaries altered were lower boundaries. The changes to the pressure variables were three bar, and the change to the molar flow variable was 500 kgmole/h. The changes increase the range of each variable by approximately 10-20 %. It was expected that the increase in variable range would allow the optimizer more room to search for an improved feasible solution. The hypothesis was proved wrong for all tests except for test 6.

The constraint violations in tests 7-10 increased to unacceptable values. The fact that the objective values for tests 7-9 decreased can be ignored due to the increased constraint violations. On the other hand, test 6 produced a better objective value along with improved constraint violations of only 0.006 °C. Overall, the result from test 6 was better than any prior result in the APCI process. Apparently, the optimizer takes advantage of choosing its own objective scale factor (objective scale factor = 0). The status of variables in the derivative utility after altering the variable bounds is shown in Table 6.17.

Name Tag	N WMR	HP Warm	C1 to NGL	HHP Cold	N CMR	MP Cold	HP Cold
Test 6	Inactive	Active Low	Inactive	Inactive	Inactive	Active Low	Inactive
Test 7	Inactive	Inactive	Inactive	Inactive	Inactive	Inactive	Inactive
Test 8	Inactive	Inactive	Inactive	Inactive	Inactive	Inactive	Inactive
Test 9	Inactive	Inactive	Inactive	Inactive	Inactive	Inactive	Inactive
Test 10	Active Low	Inactive	Inactive	Inactive	Inactive	Inactive	Inactive

Table 6.17: Status of variables in derivative utility after altering variable bounds in APCI process

Tests 7-10 have no variables blocking the search of the optimizer. Still, the objective values were worsened. Variables hindering test 6 increased to two. HP Warm kept its status as "Active Low" along with variable "MP Cold". In search of further improvement, these two variables were once again reduced to increase the searchable range of the optimizer. "HP Warm" was reduced to 29 bar, and "MP Cold" was reduced to 19 bar. The result was a further decrease of the objective value to 212.4 kWh/tonne, with a total constraint violation of 0.006 °C.

Randomly Generated Start Variables

The tests in Table 6.14 were simulated with randomly generated start values. The optimizer was studied to see how new start variables affected the outcome of the result. The new start values were within the upper and lower bounds stated in Table 6.12. The new start values for variables and the accompanying constraints are listed in Appendix I. Results of this study are presented in Figure 6.25.

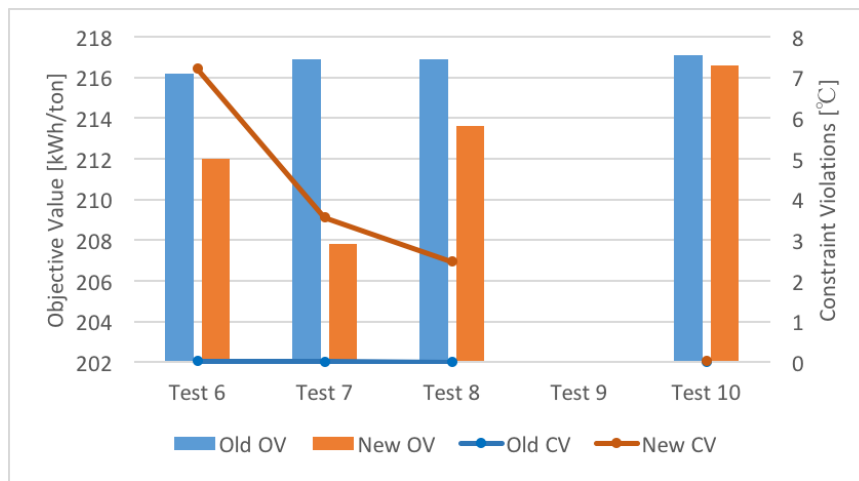


Figure 6.25: Effect of using randomly generated variable values as starting values in APCI process

Values for test 9 are not presented because the RAM cap was reached before a simulation result was found. Tests 6-8 resulted in a decrease in objective value, along with a major increase of constraint violations. Note the constraint violations are all above 3 °C. An improved result was observed in Test 10. A small decrease in objective value with equal constraint violations. The randomly generated start variables provided the optimizer with starting values that had difficulties finding solutions that upheld the constraints. This means that appropriately chosen start values helps the optimizer in upholding the

constraints. The constraint that was problematic in this case was the minimum approach in the heat exchangers. The other constraint were all upheld in respect to their tolerances.

Best Overall Test Result

The best result in the APCI process was obtained from test 6 after altering the variable bounds twice. This test result will be used in the process comparison in Chapter 7. The final values of all variables and constraints in the test can be seen in Appendix L. Figure 6.26 shows an overview of the degree of constraint violations in this result.

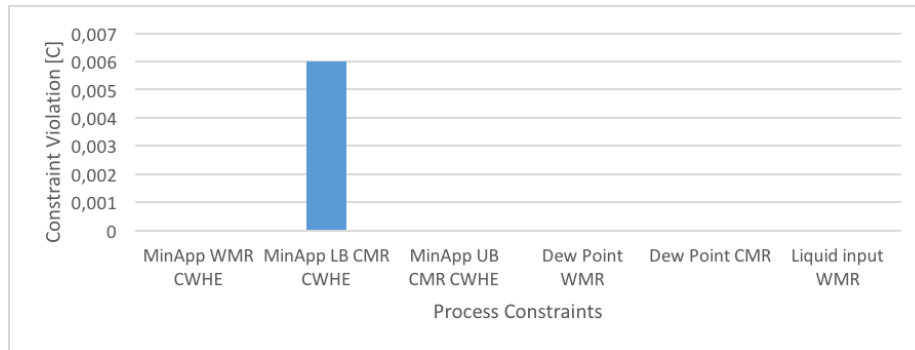


Figure 6.26: Overview of constraint violations in best test result in APCI process

6.2.2.2 CPU Time

Results of all the tests done in the APCI process are displayed in Appendix F. As in the results in the Turbo-expander process, the CPU time followed closely with the number of gradient evaluations in the simulation.

The average CPU time for test results that were within the allowable constraints was 19.3 minutes. The average CPU time for all tests done with the APCI process was 13.2 minutes. Once again, the simulations that resulted in what has been characterized as good results lasted longer than the average.

Figure 6.27 illustrates the average CPU time and gradient calculations for the different objective scale factors tested. Objective scale factors of 0 and 10 show reduced calculation time and gradient evaluations. Equal values are found for scale factors 0.001, 0.01, 0.1, and 1. This observation is compared to the earlier statement that longer simulation times result in better results

The observation does not correspond to the test results presented in Tables 6.17 - 6.22.

Objective scale values of 0.001 and 0.01 show only one accepted test result, although they use in average use the most time to solve an optimization problem. This shows that longer calculation times don't necessarily always produce good results.

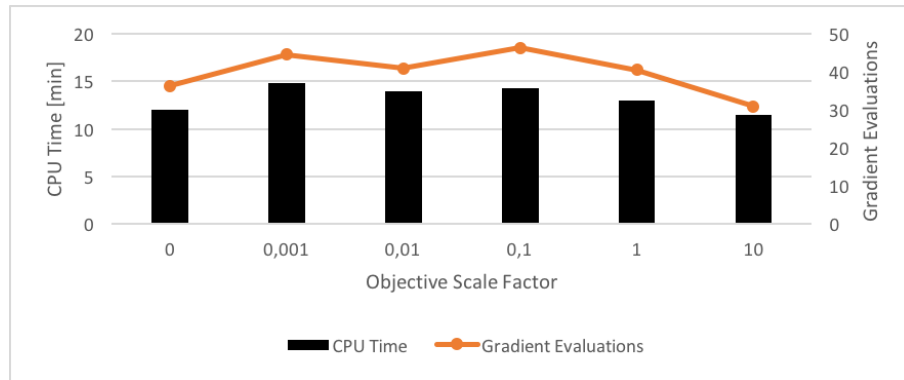


Figure 6.27: Average CPU time and gradient evaluations for simulations in APCI process

6.3 Shell

6.3.1 Derivative Utility

The start values and boundaries of variables in the Shell process are listed in Table 6.18. The variable bounds and starting values are very similar to the ones of the Turbo-expander process and the APCI process. Small changes to the starting values of the WMR and CMR compositional flow is necessary to account for slight changes in the composition of the processed gas exiting the scrub column. This is dependent on the removal efficiency of HHC in the scrub column. The values for the variables "ScrubCol Pressure" and "Booster Pressure" have also been modified. The values have been decided after finding the maximum possible operational pressure of the scrub column that achieves the required HHC removal. Values above 53 bar in the scrub column resulted in unconvergence of the column.

Tag Name	Variable	Unit	Lower Bound	Start Value	Upper Bound
N WMR	Molar Flow	kgmole/h	0	0	2000
C1 WMR	Molar Flow	kgmole/h	1000	10370	13000
C2 WMR	Molar Flow	kgmole/h	20000	32999	38000
C3 WMR	Molar Flow	kgmole/h	2000	7747	14000
i-C4 WMR	Molar Flow	kgmole/h	100	4590	9000
n-C4 WMR	Molar Flow	kgmole/h	100	2924	9000
N CMR	Molar Flow	kgmole/h	1000	6411	10000
C1 CMR	Molar Flow	kgmole/h	10000	17489	25000
C2 CMR	Molar Flow	kgmole/h	10000	19405	25000
C3 CMR	Molar Flow	kgmole/h	500	1780	12000
LP Warm	Pressure	bar	5	10	13
MP Warm	Pressure	bar	15	20.56	29
HP Warm	Pressure	bar	33	52.39	55
LLP Cold	Pressure	bar	2	5	8
LP Cold	Pressure	bar	8	15.5	23
MP Cold	Pressure	bar	22	38	46
HP Cold	Pressure	bar	30	45.5	52
HHP Cold	Pressure	bar	38	55.5	62
Temp WMR CWHE	Temperature	°C	-53	-48.3	-30
Temp LB CMR CWHE	Temperature	°C	-135	-125.7	-110
Temp Upstream	Temperature	°C	-25	-20	-15
ScrubCol Pressure	Pressure	bar	38	50	53
Split Ratio	Molar Fraction	-	0.7	0.8	1
Booster Pressure	Pressure	bar	40	59.6	70
C1 to NGL	Molar Fraction	-	0.01	0.02	0.06

Table 6.18: Derivative utility values for variables in Shell process

The accompanying initial value of constraints are shown in Table 6.19. The values here are in direct relation to the starting variable values. Notice that multiple of the constraints are violated at the starting conditions in the process. It proved to be extremely difficult to find starting values which upheld every constraint. The reason for this is the split WMR stream prior to entering the WMR CWHE. The split ratio needed to be low enough to allow enough cooling in the upstream heat exchanger, while still providing sufficient cooling in the WMR CWHE. This could affect the results in the Shell process, as it has been acknowledged that starting values play an important role in the optimizer's test results. However, the start values are expected to be good enough for the optimizer to find a solution which uphold constraints that are not already upheld.

Tag Name	Constraint	Unit	Minimum	Start Value	Maximum
MinApp WMR CWHE	Minimum Approach	°C	3	2.9922	-
MinApp LB CMR CWHE	Minimum Approach	°C	3	2.9331	-
MinApp UP CMR CWHE	Minimum Approach	°C	3	4.8085	-
Dew Point WMR	Minimum Approach	°C	5	0.3082	-
Dew Point CMR	Minimum Approach	°C	5	9.2252	-
MinApp Upstream	Minimum Approach	°C	3	4.897	-
C5+ to LNG	Molar Fraction	-	-	0.0004	0.0010
Liquid input WMR	Fraction	-	1	1	-
BTX to LNG	Molar Fraction	ppm	-	4.5980	10

Table 6.19: Derivative utility values for constraints in Shell process

The starting objective value with start values from Tables 6.18 and 6.19 is 273.6 kWh/ton.

6.3.2 Optimizer Setup Study

The results of the optimizer setup study in the Shell process are shown in Figures 6.28 - 6.33. The procedure providing the results was performed in the same way as for the Turbo-expander process as explained in Section 6.1.3.

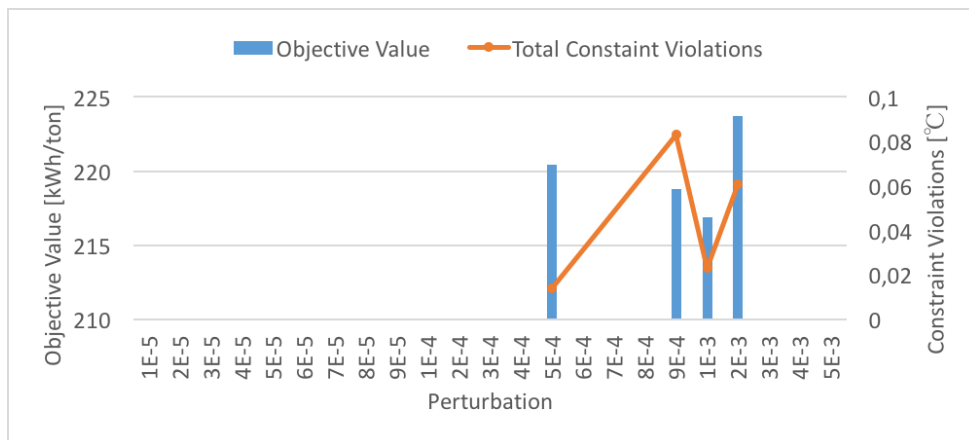


Figure 6.28: Optimizer setup test for Shell process with Objective Scale Factor = 0

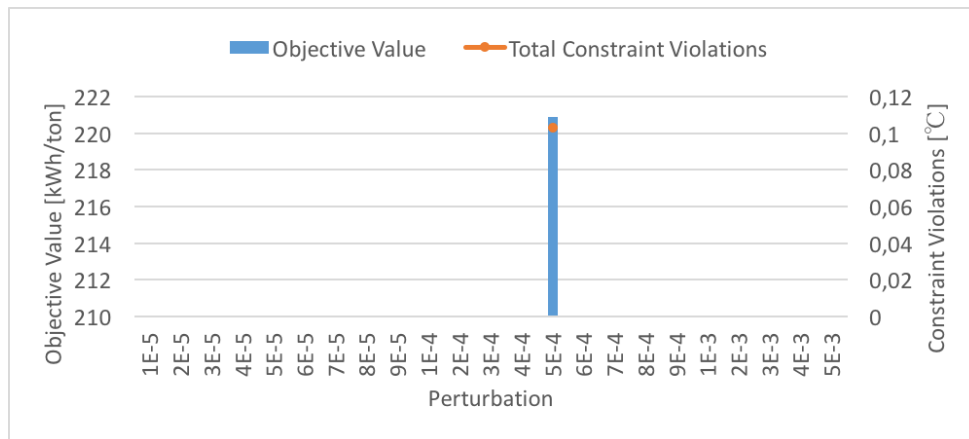


Figure 6.29: Optimizer setup test for Shell process with Objective Scale Factor = 0.001

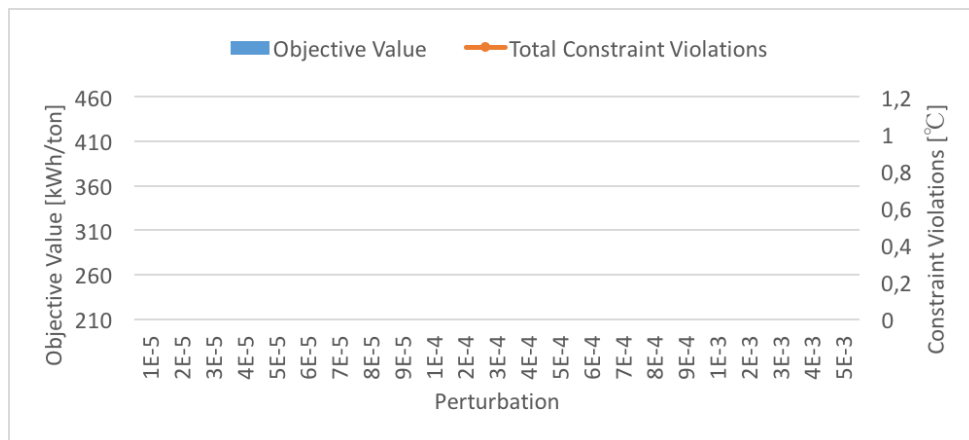


Figure 6.30: Optimizer setup test for Shell process with Objective Scale Factor = 0.01

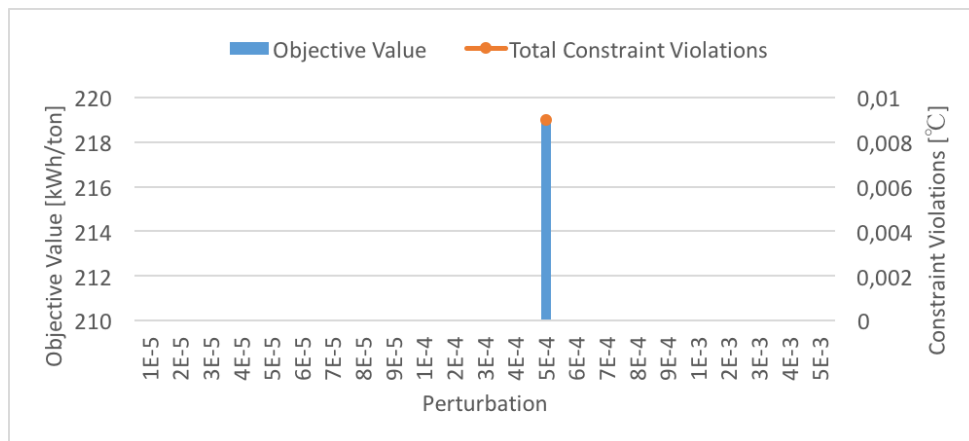


Figure 6.31: Optimizer setup test for Shell process with Objective Scale Factor = 0.1

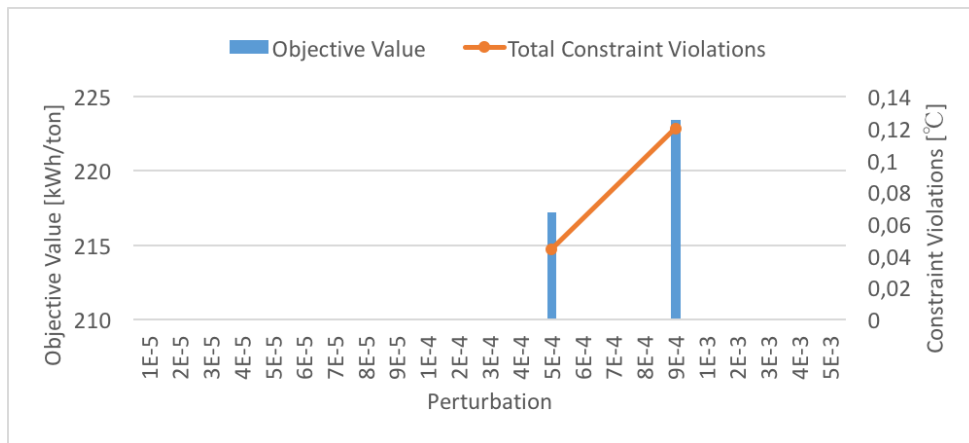


Figure 6.32: Optimizer setup test for Shell process with Objective Scale Factor = 1

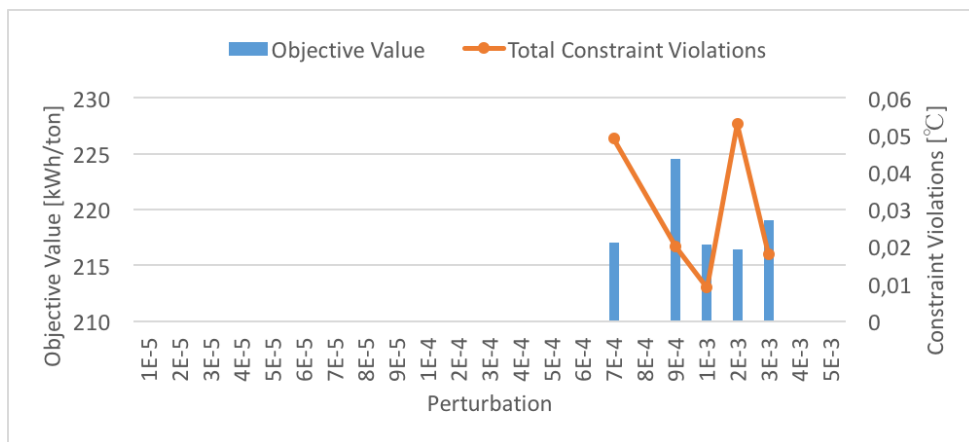


Figure 6.33: Optimizer setup test for Shell process with Objective Scale Factor = 10

A total of 13 test results were accepted in the Shell process. 13 tests account for only 9 % of all the simulation tests performed in the Shell process. This time, most of the results were provided for an objective scale factor of 0 and 10. The remaining objective values only provided four results among the 4 sets of tests. Three out of the four results were for a perturbation value of 5E-4, while the last one was also in the E-4 range. An objective scale factor of 0 provided results for a broad range of perturbation values varying from 5E-4 to 2E-3. Test results for an objective scale factor of 10 preferred perturbation values in the E-3 range, or close to it. Once again, one thing common for all tests is that perturbation values in the E-5 range have difficulty in solving the optimization algorithm while upholding the given constraints.

The objective values obtained varied from 216 - 225 kWh/ton, all providing good improve-

ment to the starting objective function value of the process. The constraint violations varied from 0.01 - 0.12 °C.

6.3.2.1 Robustness

The optimizer was tested in different ways to see how it coped with changes in the derivative utility. The top five results from Section 6.3.2, presented in Table 6.20, were used to test the robustness of the optimizer. Three of the five results have an objective scale factor of 10.

Name Tag	Objective Scale Factor	Perturbation	Objective Value	Total Constraint Violations
Test 11	0	1E-03	216.9	0.023
Test 12	1	5E-04	217.2	0.044
Test 13	10	1E-03	216.9	0.009
Test 14	10	2E-03	216.4	0.053
Test 15	10	7E-04	217	0.049

Table 6.20: Top five results from optimizer setup tests in the Shell process

Altering Variable Boundaries

The test results presented in Table 6.20 have reached the outer boundaries for different variables. The derivative utility status in common for all tests are MP Cold, HP Cold, and ScrubCol Pressure. The status for these variables is "Active Low", "Active Low", and "Active High", respectively. The upper boundary of variable ScrubCol Pressure is unchangeable. Higher operational pressure in the scrub column will not provide convergence, and therefore no simulation result. Lower boundaries of variables MP Cold and HHP Cold can be altered in an attempt to improve the objective value of the process.

Name Tag	MP Cold	HP Cold	HHP Cold	ScrubCol Pres	HP Warm	i-C4 WMR	N WMR
Test 11	Active Low	Active Low	Inactive	Active High	Inactive	Inactive	Inactive
Test 12	Active Low	Active Low	Active Low	Active High	Active Low	Inactive	Inactive
Test 13	Active Low	Active Low	Active Low	Active High	Active Low	Active High	Active Low
Test 14	Active Low	Active Low	Inactive	Active High	Inactive	Inactive	Active Low
Test 15	Active Low	Active Low	Active Low	Active High	Active Low	Inactive	Active Low

Table 6.21: Stats of variables in derivative utility for test results in Table 6.20 in Shell process

In addition to the common variables, boundaries of other variables have also been reached.

Once again, the lower boundary of variable N WMR has been reached but can not be reduced. The other variable statuses are listed in Table 6.21. The variable boundaries test for this process will be carried out slightly different than for the Turbo-expander process and the APCI process. This time the variables for each test will be altered according to the ones that are disrupting the specific test result. For example, Test 11 will only lower the boundaries of MP Cold and HP Cold. The new variable boundaries are listed in Table 6.22, with simulation results presented in Figure 6.34.

Variable	Altered Boundary	Old Value	New Value	Unit
MP Cold	Lower	22	19	bar
HP Cold	Lower	30	27	bar
HHP Cold	Lower	38	35	bar
HP Warm	Lower	33	30	bar
i-C4 WMR	Higher	9000	11000	Molar Flow

Table 6.22: New variable boundaries in optimizer test for Shell process

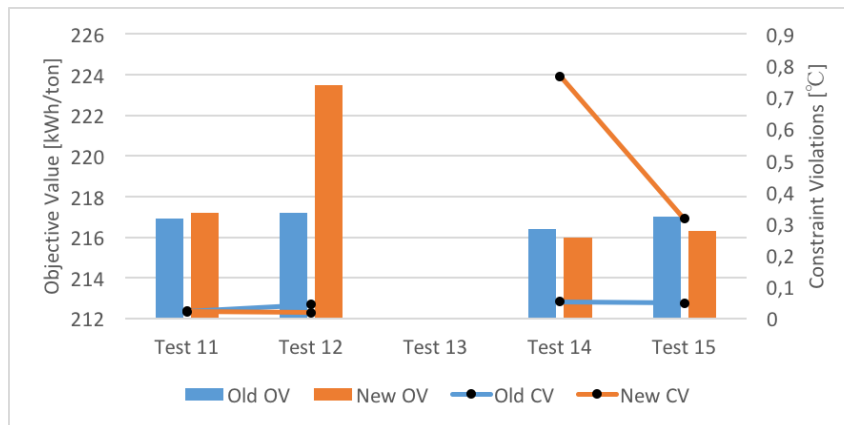


Figure 6.34: Effect of altering variable boundaries in Shell process

The changes in Table 6.22 roughly increase the variables' range by 10-20 %. Changing the variable bounds would hopefully allow the optimizer to search for an improved objective value in areas that were previously restricted. The results are bad for all tests. The objective value is increased for tests 11 & 12, but also achieve a reduction in constraint violations. It should be mentioned that the test with an objective scale factor of 0 once again provided the best result. A test result for test 13 is not achieved due to the RAM cap being reached. Tests 14 & 15 improve their objective values, but are penalized with a

moderate increase in constraint violations. The overall effects of varying the boundaries in the Shell process is disappointing.

Randomly Generated Start Variables:

The randomly generated variables and constraints can be seen in Appendix J. The variable starting values violated the minimum temperature approach in the CMR CWHE Lower Bundle and upstream heat exchanger severely. Results of this study are presented in Figure 6.35. The effects of using randomly generated start variables were worse in the Shell process compared to the Turbo-expander and Fluor process. All tests, with no exception, resulted in increased constraint violations and objective value. The constraint violations in four of the five cases were above 2 °C. The starting condition of variables played a very important role in the simulation results in the Shell process. Knowledge of the process proves to be vital to ensure acceptable starting conditions in the process.

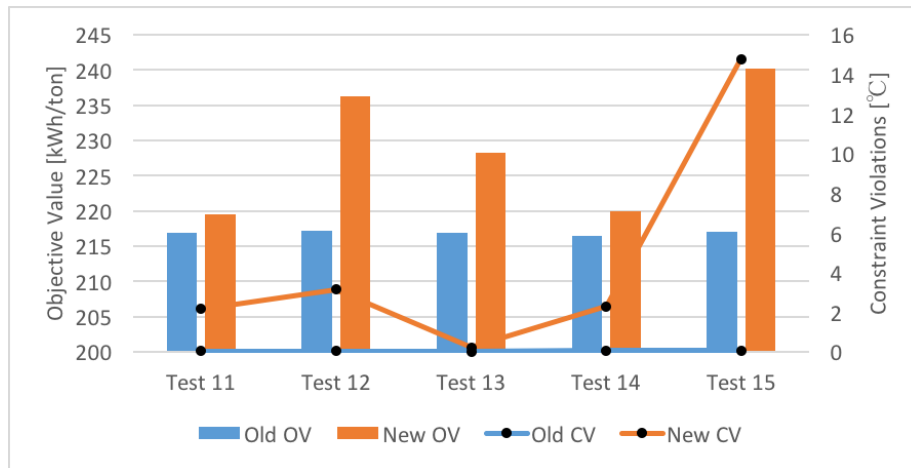


Figure 6.35: Effect of using randomly generated variable values as starting values in Shell process

Best Overall Test Result

The best result in the Shell process was obtained from the original optimizer setup test in Figure 6.33. The objective scale factor is 10 and perturbation value is 2E-3. The resulting values of all variables and constraints from this simulation test can be seen in Appendix M. Figure 6.36 shows an overview of the degree of constraint violations in this result.

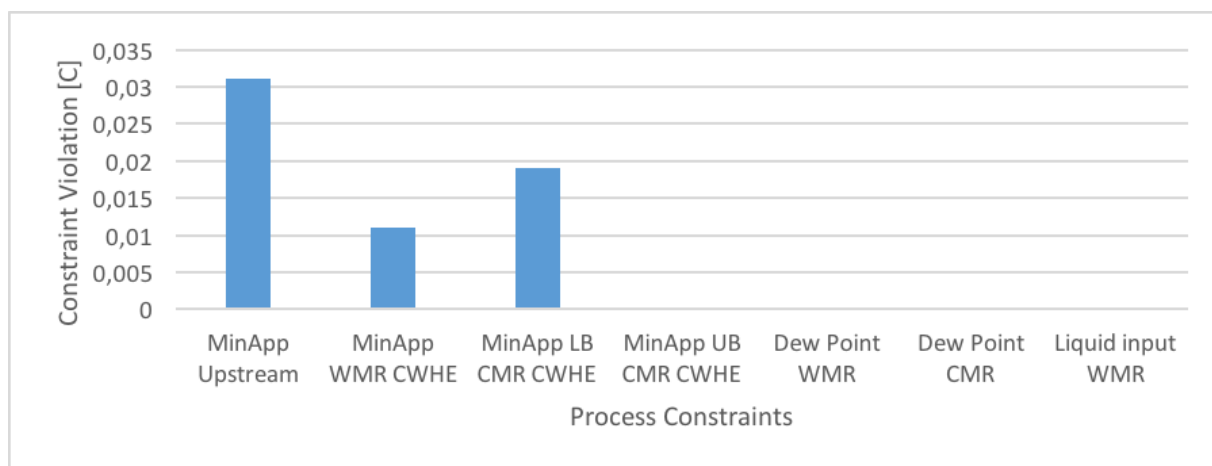


Figure 6.36: Overview of constraint violations in best test result in Shell process

6.3.2.2 CPU Time

Results of all test results in the Shell process are shown in Appendix G. Fairly identical observations are detected in this process as for the Turbo-expander and APCI process. The CPU time is therefore not studied any deeper for the Shell process.

6.4 Fluor

Optimization of the Fluor process turned out to be more complicated than expected. Setting up the derivative utility as in the above processes simply did not produce results. Reasons for why the optimizer was unable to find solutions was examined to find the cause. For all objective scale factors and perturbation values, the optimizer search was terminated due to the scrub columns inability to converge. Differences between the Fluor process and other NGL extraction processes were looked at.

The main difference is that this process utilizes two columns in the upstream extraction. The complexity also increases due to a recycle stream which exits the top of the scrub column and enters the bottom of the absorber. Due to this, the two columns have a direct relation to each other. If the scrub column is unsolvable, then the properties of the exiting top stream do not exist. The absorber also becomes unsolvable, and the stream entering the liquefaction process has no defined properties or composition.

The process included an absorber column and a reboiled absorber column. Each column is solved using an iteration process, where heat and equilibrium calculations are solved in each tray of the column prior to convergence is a possibility. The optimizer was first tested by changing the column specifications listed in Table 4.6 in Section 4.8. A trial and error method was used to see if changes to these specifications would produce results. These changes did not resolve the problem.

Next, the range of optimizer variables was tightened. Upper and lower boundary values were adjusted, especially for the operational pressure of the absorber and scrub column. Multiple optimizer tests were once again initiated, but resulted in a lack of convergence in both columns. A solution to the optimization problem was solved by splitting the optimizers search in two separate parts. The optimizer was tested by tearing the connection between the upstream extraction unit and the liquefaction unit. The results of the study are further discussed in Section 6.4.2.

6.4.1 Derivative Utility

The start values and boundaries of variables in the Fluor process are listed in Table 6.23. The accompanying constraints are shown in Table 6.24.

Tag Name	Variable	Unit	Lower Bound	Start Value	Upper Bound
N WMR	Molar Flow	kgmole/h	0	0	2000
C1 WMR	Molar Flow	kgmole/h	1000	7597	13000
C2 WMR	Molar Flow	kgmole/h	20000	35000	38000
C3 WMR	Molar Flow	kgmole/h	2000	8000	14000
i-C4 WMR	Molar Flow	kgmole/h	100	2886	9000
n-C4 WMR	Molar Flow	kgmole/h	100	2886.4	9000
N CMR	Molar Flow	kgmole/h	2000	6523	10000
C1 CMR	Molar Flow	kgmole/h	10000	17794	25000
C2 CMR	Molar Flow	kgmole/h	10000	19743	25000
C3 CMR	Molar Flow	kgmole/h	500	1811	12000
LP Warm	Pressure	bar	5	10	13
MP Warm	Pressure	bar	15	20.56	29
HP Warm	Pressure	bar	35	48.13	55
LLP Cold	Pressure	bar	2	5	8
LP Cold	Pressure	bar	8	15.5	23
MP Cold	Pressure	bar	22	38	46
HP Cold	Pressure	bar	30	45.5	52
HHP Cold	Pressure	bar	40	55.5	62
Temp WMR	Temperature	°C	-53	-48.3	-30
Temp LB CMR	Temperature	°C	-135	-125.7	-110
Absorber Pressure	Temperature	°C	35	42	60
ScrubCol Pressure	Pressure	bar	25	31	58
Upstream CWHE	Temperature	°C	-75	-50	-30
Booster Pressure	Pressure	bar	55.00	57.00	65.00
C1 in NGL	Molar Fraction	-	0.01	0.02	0.06

Table 6.23: Derivative utility values for variables in Fluor process

Tag Name	Constraint	Unit	Lower Bound	Start Value	Upper Bound
MinApp WMR CWHE	Minimum Approach	°C	3	3.531	
MinApp LB CMR CWHE	Minimum Approach	°C	3	3.991	
MinApp UP CMR CWHE	Minimum Approach	°C	3	5.6636	
Dew Point WMR	Minimum Approach	°C	5	-0.2844	
Dew Point CMR	Minimum Approach	°C	5	7.2946	
MinApp Upstream	Minimum Approach	°C	3	3.2894	
C5+ to LNG	Molar Fraction	-	-	0.0001	0.001
Liquid Input WMR	Fraction	-	1	1	-
BTX to LNG	Molar Fraction	ppm	-	0.8	10

Table 6.24: Derivative utility values for constraints in Fluor process

The starting objective value with start values from Tables 6.23 and 6.24 is 260.5 kWh/ton.

6.4.2 Optimizer Setup Study

The upstream unit was first partly optimized for only a few of the variables and constraints listed in Tables 6.23 & 6.24. The variables that were selected to be optimized were; Absorber Pressure, ScrubCol Pressure, Upstream CWHE, Booster Pressure, and C1 in NGL. The following constraints were ticked: MinApp Upstream, C5+ to LNG, and BTX to LNG. All of the mentioned variables and constraints affected the upstream extraction process. A new objective function was also defined for this part of the process. The new objective function for this optimization was to minimize compressor work in compressors C1 and Booster illustrated in Figure 5.7. The starting objective value was 5.36 MW.

Multiple optimization tests were run to find a solution which upheld the constraints and reduced the objective value. The best result was obtained using an objective scale factor of 0, and a perturbation value of 6E-4. The new values of the relevant variables and constraints are listed in Table 6.25. The values listed were used to further optimize the full Fluor process.

Tag Name	Variable	Unit	Lower Bound	New Value	Upper Bound
Absorber Pressure	Temperature	°C	35	50.99	60
ScrubCol Pressure	Pressure	bar	25	56.87	58
Upstream CWHE	Temperature	°C	-75	-31.66	-30
Booster Pressure	Pressure	bar	55.00	55.00	65.00
C1 in NGL	Molar Fraction	-	0.01	0.0475	0.06
Tag Name	Constraint	Unit	Lower Bound	New Value	Upper Bound
MinApp Upstream	Minimum Approach	°C	3	3.028	
C5+ to LNG	Molar Fraction	-	-	0.0006	0.001
BTX to LNG	Molar Fraction	ppm	-	9.99	10

Table 6.25: New values for variables and constraints in Fluor process after optimization of the upstream extraction unit.

The optimizer was now tested with all optimization variables and constraints activated. Due to appropriate variable values in the upstream extraction unit, the optimizer was able to converge both columns in simulations of the entire Fluor process. This time, simulations were only done using an objective scale factor of 0. Perturbation values were still varied to find the best setup parameter for the optimizer. The results of the test are illustrated in Figure 6.37.

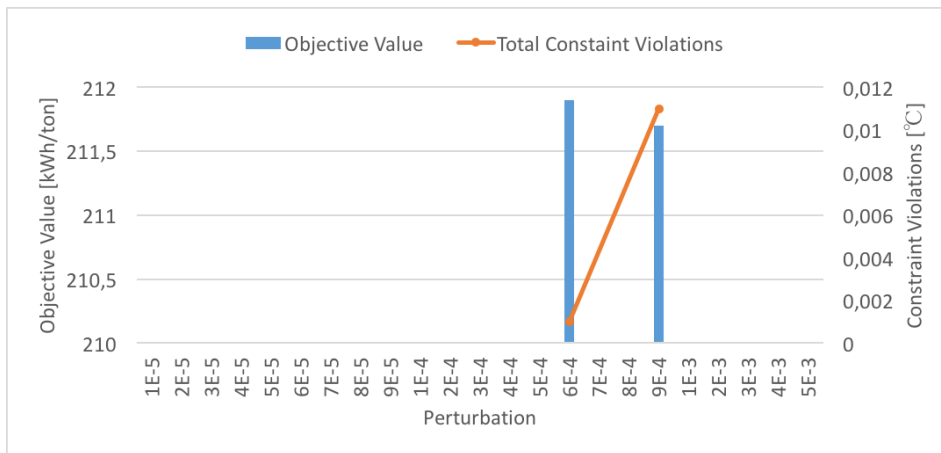


Figure 6.37: Optimizer setup test for Fluor process with Objective Scale Factor = 0

Two test results were confirmed for perturbation values of 6E-4 and 9E-4. Both proved to be excellent results, with a low objective value obtained and very small constraint violations. It was unexpected that the simulation of the Fluor process would go from unworkable to produce such amazing results. This means that the optimizer takes advantage of separating a large and complicated flowsheet into smaller optimizable sections. This is

only possible for upstream extraction processes which are independent of the liquefaction process.

No additional robustness tests were performed for the Fluor process. CPU time and gradient evaluation analysis was not performed, as similar results to the ones presented for the Turbo-expander and APCI process were expected. The optimizer test using a perturbation of $9E-4$ was used as the best Fluor result in the process comparison study. The final values of all variables and constraints in the test can be seen in Appendix N. Figure 6.38 shows an overview of the degree of constraint violations in this result.

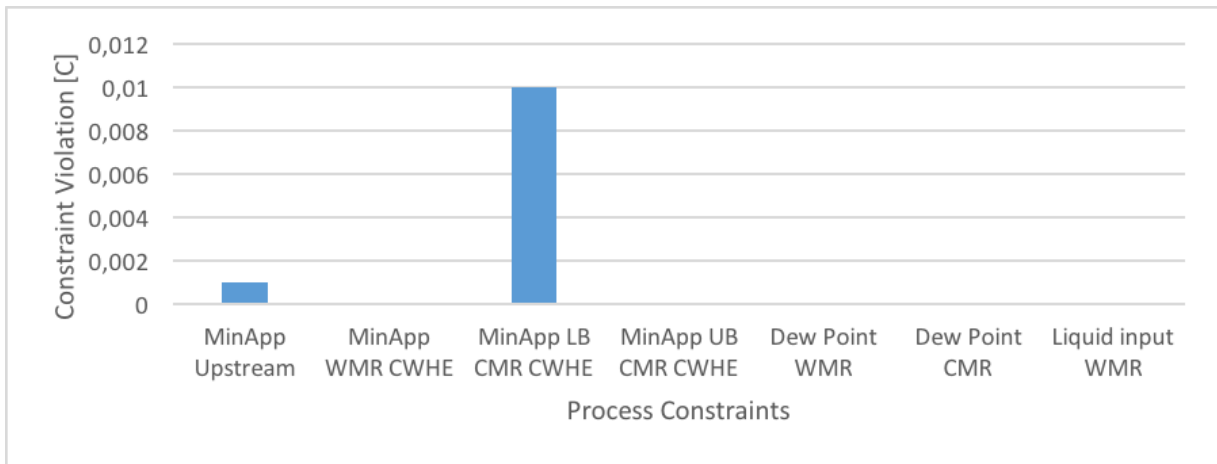


Figure 6.38: Overview of constraint violations in best test result in Fluor process

6.5 Optimizer Setup Trends

Results of all the original simulation tests, before robustness testing, have been studied. All the tests were collected and compared with respect to which objective scale factors and perturbation values that provided the majority of accepted results. The intention was to find out if a certain objective scale factor or perturbation value was superior to the others. Table 6.26 presents the number of accepted results for each objective scale factor in each process. The Fluor was only tested using an objective scale factor of 0, and is therefore not included in the table.

Objective Scale Factor	Turbo-expander	APCI	Shell	Fluor	Total
0	7	4	4	-	15
0.001	0	5	1	-	6
0.01	1	2	0	-	3
0.1	5	5	1	-	11
1	5	5	2	-	12
10	1	5	5	-	11

Table 6.26: Accepted results for each process model considering different objective scale factors

The table shows that an objective scale factor of 0 is preferred. It should be mentioned once again that when using a value of 0, the optimizer picks its own suitable objective scale factor. The lowest objective scale factors of 0.001 and 0.01 result in very few good test results. In Section 2.5.2 under the explanation of the objective scale factor it was stated that low values can help in solving non-linear optimization problems. Although all the process models studied in this thesis are non-linear, a low objective scale factor seemed to do just the opposite. Table 6.26 shows that the higher values, 0.1, 1 and 10, produced better results. It is unknown how the optimizer behaves for Objective scale factors larger than 10, as this was not tested.

The total number of successful (accepted) results does not give a good indication on how often a test was positive. Figure 6.39 illustrated the number of accepted results in comparison to the total number of tests performed for each objective scale factor. The figure shows that a little over 20 % of tests were accepted using an objective scale factor of 0, while for other scale factors they were below 20 %. The figure does not provide information on whether or not certain perturbation values worked well with certain objective scale factors.

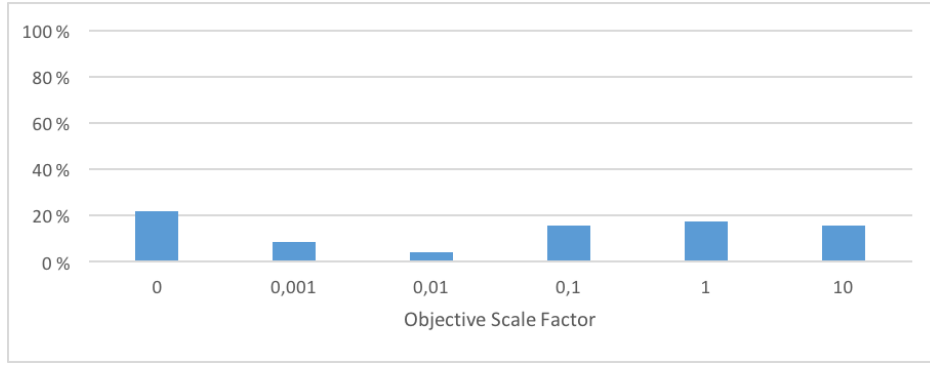


Figure 6.39: Total accepted results for each objective scale factor relative to the number of simulation tests performed

Another investigation was performed to find which perturbation values that provided good test results. Figure 6.40 shows for which perturbation values test results were accepted. It clearly shows that values in the E-5 range produced a total of seven results. None of these seven results were part of the top 5 results in any of the extraction processes. It can therefore be stated that values in this perturbation range do not produce good results for the extraction processes studied.

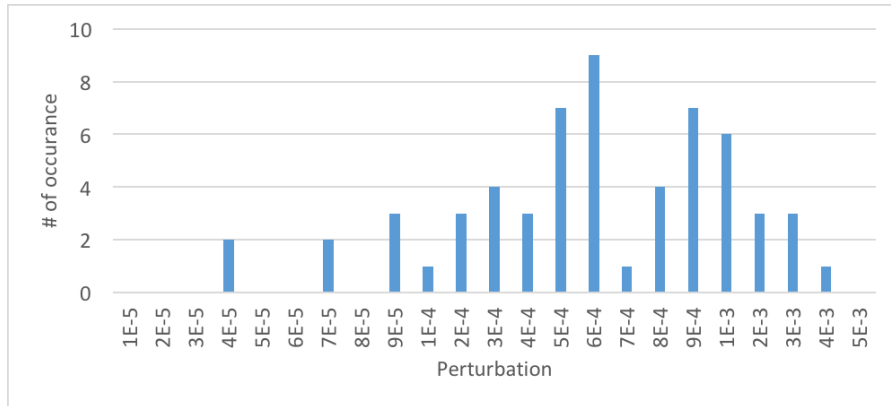


Figure 6.40: Total accepted results considering perturbation values

Simulation tests using perturbation values in the E-4 and E-3 range provide good results, specifically for values 5E-4 and 6E-4. In addition perturbation values 9E-4 and 1E-3 result in many good results. Focus on future optimizer testing for identical or similar process should utilize these values. The four mentioned values contributed to 9 of the best 17 results (Turbo-expander, APCI, and Shell have 5, Fluor has 2) distributed among the four processes.

Chapter 7 Process Comparison

A short comparison of the four NGL extraction process configurations i.e. Turbo-expander, Fluor, APCI, and Shell, is presented in this chapter. The best optimization result from each process in Chapter 6 were used in the comparison. The comparison focuses on process efficiency, production capacity, product recovery, process complexity, and process safety. Table 7.1 shows the main results for each of the processes.

Property	Unit	Turbo-expander	Fluor	Shell	APCI
Specific Power (Process Efficiency)	kWh/ton	214.1	211.7	216.4	212.4
Annual LNG production rate	MTPA	4.271	4.342	4.366	4.222
Annual NGL production rate	MTPA	0.338	0.266	0.2373	0.394
Total power demand	MW	124.6	123.2	125.8	123.8
Total cooling duty	MW	256.8	249.1	258.05	256.5
Total heating duty	MW	5.508	4.134	4.913	7.809
LNG Higher Heating Value	MJ/Sm ³	39.74	40.01	40.23	39.48

Table 7.1: Simulation results for the best optimizer results for each NGL extraction process in Chapter 6

7.1 Process Efficiency

The specific power is the performance parameter which describes the process efficiency. It is defined as the amount of power needed per mass of product produced. The products in this simulation work have been NGL and LNG. The total power in each process is a sum of the compression power from the WMR refrigerant cycle, CMR refrigerant cycle, and additional compressors used in the NGL extraction process.

The specific power results are illustrated in Figure 7.1. The calculations are based on equal plant availability of 330 days/year for each process. The results show that the Fluor process is the most efficient process when utilizing the design basis described in Chapter 4. The difference between the most efficient process and the least efficient, Shell process, is only 2%.

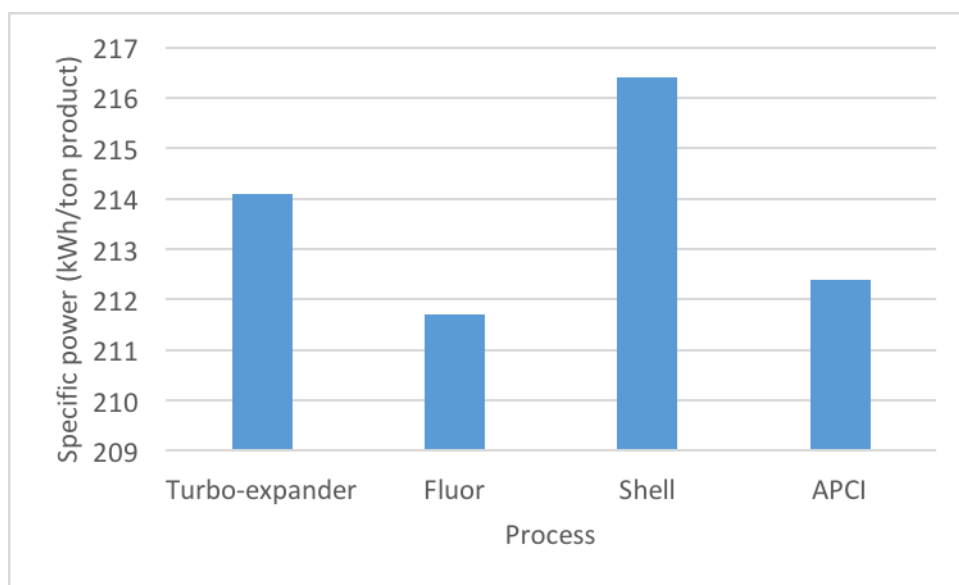


Figure 7.1: Specific power after optimization of NGL extraction processes

The reason for small differences in process efficiency is that the liquefaction process accounts for most the compressor power. This is illustrated in Table 7.2. The WMR and CMR refrigeration cycles justify most of the power usage. The compressor power in the WMR refrigeration cycle is smaller for the upstream processes than the integrated ones. This is due to a lower molar flow of the gas in upstream processes because HHC have already been extracted. On the other hand, the compressor power is higher for the upstream processes in the CMR refrigeration cycle. This is because they have a higher exit

temperature exiting the WMR CWHE. Increased cooling duty is therefore needed in the two CMR CWHE's to cool the gas to design specifications.

Compressor power	Turbo-expander	Fluor	Shell	APCI
WMR refrigeration cycle	42.22	40.22	46.00	52.02
CMR refrigeration cycle	78.53	82.27	77.94	71.38
Booster compressor	3.87	0.68	1.83	0.36
Total power demand	124.62	123.17	125.77	123.76

Table 7.2: Comparison of compressor power in NGL extraction processes

Since the power demand in each extraction process is very similar, the number of gas turbines necessary are equal. Assuming an ambient air temperature of 25 °C, the power output of the GE LM6000 (displayed in Figure 4.2) is 35 MW. Four such gas turbines produce a total power output of 140 MW, covering the power demand for all processes. No advantage in any process compared to another comes in the form of number of turbines.

All processes have improved immensely by the use of the Hyprotech SQP optimizer. Table 7.3 shows how the optimizer has affected the specific power in each of the processes.

Process	Starting specific power [kWh/ton]	Optimized specific power [kWh/ton]	Reduced Objective Value [%]
Turbo-expander	264.3	214.1	18.99
Fluor	260.5	211.7	18.73
Shell	273.6	216.4	20.91
APCI	267.7	212.4	20.66

Table 7.3: Comparison between the objective value of the extraction models prior to and after optimization using the Hyprotech SQP optimizer.

7.2 Product Recovery

The operation of the scrub column is the main deciding factor of the overall separation in each recovery scheme. In all cases, the bottom product of the scrub column is the NGL product. The operational parameters of the scrub column in each scheme are presented in Table 7.4.

Scrub Column parameters	Unit	Turbo-expander	Fluor	Shell	APCI
Operating pressure	bar	44.49	58	53	53.23
Reflux temperature	°C	-44.12	18.86	-23.62	-50.52
Reboiler temperature	°C	113.2	159.3	173.3	122.9
Reboiler heat duty	MW	5.508	4.134	4.913	7.809

Table 7.4: Scrub column operational parameters in NGL extraction processes

The scrub column in each scheme has different operational parameters. The only specified parameter is the amount of methane allowed in the NGL product stream, which exits the bottom of the scrub column. In general, the operational pressure of the scrub column is desired as high as possible, while still achieving the necessary removal of BTX and C5+ components. High scrub column operational pressure reduces the power needed in the booster compressor before liquefaction.

The reflux temperature is dependant on how the gas has been treated before entering the scrub column. The reflux temperature depends on the composition of the stream when entering the column. If the gas has been partly separated prior to the scrub column, a higher temperature can be used. This is because the lighter components are already separated, and the heavier components remaining have higher boiling points. The stream entering the scrub column in the Fluor and Shell process have already been partly separated, explaining the higher reflux temperatures.

Reboiler temperature and reboiler heat duty are settled by upholding the defined molar composition of methane in the NGL product.

The product recovery in each process is compared in Table 7.5. The recovered amount of each component has been divided by the amount of the component in the feed stream. In FLNG projects, it is beneficial that enough of each component of ethane, propane, and butane is extracted to supply the refrigeration circuits. Methane is obtained from the produced LNG. A rule of thumb is that 0.2 mol-% of each refrigerant molar flow rate should be extracted. This was examined for the extraction process although it was not a specification in the design basis of the models. Figure 7.2 illustrates whether or not enough of each component has been extracted in the extraction processes. A value of 100% means that more than enough of the component is available. The necessary amount of recovery is achieved for all components except for ethane in the Shell and Fluor processes.

Component	Turbo-expander	Fluor	Shell	APCI
C1	0.1 %	0.1 %	0.0 %	0.0 %
C2	9.8 %	4.7 %	3.9 %	15.9 %
C3	34.5 %	21.0 %	15.4 %	45.1 %
i-C4	59.7 %	42.0 %	34.0 %	67.8 %
n-C4	69.9 %	53.1 %	45.4 %	75.9 %
C5+	94.0 %	90.4 %	89.1 %	94.8 %
BTX	98.1 %	98.6 %	98.6 %	98.3 %

Table 7.5: Product recovery of components divided by component molar flow in feed stream in NGL extraction processes

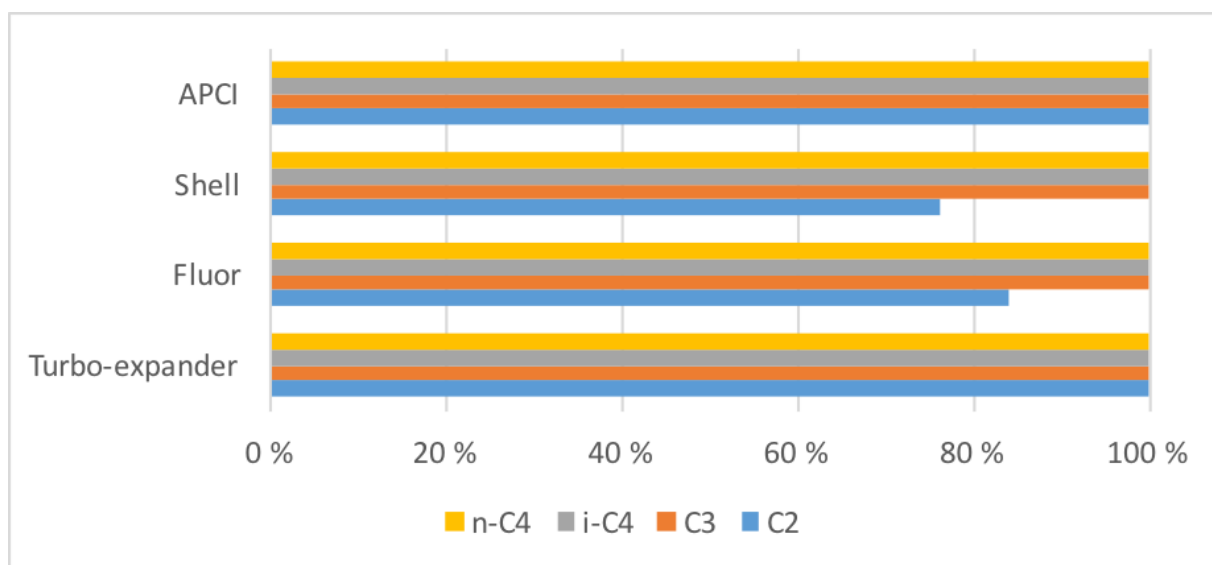


Figure 7.2: Illustration of the degree to which the necessary refrigeration make-up is extracted in each of the NGL extraction schemes

The Turbo-expander and APCI processes stand out as the processes which have the best separation efficiency. Both of the processes have great recovery of pentanes and heavier components. The APCI process also has the best recovery rates for the lighter components ethane, propane and butanes. The recovery rates in the Fluor and Shell process are similar. They are both extracting the needed amount of C5+ and BTX, but fewer of the lighter components.

It should be mentioned that the processes did not have specifications for recovery of the lighter components. Therefore it is hard to know if these processes have the ability to

extract more of the lighter components, or if they are operating the way they are just to increase the process efficiency. From an economical point of view, it is most important to have a good separation of the C5+ components as these components return the highest revenue.

7.3 Production Capacity

Production capacity is the amount of product that can be achieved by a production plant in a give time period using the available resources. The specifications set in Chapter 4 prevent the overall production from varying to a great degree. Two main parameters that manipulate the production capacity are the molar flow rate of the feed and the type of liquefaction process. Both of them are pre-defined, resulting in minor differences in total production between the NGL extraction schemes. The production capacity of each scheme is presented in Table 7.6.

Production Capacity	Unit	Turbo-expander	Fluor	Shell	APCI
Annual LNG production rate	MTPA	4.271	4.342	4.366	4.222
Annual NGL production rate	MTPA	0.338	0.266	0.2373	0.394

Table 7.6: Comparison of production capacity in NGL extraction processes

The ability to extract as much of the HHC as possible from the feed stream is an advantage from an economic point of view. The value of NGL exceeds the value of LNG, and will increase the profitability of the FLNG project. Comparing the yearly production rate of NGL, the integrated APCI process produces 14-40 % more than the other processes. Nothing indicates whether the upstream or integrated processes are better at producing NGL. The integrated Shell process provides the lowest production of NGL.

7.4 Process Complexity

All configurations have been modelled using available equipment in the LNG industry. The integrated cases have the advantage of only needing stationary equipment, while the upstream cases depend on turbo machinery. The major equipment count for each recovery scheme is presented in Table 7.7. The equipment count gives a good indication of the complexity of the NGL extraction scheme. The more equipment, the more complex the scheme. The size of equipment was not considered. Heat exchangers utilizing cooling water, valves and stream splitters were not included.

Equipment	Turbo-expander	Fluor	Shell	APCI
Heat Exchanger	1	1	1	0
Separator	1	2	1	0
Absorber	0	1	0	0
Scrub Column	1	1	1	1
Compander	1	1	0	0
Compressor	1	2	1	1
Pump	0	0	0	0
Total	5	8	4	2

Table 7.7: Major equipment count for NGL extraction processes

Table 7.7 indicates that the integrated schemes need the lowest amount of equipment. The APCI process only needs two additional units for the extraction of NGL in this study. The equipment count for this process is very low since it only utilizes one scrub column in the separation of HHC. Additionally, it uses a booster compressor, increasing its pressure prior to liquefaction. The fact that this process does not need rotating machinery, makes it even more suitable for an offshore operation. An increase in rotating equipment on an FLNG unit will also decrease the plant availability. This is because the reliability of rotating machinery is not 100%. In other words, it will increase the downtime of the plant, which for offshore plants is more crucial than for onshore plants. The maintenance of equipment is limited, which gives the APCI process an advantage.

The Fluor process needs by far the most equipment to operate. It requires a heat exchanger, two separators, an absorber, a scrub column, a compander, and two additional compressors. The increased need of equipment, results in additional space requirement, increasing the cost of the FLNG barge. This configuration needs four additional rotating

machinery units compared to the APCI process. Due to this, the plant availability is lowered, and therefore so will the production of condensate and LNG. The result of this will be an increase in specific power of the plant. In process complexity the Fluor process seems to have a disadvantage. On the other hand, the excessive amount of equipment could prove to be useful for richer feed gas streams.

The upstream Turbo-expander process and integrated Shell process are similar in amount of equipment needed. The difference between the two is the need for a compander in the Turbo-expander process. The compander, consisting of an expander and compressor, will increase the downtime of the facility.

Although an increase in equipment will generally also increase the complexity, the upstream schemes have another advantage. The upstream extraction units can be secluded from the liquefaction unit. This is an advantage because FLNG vessels are organized in modules, and the placement of equipment is important. Adding extra equipment to the liquefaction module might be difficult. The upstream schemes have the possibility of being built as its own module. This could improve the area usage on the barge even though the equipment count is higher.

7.5 Process Safety

Process safety is an important aspect to the LNG industry. The importance of safety increases when operating a floating LNG facility. Key hazards are typically high pressure streams, together with stored LNG and NGL. Additionally, pumping large inventories of liquids and hydrocarbon refrigerants represent a major hazard. In this study, all extraction processes are liquefying the gas using a DMR liquefaction unit. The circulation rates of the highly flammable hydrocarbons varies from one process to the next, and will be compared in this section. Table 7.8 displays the amount of refrigerant circulation in each cycle.

Refrigerant Circulation	Unit	Turbo-expander	Fluor	Shell	APCI
WMR Cycle	kgmole/h	42498	45153	45048	43823.6
CMR Cycle	kgmole/h	44444	47037	41466	41169
Total Refrigerant Circulation	kgmole/h	86942	92190	86514	84992.6

Table 7.8: Refrigerant circulation for best cases of NGL extraction processes

Additionally, the processed gas stream pressure along with the WMR and CMR high cycle pressures were compared. Figure 7.3 shows the pressure levels in the different processes. The APCI process operates with the lowest pressure of the four processes in two of the three compared streams.

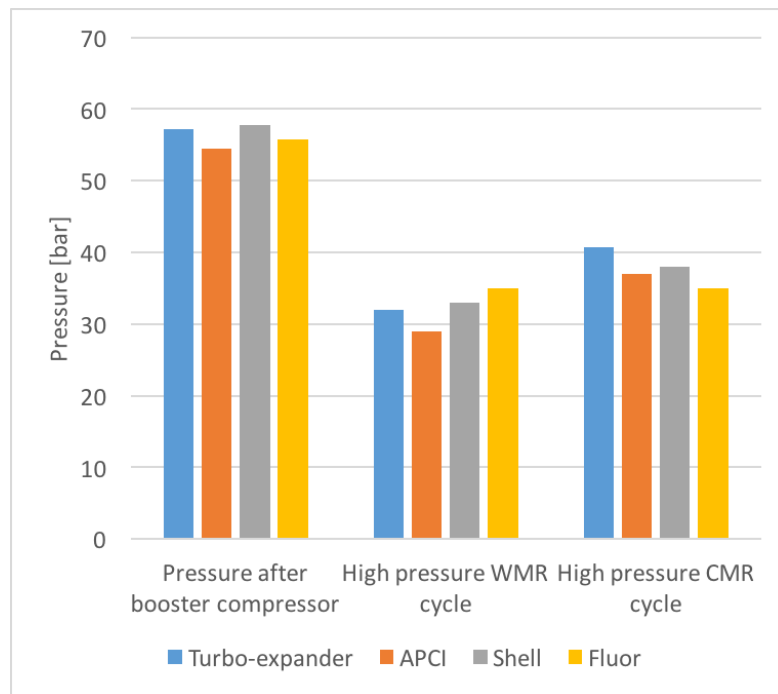


Figure 7.3: Pressure level of processed gas stream, WMR cycle high pressure and CMR cycle high pressure for best cases of NGL extraction processes

The safety of the liquefaction unit will reduce with increasing refrigerant circulation rate [24]. Relative to the molar flow of refrigerant and high pressure levels, the safest operation is APCI's, followed by Shell, Turbo-expander and lastly Fluor.

7.6 Summary

A summary of the process comparison in Chapter 7 is presented in Table 7.9. The letter A represents the best result and D the worst. In this study, the process with the best overall performance is the APCI process.

Criteria	Turbo-expander	APCI	Shell	Fluor
Process Efficiency	C	B	D	A
Complexity/ Equipment Count	C	A	B	D
Safety	C	A	B	D
Product Recovery	B	A	D	C
Production Capacity	A	A	A	A

Table 7.9: Comparison summary of NGL extraction schemes

Chapter 8 Conclusion

The main objective of this thesis has been to test the Hyprotech SQP optimizer in Aspen HYSYS. The optimizer has been tested using four different NGL extraction models, of which two are upstream and two are integrated approaches. The optimized process models are compared using the performance parameters process efficiency, product recovery, production capacity, process complexity, and process safety.

The Hyprotech SQP optimizer is very sensitive to minor changes in the setup of the derivative utility. The starting values and boundaries for variables, as well as the process constraints need to be defined appropriately. Badly defined or too broad variable boundaries result in process models not being able to converge. On the other hand, it was found that the variable ranges should be set large enough to support the optimizer in finding an improved objective function value. The most vital boundaries in the derivative utility were the ones in connection to a scrub column. Poorly defined or too broad variable boundaries result in non-convergence of the process models. Good process model knowledge when setting variable values proved to be a necessity when using the Hyprotech SQP optimizer.

The process constraints are set to restrict the optimizer in specific ways. Setting appropriate process constraints also supports in obtaining more realistic model results. The results show that upholding process constraints prior to a simulation run benefited the optimizer. The constraints were more likely to remain upheld when this was the case.

The optimizer interface in the Hyprotech SQP consists of two configuration sections, flags and setup. The flags section was tested using the Turbo-expander process. Results showed that using two of the nine available flag options supported in reducing the constraint violations and improved the objective value of the model. The flags used were "Include Variable Scales" and "Hyprotech SQP Calc Gradients".

The setup configuration in the optimizer interface was examined thoroughly. Setup parameters "Objective Scale Factor" and "Perturbation" were modified against each other. The simulation tests were performed using identical derivative utility specifications and equal flowsheets for each specific model. The computational times for the simulations varied from 5 - 30 minutes. Using an objective scale factor of 0 returned the best simulation results, while the tested values, 0.001 and 0.01, provided the worst results.

The perturbation values that provided the best results varied greatly depending on the

objective scale factor and which extraction model was tested. Overall, values of 5E-4 and 6E-4 provided the best results independent of the objective scale factor value. Perturbation values in the E-5 range rarely provided good objective values, and should not be used further.

Changes to variable starting values and variable bounds while using identical optimizer configurations resulted in different constraint violations and new objective values. This means that changing any parameters that affects the input data in the Hyprotech SQP optimizer, will also impact the results obtained. The configuration of the optimizer should therefore always be configured after the modeller has made a final decision on the variable start and boundary values. When configured correctly, the Hyprotech SQP optimizer provides great simulation results.

Considering the performance parameters of the NGL extraction models, the best optimization results of each scheme were compared. The process efficiency proved to have minor differences in all schemes, only varying from one another by 2 %. The upstream Fluor process proved to have the highest efficiency with the lowest specific power usage of 211.7 kWh/ton product produced. The integrated Shell process required the most power at 216.4 kWh/ton product. The optimized processes were improved by 19-21 % compared to the initial objective value in the processes.

The product recovery is the performance parameter that to the largest extent distinguish one process from another. All models were able to meet the product specifications considering removal of C5+ and the heavier components benzene, toluene, and xylene. The separation efficiency in the APCI and Turbo-expander processes proved to be very high, extracting more than 94 % of the C5+ components and 98 % of BTX in the gas stream. In the case of needing to extract components to be used as refrigerant make-up, the APCI and Turbo-expander processes once again met the recommended amounts. The Shell and Fluor process struggled to meet the necessary amount of ethane, but extracted more than enough of the other refrigerant components. The total production capacity in all processes were almost identical due to having equal feed streams and the same two products, NGL and LNG. The processes with higher separation efficiency, APCI and Turbo-expander, produced more NGL than the other two, Fluor and Shell. The opposite is true for LNG production.

When it comes to process complexity, the integrated schemes, especially the APCI process, were better than the upstream solutions. Low equipment count, as well as not using rotat-

ing machinery brings advantages when considering an FLNG project. The Fluor process needs the most equipment, as well as the largest number of rotating equipment. Considering process safety, the APCI process is slightly better than the other processes when it comes to low circulation rate of flammable components and low maximum operational pressure.

It is difficult to clearly point out the best NGL extraction scheme among the ones proposed. Each process will have advantages and disadvantages, which will vary heavily depending on factors such as feed composition and product specifications. In accordance to the design specifications in this thesis, the APCI process has the best overall performance.

Chapter 9 Further Work

The Hyprotech SQP optimizer is relatively unexplored with respect to the setup of the derivative utility and optimizer interface. Testing the optimizer is a time intensive study and the testing possibilities are endless. Using the optimizer in optimization of NGL extraction methods is beneficial to improve the objective function of the process. Following are a couple of suggestions for further research topics.

- The optimizer could be tested with an objective function based on cost analysis. The plant revenue will vary depending on equipment count, product recovery, product value, and production capacity. Establishing a cost parameter as the objective function which adopts all the necessary parameters will improve the process comparison basis.
- The evaluation of NGL extraction methods use the same process availability in all case studies in this thesis. In reality, the addition of equipment used for NGL extraction affects this parameter. A reliability study on the additional equipment used for NGL extraction can be studied to see how it affects the process availability of the plant, and therefore also the production capacity and process efficiency.
- A sensitivity analysis of the process configurations in the design basis can be performed. Testing the optimizer, as well as the NGL extraction processes with different feed gas compositions, process temperatures, product recovery restrictions could provide valuable insight.

References

- [1] Chapter 1 - LNG fundamentals. In Saeid MokhatabJohn Y. MakJaleel V. ValappilDavid A. Wood, editor, *Handbook of Liquefied Natural Gas*, pages 1 – 106. Gulf Professional Publishing, Boston, 2014. ISBN 978-0-12-404585-9. doi: <http://dx.doi.org/10.1016/B978-0-12-404585-9.00001-5>. URL <http://www.sciencedirect.com/science/article/pii/B9780124045859000015>.
- [2] Mohd Shariq Khan, Yus Donald Chaniago, Mesfin Getu, and Moonyong Lee. Energy saving opportunities in integrated NGL/LNG schemes exploiting: Thermal-coupling common-utilities and process knowledge. *Chemical Engineering and Processing: Process Intensification*, 82(0):54 – 64, 2014. ISSN 0255-2701. doi: <http://dx.doi.org/10.1016/j.cep.2014.06.001>. URL <http://www.sciencedirect.com/science/article/pii/S0255270114001184>.
- [3] Daniel Sætre. NGL Extraction in Floating LNG Processes. Specialization project, Institute for Energy and Process Technology, NTNU, Trondheim, Norway, June 2015.
- [4] Jorge Nocedal and Steve J. Wright. *Numerical optimization*. Springer Series in Operations Research and Financial Engineering. Springer, Berlin, 2006. ISBN 978-0387-30303-1. URL <http://opac.inria.fr/record=b1120179>. NEOS guide <http://www-fp.mcs.anl.gov/otc/Guide/>.
- [5] David G. Luenberger and Yinyu Ye. *Linear and Nonlinear Programming*. Springer Publishing Company, Incorporated, 2015. ISBN 3319188410, 9783319188416.
- [6] Eduardo D. Glandt, Michael T. Klein, and Thomas F. Edgar. *Optimization of chemical processes second edition*. McGraw-Hill chemical engineering series.
- [7] Aspen Technology. *Aspen HYSYS Unit Operations Guide*. Aspen Technology Inc., Burlington, Massachusetts, 2011.
- [8] Eirik Rødstøl. Optimization of FLNG processes. Masters thesis, Institute for Energy and Process Technology, NTNU, Trondheim, Norway, June 2015.
- [9] Aspen Technology. *HYSYS.RTO Reference Guide*. Aspen Technology Inc., Massachusetts, 2003.

-
- [10] Aspen Technology. *Aspen HYSYS SQP Optimization, A practical Guide*. Aspen Technology Inc., Massachusetts.
- [11] Saeid Mokhatab, William A. Poe, and John Y. Mak. Chapter 8 - natural gas liquids recovery. In Saeid MokhatabWilliam A. PoeJohn Y. Mak, editor, *Handbook of Natural Gas Transmission and Processing (Third Edition)*, pages 265 – 299. Gulf Professional Publishing, Boston, third edition edition, 2015. ISBN 978-0-12-801499-8. doi: <http://dx.doi.org/10.1016/B978-0-12-801499-8.00008-0>. URL <http://www.sciencedirect.com/science/article/pii/B9780128014998000080>.
- [12] Sojung Kim, Kiil Nam, and Woo Young Byun. Selection study on natural gas liquid extraction processes in offshore plants. *Proceedings of the Twenty-fourth International Ocean and Polar Engineering Conference*, pages 599–602, 2014. URL <http://www.isopec.org/publications/proceedings/ISOPE/ISOPE%202014/papers/vol4/14TPC-0795Kim.pdf>.
- [13] J. Mak. Configurations and methods for offshore NGL recovery, March 6 2014. URL <https://www.google.no/patents/US20140060114>. US Patent App. 14/014,226.
- [14] M.J. Roberts and R. Agrawal. Dual mixed refrigerant cycle for gas liquefaction, August 7 2001. URL <https://www.google.no/patents/US6269655>. US Patent 6,269,655.
- [15] Grootjans, H.F, , R.K. Nagelvoort, and K.J. Vink. Liquefying a stream enriched in methane, April 16 2002. URL <https://www.google.no/patents/US6370910>. US Patent 6,370,910.
- [16] Mesfin Getu, Shuhaimi Mahadzir, Nguyen Van Duc Long, and Moonyong Lee. Techno-economic analysis of potential natural gas liquid (NGL) recovery processes under variations of feed compositions. *Chemical Engineering Research and Design*, 91(7):1272 – 1283, 2013. ISSN 0263-8762. doi: <http://dx.doi.org/10.1016/j.cherd.2013.01.015>. URL <http://www.sciencedirect.com/science/article/pii/S026387621300035X>.
- [17] A. P. F. Teles, A. S. de Abreu, A. C. Saad, D. C. de Mello, F. B. Campos, J. P. Silva, L. F. N Quintanilha, , and M. D. A. S. Ferreira. Evaluation of a floating liquefied natural gas for brazilian scenarios. *Offshore Technology Conference*, May 2010. Petrobas’s Research and Development Center.

- [18] Dr. Justin D. Bukowski. Innovations in natural gas liquefaction technology for future LNG plants and floating LNG facilities. *International Gas Union Research Conference 2011*, 2011.
- [19] Joe Wehrman, Mark Roberts, and Bill Kennington. Machinery/Process Configurations for an Evolving LNG Landscape Air Products. *LNG Journal May 2012*, February 2011.
- [20] Craig Thomas and Robert Burlingame. Direct seawater cooling in LNG liquefaction plants. *15th International Conference & Exhibition on Liquefied Natural Gas*, 2007.
- [21] Dr. Justin D. Bukowski. Natural gas liquefaction technology for floating LNG facilities. *17th International Conference & Exhibition on Liquefied Natural Gas*, April 2013. Houston Texas.
- [22] Donghoi Kim. Comparison of New Liquefaction Processes for FLNG. Master's thesis, NTNU, Trondheim, Norway, June 2014. Master Project.
- [23] Yuli Amalia Husnil and Moonyong Lee. Synthesis of an optimizing control structure for dual mixed refrigerant process. *JOURNAL OF CHEMICAL ENGINEERING OF JAPAN*, 47(8):678–686, 2014. doi: 10.1252/jcej.14we098.
- [24] Michael Barclay and Noel Denton. Selecting offshore LNG processes. *LNG Journal*, 2005.

Appendix A

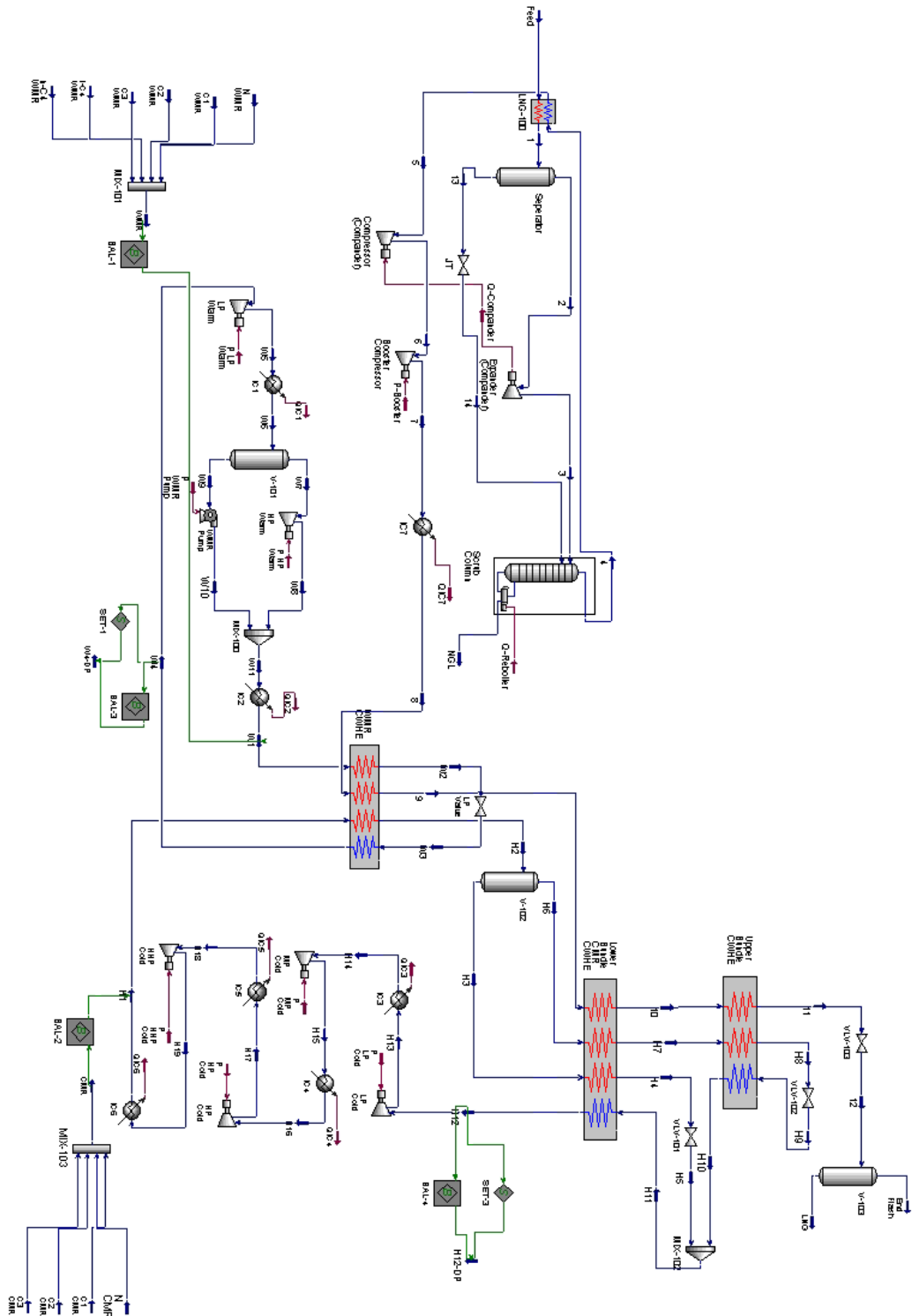


Figure A.1: Full HYSYS model of Turbo-expander process

Appendix B

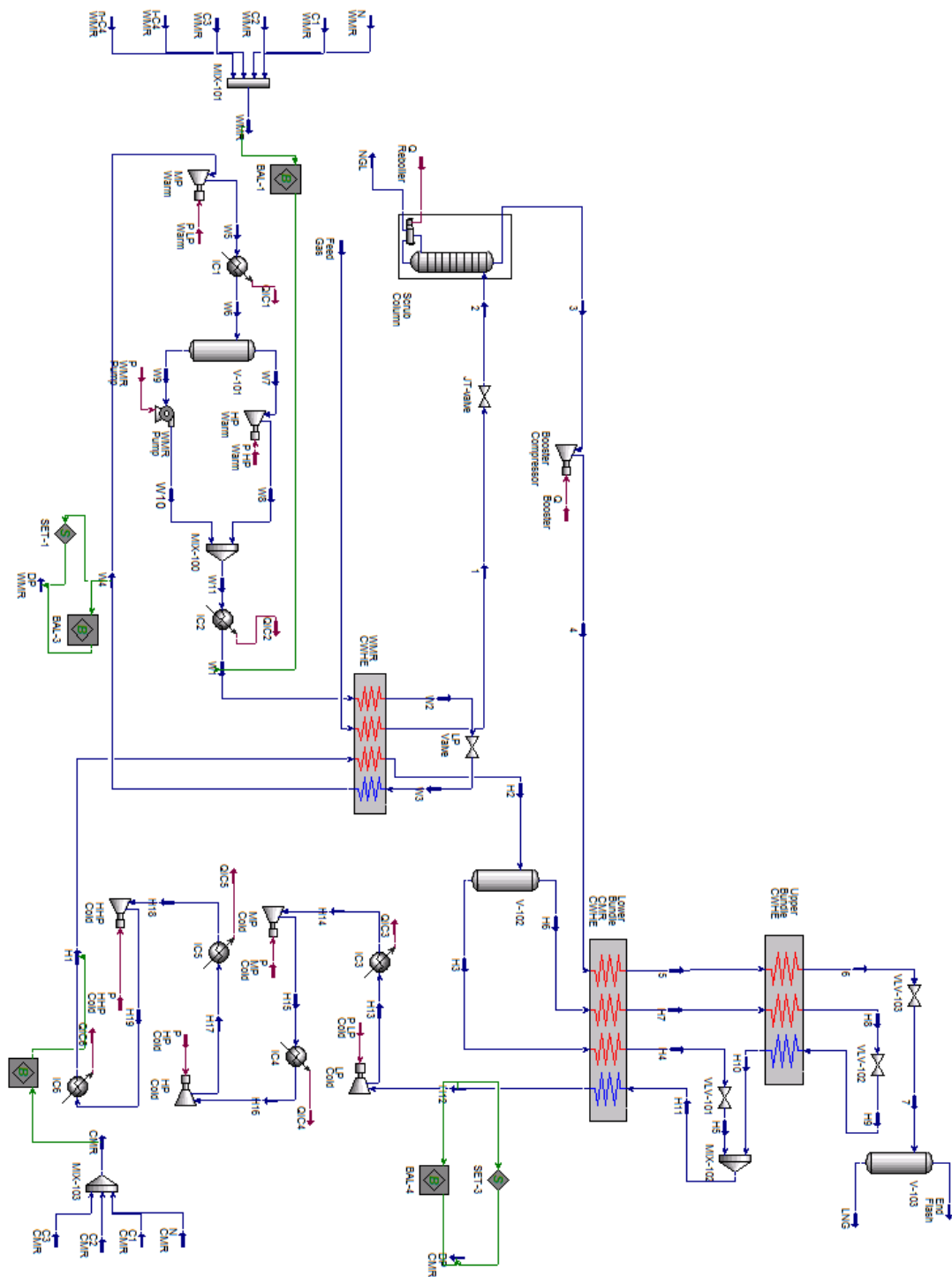


Figure B.1: Full HYSYS model of APCI process

Appendix D

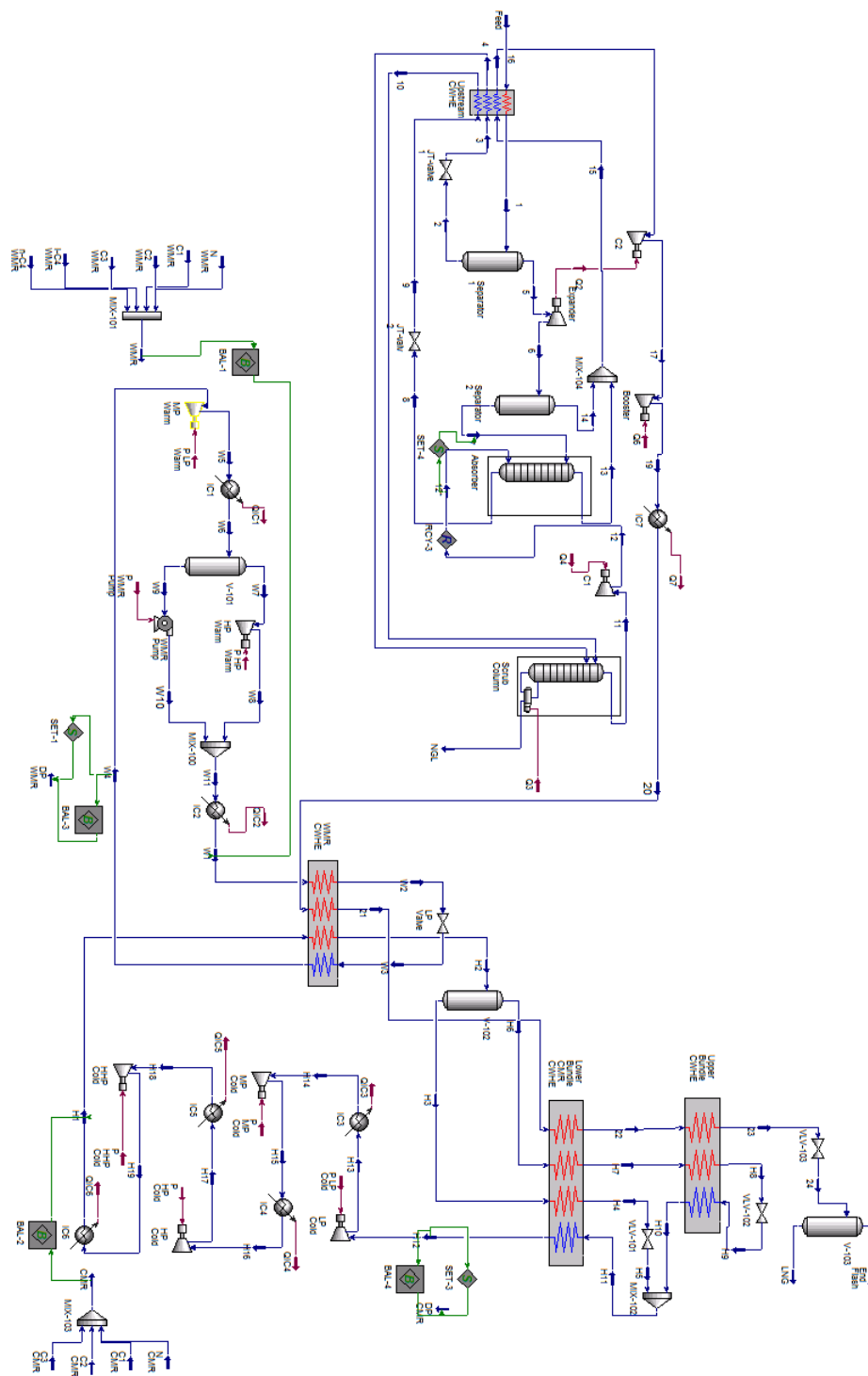


Figure D.1: Full HYSYS model of Fluor process

Recycle

The capability of any flowsheet simulator to solve recycles reliably and efficiently is critical. HYSYS has inherent advantages over other simulators in this respect. It has the unique ability to back-calculate through many operations in a non-sequential manner, allowing many problems with recycle loops to be solved explicitly. For example, most heat recycles can be solved explicitly (without a Recycle operation). Material recycles, where downstream material mixes with upstream material, require a Recycle operation.

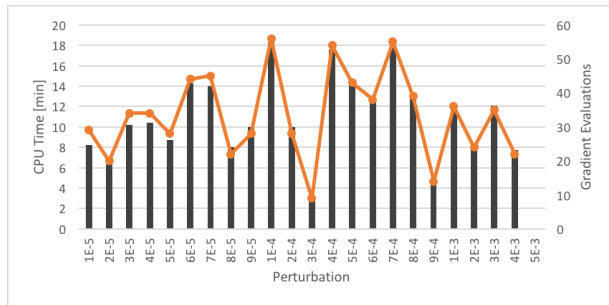
The Recycle installs a theoretical block in the process stream. The stream conditions can be transferred either in a forward or backward direction between the inlet and outlet streams of this block. In terms of the solution, there are assumed values and calculated values for each of the variables in the inlet and outlet streams. Depending on the direction of transfer, the assumed value can exist in either the inlet or outlet stream. For example, if the user selects Backward for the transfer direction of the Temperature variable, the assumed value is the Inlet stream temperature and the calculated value is the Outlet stream temperature. The following steps take place during the convergence process:

1. HYSYS uses the assumed values and solves the flowsheet around the recycle.
2. HYSYS then compares the assumed values in the attached streams to the calculated values in the opposite stream.
3. Based on the difference between the assumed and calculated values, HYSYS generates new values to overwrite the previous assumed values.
4. The calculation process repeats until the calculated values match the assumed values within specified tolerances.

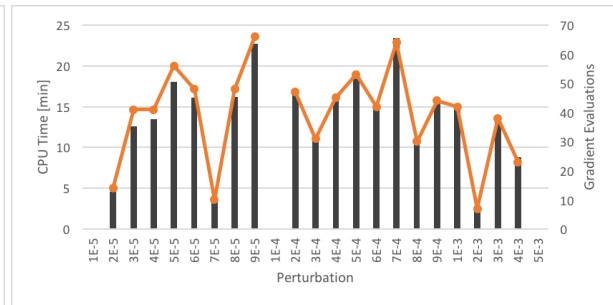
[7]

In the NGL extraction processes, Shell and Fluor, the scrub column terminates the optimizer due to an "Inconsistency Error" if a recycle icon is not used. The maximum number of iterations in the recycle icon is set down from 1000 to 2. This way it does not prevent the optimizer in its search for an improved solution.

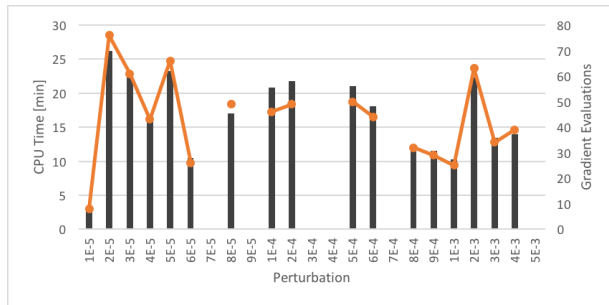
Appendix E



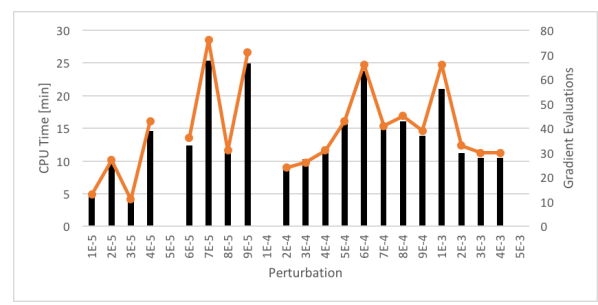
(a) Objective Scale Factor = 0



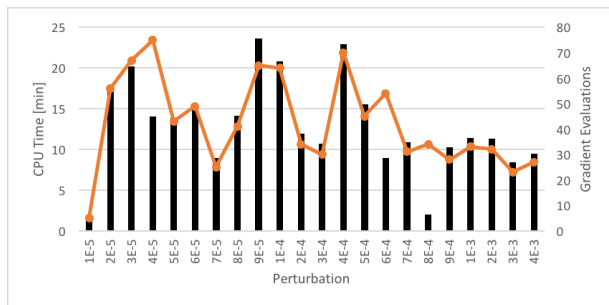
(b) Objective Scale Factor = 0.001



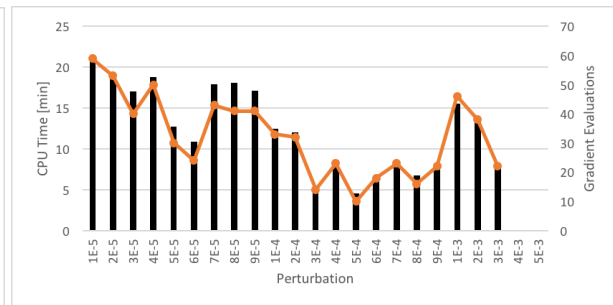
(c) Objective Scale Factor = 0.01



(d) Objective Scale Factor = 0.1



(e) Objective Scale Factor = 1

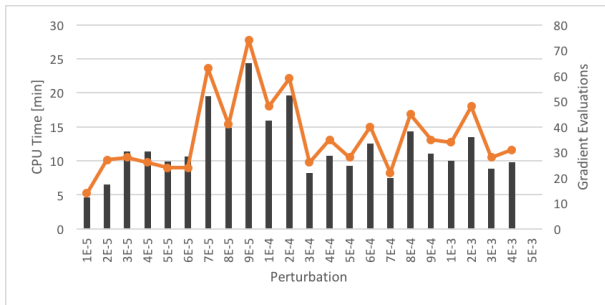


(f) Objective Scale Factor = 10

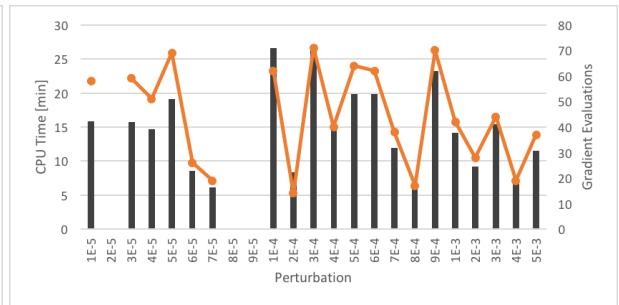
Figure E.1: CPU Time vs Gradient Calculations for Turbo-expander process

The orange line represents gradient calculations, and the black columns represent CPU time. For perturbation values showing no results, the simulation process failed.

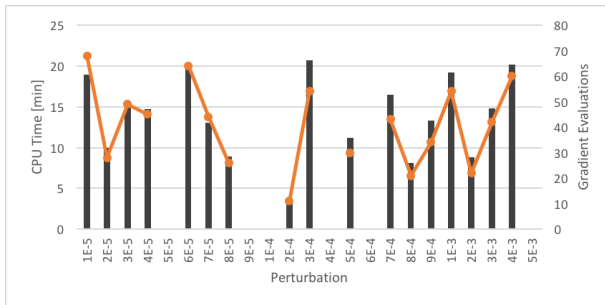
Appendix F



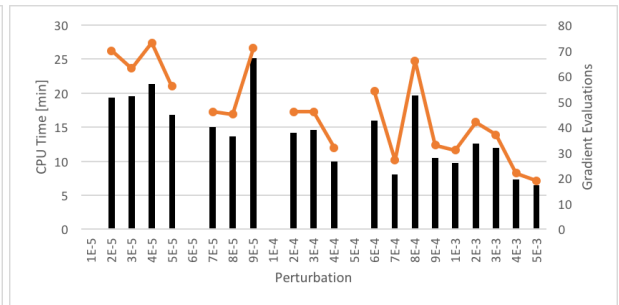
(a) Objective Scale Factor = 0



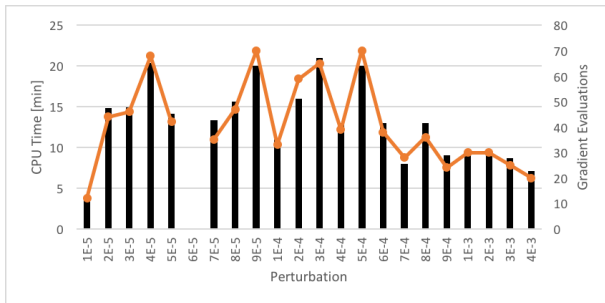
(b) Objective Scale Factor = 0.001



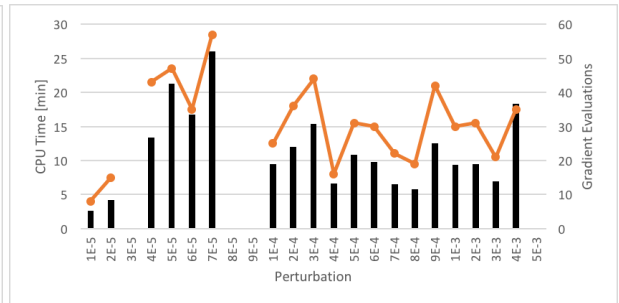
(c) Objective Scale Factor = 0.01



(d) Objective Scale Factor = 0.1



(e) Objective Scale Factor = 1

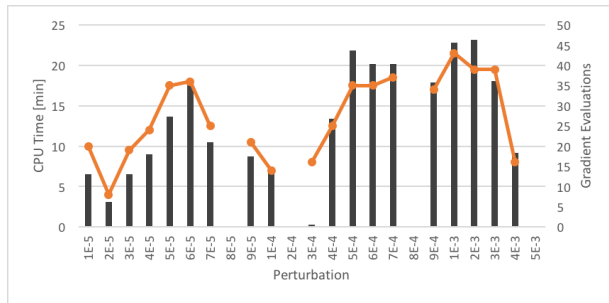


(f) Objective Scale Factor = 10

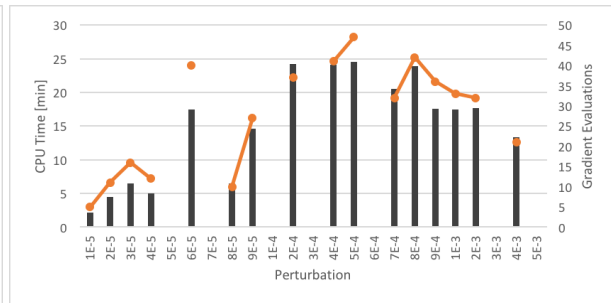
Figure F.1: CPU Time vs Gradient Calculations for APCI process

The orange line represents gradient calculations, and the black columns represent CPU time. For perturbation values showing no results, the simulation process failed.

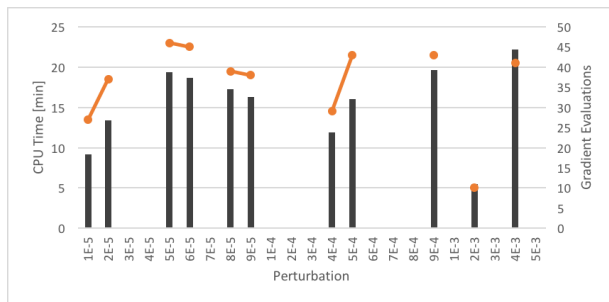
Appendix G



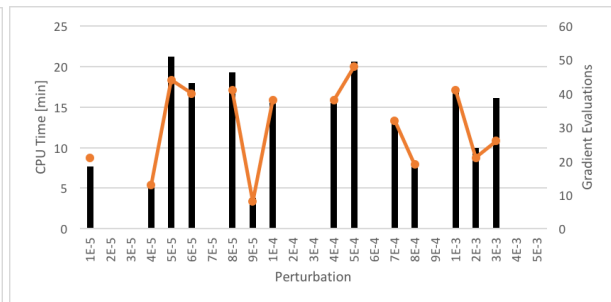
(a) Objective Scale Factor = 0



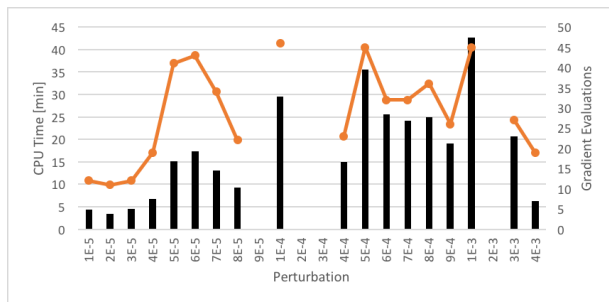
(b) Objective Scale Factor = 0.001



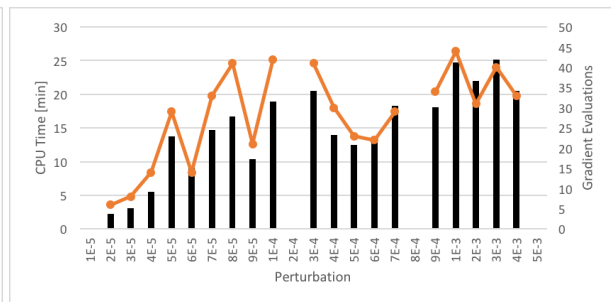
(c) Objective Scale Factor = 0.01



(d) Objective Scale Factor = 0.1



(e) Objective Scale Factor = 1



(f) Objective Scale Factor = 10

Figure G.1: CPU Time vs Gradient Calculations for Shell process

The orange line represents gradient calculations, and the black columns represent CPU time. For perturbation values showing no results, the simulation process failed.

Appendix H

Tag Name	Variable	Unit	Lower Bound	Start Value	Upper Bound
N WMR	Molar Flow	kgmole/h	0	611	2000
C1 WMR	Molar Flow	kgmole/h	1000	5803	13000
C2 WMR	Molar Flow	kgmole/h	20000	25339	38000
C3 WMR	Molar Flow	kgmole/h	2000	12419	14000
i-C4 WMR	Molar Flow	kgmole/h	100	6883	9000
n-C4 WMR	Molar Flow	kgmole/h	100	7873	9000
N CMR	Molar Flow	kgmole/h	2000	6580	10000
C1 CMR	Molar Flow	kgmole/h	10000	14340	25000
C2 CMR	Molar Flow	kgmole/h	10000	23646	25000
C3 CMR	Molar Flow	kgmole/h	500	9046	12000
LP Warm	Pressure	bar	5	7	13
MP Warm	Pressure	bar	15	28	29
HP Warm	Pressure	bar	35	42	55
LLP Cold	Pressure	bar	2	2	8
LP Cold	Pressure	bar	8	15	23
MP Cold	Pressure	bar	22	36	46
HP Cold	Pressure	bar	30	41	52
HHP Cold	Pressure	bar	40	52	62
Temp WMR CWHE	Temperature	°C	-53	-49	-30
Temp LB CMR CWHE	Temperature	°C	-135	-113	-110
Temp Upstream	Temperature	°C	-40	-31	-20
ScrubCol Pressure	Pressure	bar	30	43	50
Booster Pressure	Pressure	bar	50	60	70
C1 to NGL	Molar Fraction	-	0.0100	0.0345	0.0600

Table H.1: Start values for randomly generated variables in Turbo-expander process for tests done in Section 6.1.3.1

Tag Name	Constraint	Unit	Minimum	Start Value	Maximum
MinApp WMR CWHE	Minimum Approach	°C	3	0.5941	-
MinApp LB CMR CWHE	Minimum Approach	°C	3	6.205	-
MinApp UP CMR CWHE	Minimum Approach	°C	3	-174.1925	-
Dew Point WMR	Minimum Approach	°C	5	-2.104	-
Dew Point CMR	Minimum Approach	°C	5	-11.2835	-
MinApp Upstream	Minimum Approach	°C	3	2.8678	-
C5+ to LNG	Molar Fraction	-	-	0.0003	0.0010
Liquid input WMR	Fraction	-	1	1	-
BTX to LNG	Molar Fraction	ppm	-	7.3810	10

Table H.2: Start values for randomly generated constraints in Turbo-expander process for tests done in Section 6.1.3.1

Appendix I

Tag Name	Variable	Unit	Lower Bound	Start Value	Upper Bound
N WMR	Molar Flow	kgmole/h	0	1323	2000
C1 WMR	Molar Flow	kgmole/h	1000	8067	13000
C2 WMR	Molar Flow	kgmole/h	20000	32202	38000
C3 WMR	Molar Flow	kgmole/h	2000	3647	14000
i-C4 WMR	Molar Flow	kgmole/h	100	8558	9000
n-C4 WMR	Molar Flow	kgmole/h	100	7059	9000
N CMR	Molar Flow	kgmole/h	2000	5121	10000
C1 CMR	Molar Flow	kgmole/h	10000	18042	25000
C2 CMR	Molar Flow	kgmole/h	10000	19979	25000
C3 CMR	Molar Flow	kgmole/h	500	9950	12000
LP Warm	Pressure	bar	5	9	13
MP Warm	Pressure	bar	15	15	29
HP Warm	Pressure	bar	35	35	55
LLP Cold	Pressure	bar	2	2	8
LP Cold	Pressure	bar	8	20	23
MP Cold	Pressure	bar	22	42	46
HP Cold	Pressure	bar	30	51	52
HHP Cold	Pressure	bar	40	59	62
Temp WMR	Temperature	°C	-53	-43	-30
Temp LB CMR	Temperature	°C	-135	-132	-110
ScrubCol Pressure	Pressure	bar	40	50	55
Booster Pressure	Pressure	bar	50	56	70
C1 to NGL	Molar Fraction	-	0.01	0.013	0.06

Table I.1: Start values for randomly generated variables in APCI process for tests done in Section 6.2.2.1

Tag Name	Constraint	Unit	Minimum	Start Value	Maximum
MinApp WMR CWHE	Minimum Approach	°C	3	-3.77	-
MinApp LB CMR CWHE	Minimum Approach	°C	3	10.17	-
MinApp UP CMR CWHE	Minimum Approach	°C	3	-21.02	-
Dew Point WMR	Minimum Approach	°C	5	5.68	-
Dew Point CMR	Minimum Approach	°C	5	-7.68	-
C5+ to LNG	Molar Fraction	-	-	0.00	0.0010
Liquid input WMR	Fraction	-	1	0.73	-
BTX to LNG	Molar Fraction	ppm	-	8.76	10

Table I.2: Start values for randomly generated constraints in APCI process for tests done in Section 6.2.2.1

Appendix J

Tag Name	Variable	Unit	Lower Bound	Start Value	Upper Bound
N WMR	Molar Flow	kgmole/h	0	479	2000
C1 WMR	Molar Flow	kgmole/h	1000	12010	13000
C2 WMR	Molar Flow	kgmole/h	20000	31124	38000
C3 WMR	Molar Flow	kgmole/h	2000	3109	14000
i-C4 WMR	Molar Flow	kgmole/h	100	7943	9000
n-C4 WMR	Molar Flow	kgmole/h	100	5214	9000
N CMR	Molar Flow	kgmole/h	1000	6516	10000
C1 CMR	Molar Flow	kgmole/h	10000	16794	25000
C2 CMR	Molar Flow	kgmole/h	10000	10793	25000
C3 CMR	Molar Flow	kgmole/h	500	3934	12000
LP Warm	Pressure	bar	5	10	13
MP Warm	Pressure	bar	15	24	29
HP Warm	Pressure	bar	33	42	55
LLP Cold	Pressure	bar	2	6	8
LP Cold	Pressure	bar	8	17	23
MP Cold	Pressure	bar	22	26	46
HP Cold	Pressure	bar	30	45	52
HHP Cold	Pressure	bar	38	57	62
Temp WMR CWHE	Temperature	°C	-53	-49	-30
Temp LB CMR CWHE	Temperature	°C	-135	-135	-110
Temp Upstream	Temperature	°C	-25	-19	-15
ScrubCol Pressure	Pressure	bar	38	40	53
Split Ratio	Molar Fraction	-	0.7	0.93	1
Booster Pressure	Pressure	bar	40	54	70
C1 to NGL	Molar Fraction	-	0.01	0.0462	0.06

Table J.1: Start values for randomly generated variables in Shell process for tests done in Section 6.3.2.1

Tag Name	Constraint	Unit	Minimum	Start Value	Maximum
MinApp WMR CWHE	Minimum Approach	°C	3	7.5849	-
MinApp LB CMR CWHE	Minimum Approach	°C	3	-53.4406	-
MinApp UP CMR CWHE	Minimum Approach	°C	3	20.887	-
Dew Point WMR	Minimum Approach	°C	5	-3.1255	-
Dew Point CMR	Minimum Approach	°C	5	52.1065	-
MinApp Upstream	Minimum Approach	°C	3	-133.2229	-
C5+ to LNG	Molar Fraction	-	-	0.0002	0.0010
Liquid input WMR	Fraction	-	1	0.7096	-
BTX to LNG	Molar Fraction	ppm	-	2.2380	10

Table J.2: Start values for randomly generated constraints in Shell process for tests done in Section 6.3.2.1

Appendix K

Tag Name	Variable	Unit	Lower Bound	Final Value	Upper Bound
N WMR	Molar Flow	kgmole/h	0	0.10	2000
C1 WMR	Molar Flow	kgmole/h	1000	2686.80	13000
C2 WMR	Molar Flow	kgmole/h	20000	23924.80	38000
C3 WMR	Molar Flow	kgmole/h	2000	5910.97	14000
i-C4 WMR	Molar Flow	kgmole/h	100	8954.70	9000
n-C4 WMR	Molar Flow	kgmole/h	100	1024.00	9000
N CMR	Molar Flow	kgmole/h	2000	2000.00	10000
C1 CMR	Molar Flow	kgmole/h	10000	18662.00	25000
C2 CMR	Molar Flow	kgmole/h	10000	19207.50	25000
C3 CMR	Molar Flow	kgmole/h	500	4576.00	12000
LP Warm	Pressure	bar	5	7.30	13
MP Warm	Pressure	bar	15	17.88	29
HP Warm	Pressure	bar	35	32.02	55
LLP Cold	Pressure	bar	2	4.22	8
LP Cold	Pressure	bar	8	16.18	23
MP Cold	Pressure	bar	22	22.88	46
HP Cold	Pressure	bar	30	31.24	52
HHP Cold	Pressure	bar	40	40.71	62
Temp WMR CWHE	Temperature	°C	-53	-39.19	-30
Temp LB CMR CWHE	Temperature	°C	-135	-120.95	-110
Temp Upstream	Temperature	°C	-40	-29.15	-20
ScrubCol Pressure	Pressure	bar	30	44.49	50
Booster Pressure	Pressure	bar	50	57.20	70
C1 to NGL	Molar Fraction	-	0.0100	0.02	0.0600

Table K.1: Final variable values for the best result in simulation work done by the Hyprotech SQP optimizer for the Turbo-expander process.

Tag Name	Constraint	Unit	Minimum	Final Value	Maximum
MinApp WMR CWHE	Minimum Approach	°C	3	2.988	-
MinApp LB CMR CWHE	Minimum Approach	°C	3	2.996	-
MinApp UP CMR CWHE	Minimum Approach	°C	3	2.999	-
Dew Point WMR	Minimum Approach	°C	5	7.389	-
Dew Point CMR	Minimum Approach	°C	5	9.607	-
MinApp Upstream	Minimum Approach	°C	3	3.001	-
C5+ to LNG	Molar Fraction	-	-	0.0004	0.0010
Liquid input WMR	Fraction	-	1	1	-
BTX to LNG	Molar Fraction	ppm	-	9.99	10

Table K.2: Final constraint values for the best result in simulation work done by the Hyprotech SQP optimizer for the Turbo-expander process.

Appendix L

Tag Name	Variable	Unit	Lower Bound	Final Value	Upper Bound
N WMR	Molar Flow	kgmole/h	0	0.00	2000
C1 WMR	Molar Flow	kgmole/h	1000	2353.58	13000
C2 WMR	Molar Flow	kgmole/h	20000	22901.29	38000
C3 WMR	Molar Flow	kgmole/h	2000	6205.24	14000
i-C4 WMR	Molar Flow	kgmole/h	100	8714.25	9000
n-C4 WMR	Molar Flow	kgmole/h	100	3650.42	9000
N CMR	Molar Flow	kgmole/h	2000	1500.00	10000
C1 CMR	Molar Flow	kgmole/h	10000	17913.65	25000
C2 CMR	Molar Flow	kgmole/h	10000	18485.79	25000
C3 CMR	Molar Flow	kgmole/h	500	3271.55	12000
LP Warm	Pressure	bar	5	5.13	13
MP Warm	Pressure	bar	15	15.07	29
HP Warm	Pressure	bar	35	29.00	55
LLP Cold	Pressure	bar	2	3.91	8
LP Cold	Pressure	bar	8	16.15	23
MP Cold	Pressure	bar	22	21.60	46
HP Cold	Pressure	bar	30	28.46	52
HHP Cold	Pressure	bar	40	37.02	62
Temp WMR	Temperature	°C	-53	-46.14	-30
Temp LB CMR	Temperature	°C	-135	-123.04	-110
ScrubCol Pressure	Pressure	bar	40	53.23	55
Booster Pressure	Pressure	bar	50	54.45	70
C1 to NGL	Molar Fraction	-	0.01	0.01	0.06

Table L.1: Final variable values for the best result in simulation work done by the Hyprotech SQP optimizer for the APCI process.

Tag Name	Constraint	Unit	Minimum	Final Value	Maximum
MinApp WMR CWHE	Minimum Approach	°C	3	3	-
MinApp LB CMR CWHE	Minimum Approach	°C	3	2.994	-
MinApp UP CMR CWHE	Minimum Approach	°C	3	3.007	-
Dew Point WMR	Minimum Approach	°C	5	5.002	-
Dew Point CMR	Minimum Approach	°C	5	7.327	-
C5+ to LNG	Molar Fraction	-	-	0.0003	0.0010
Liquid input WMR	Fraction	-	1	1	-
BTX to LNG	Molar Fraction	ppm	-	10	10

Table L.2: Final constraint values for the best result in simulation work done by the Hyprotech SQP optimizer for the APCI process

Appendix M

Tag Name	Variable	Unit	Lower Bound	Final Value	Upper Bound
N WMR	Molar Flow	kgmole/h	0	0.00	2000
C1 WMR	Molar Flow	kgmole/h	1000	2836.90	13000
C2 WMR	Molar Flow	kgmole/h	20000	27153.40	38000
C3 WMR	Molar Flow	kgmole/h	2000	3662.10	14000
i-C4 WMR	Molar Flow	kgmole/h	100	8921.40	9000
n-C4 WMR	Molar Flow	kgmole/h	100	2485.10	9000
N CMR	Molar Flow	kgmole/h	1000	1192.50	10000
C1 CMR	Molar Flow	kgmole/h	10000	17400.60	25000
C2 CMR	Molar Flow	kgmole/h	10000	17176.90	25000
C3 CMR	Molar Flow	kgmole/h	500	5697.30	12000
LP Warm	Pressure	bar	5	7.29	13
MP Warm	Pressure	bar	15	17.71	29
HP Warm	Pressure	bar	33	33.00	55
LLP Cold	Pressure	bar	2	3.45	8
LP Cold	Pressure	bar	8	15.48	23
MP Cold	Pressure	bar	22	22.00	46
HP Cold	Pressure	bar	30	30.00	52
HHP Cold	Pressure	bar	38	38.00	62
Temp WMR CWHE	Temperature	°C	-53	-40.33	-30
Temp LB CMR CWHE	Temperature	°C	-135	-124.11	-110
ScrubCol Pressure	Pressure	bar	38	53.00	53
Split Ratio	Molar Fraction	-	0.7	0.86	1
Booster Pressure	Pressure	bar	40	57.75	70
C1 to NGL	Molar Fraction	-	0.01	0.02	0.06

Table M.1: Final variable values for the best result in simulation work done by the Hyprotech SQP optimizer for the Shell process.

Tag Name	Constraint	Unit	Minimum	Final Value	Maximum
MinApp WMR CWHE	Minimum Approach	°C	3	2.989	-
MinApp LB CMR CWHE	Minimum Approach	°C	3	2.981	-
MinApp UP CMR CWHE	Minimum Approach	°C	3	3.011	-
Dew Point WMR	Minimum Approach	°C	5	5.04	-
Dew Point CMR	Minimum Approach	°C	5	8.428	-
MinApp Upstream	Minimum Approach	°C	3	2.969	-
C5+ to LNG	Molar Fraction	-	-	0.0007	0.0010
Liquid input WMR	Fraction	-	1	1	-
BTX to LNG	Molar Fraction	ppm	-	10	10

Table M.2: Final constraint values for the best result in simulation work done by the Hyprotech SQP optimizer for the Shell process

Appendix N

Tag Name	Variable	Unit	Lower Bound	Final Value	Upper Bound
N WMR	Molar Flow	kgmole/h	0	0	2000
C1 WMR	Molar Flow	kgmole/h	1000	3231.3	13000
C2 WMR	Molar Flow	kgmole/h	20000	26909.7	38000
C3 WMR	Molar Flow	kgmole/h	2000	8004.5	14000
i-C4 WMR	Molar Flow	kgmole/h	100	3711.9	9000
n-C4 WMR	Molar Flow	kgmole/h	100	3298.7	9000
N CMR	Molar Flow	kgmole/h	2000	2057.3	10000
C1 CMR	Molar Flow	kgmole/h	10000	19133.7	25000
C2 CMR	Molar Flow	kgmole/h	10000	20780.5	25000
C3 CMR	Molar Flow	kgmole/h	500	5067.7	12000
LP Warm	Pressure	bar	5	9.15	13
MP Warm	Pressure	bar	15	20.67	29
HP Warm	Pressure	bar	35	35	55
LLP Cold	Pressure	bar	2	4.3	8
LP Cold	Pressure	bar	8	15.67	23
MP Cold	Pressure	bar	22	22	46
HP Cold	Pressure	bar	30	30	52
HHP Cold	Pressure	bar	40	40	62
Temp WMR	Temperature	°C	-53	-35.27	-30
Temp LB CMR	Temperature	°C	-135	-118.08	-110
Absorber Pressure	Temperature	°C	35	51.01	60
ScrubCol Pressure	Pressure	bar	25	58	58
Upstream CWHE	Temperature	°C	-75	-31.7	-30
Booster Pressure	Pressure	bar	55.00	55.79	65.00
C1 in NGL	Molar Fraction	-	0.01	0.06	0.06

Table N.1: Final variable values for the best result in simulation work done by the Hypro-tech SQP optimizer for the Fluor process.

Tag Name	Constraint	Unit	Lower Bound	Final Value	Upper Bound
MinApp WMR CWHE	Minimum Approach	°C	3	3.0001	
MinApp LB CMR CWHE	Minimum Approach	°C	3	2.9895	
MinApp UP CMR CWHE	Minimum Approach	°C	3	2.9998	
Dew Point WMR	Minimum Approach	°C	5	5.3985	
Dew Point CMR	Minimum Approach	°C	5	12.6842	
MinApp Upstream	Minimum Approach	°C	3	2.9989	
C5+ to LNG	Molar Fraction	-	-	0.0006	0.001
Liquid Input WMR	Fraction	-	1	1	-
BTX to LNG	Molar Fraction	ppm	-	9.96	10

Table N.2: Final constraint values for the best result in simulation work done by the Hyprotech SQP optimizer for the Fluor process